MULTI-BODY DYNAMIC ANALYSIS OF CERVICAL SPINE FOR HELICOPTER PILOTS

by

Hojjat Fathollahi

BSc, Mechanical Engineering, Shiraz University, Iran, 1991

A THESIS

PRESENTED TO RYERSON UNIVERSITY

In partial fulfillment of the

Requirement for the degree of

Master of Applied Science

In the program of

Aerospace Engineering

Toronto, Ontario, Canada, 2012

Author's Declaration

I hereby declare that I am the sole author of this thesis. This is a true copy of the thesis, including any required final revisions, as accepted by my examiners.

I authorize Ryerson University to lend this thesis to other institutions or individuals for the purpose of scholarly research.

I further authorize Ryerson University to reproduce this thesis by photocopying or by other means, in total or in part, at the request of other institutions or individuals for the purpose of scholarly research.

I understand that my thesis may be made electronically available to the public.

Signature

ABSTRACT

Multi-Body Dynamic Analysis of Cervical Spine for Helicopter pilots

Master of Applied Science 2011

Hojjat Fathollahi

Aerospace Engineering

School of Graduate Studies, Ryerson University

Helicopter pilots use helmets equipped with night vision goggle and counter weight. This increased load can lead to disc injury, so it is necessary to evaluate the load and moments applied to each cervical disc when pilot head is moving in different flight conditions. A 3D multi-body dynamic model of cervical spine is provided to investigate the effect of weight of the helmet in flexion, extension, lateral bending and axial rotation of the spine. The whole study was done in several steps: 1) to develop a non-linear dynamic model of spine. 2) to validate the model against the published data under flexion, extension, lateral bending and torsinal moments. 3) to solve three case studies to simulate a moving head in different direction. 4) to run the simulations again with consideration of adding a helmet into the model with different weight to find out the effects on the cervical discs loading. The results demonstrate that C2C3, C4C5 and C7T1 carry the highest loads depending on direction of imposed displacement on the head. Experts in the area of neck injury can study the results and locate the regions at risk of injury or they can feed this information into FEA model to get stress distribution in discs, bones or ligaments.

Acknowledgment

I would like to give my special thanks and express my deepest sense of gratitude to my supervisor Dr. Kamran Behdinan for his great support during my study.

Table of contents

List of Tables

Table 7.1: Muscles geometry data [Jager, Johannes, 1998]

List of Figures

List of Abbreviations

2D	Two dimentional
3D	Three dimentional
AL	Alar Ligament
ALL	Anterior Longitudinal Ligament
CAD	Computer aided design
CL	Capsular Ligaments
CLV	Vertical Cruciate Ligament
CW	Counter weight
G	Gravity
ISL	Interspinous Ligaments
JC	Capsular Joint
LF	Ligamentum Flavum
NVG	Night vision goggle
NZ	Neutral zone
PLL	Posterior Longitudinal Ligament
ROM	Range of motion
SSL	Superspinous Ligaments
TL	Transverse Ligament
TM	Tectorial Membrane
AA-OM	Anterior Atlanto-Occipital Membrane
PA-OM	Posterior Atlanto-Occipital Membrane

Chapter 1

Introduction

The cervical spine is one of the most complicated structures in the human body. Its exclusive anatomy makes this structure extremely flexible. The cervical spine is also responsible for providing appropriate support for the skull and protecting the spinal cord from injury. Although the cervical spine is very flexible, it is highly at risk of injury from strong, sudden movements, such as whiplash-type and high gravitational (G) force impact injuries.

Researchers have chosen different approaches to investigate the area of cervical spine injuries. Statistical survey is the basic approach to determining populations at risk of cervical spine injury and the external causes of injury. Clinical studies of cervical spine injuries can assist researchers to define the mechanism and severity of a neck injury. Investigating cervical spine injuries experimentally is the ideal method of simulating the mechanism of injury and its initialization, as controlled loads can be applied to the neck while performing the experiments. Numerical analysis is another method of simulating real life accidents and is more efficient than the experimental approach. This method enables researchers to develop highly detailed models in which the distribution of stresses and strains can be studied for all of the different components of the cervical spine. All of these approaches are extremely important and considering them together will offer a great opportunity to increase the knowledge of neck injury mechanisms.

The numerous advantages of multi-body dynamic analysis and the finite element method have motivated researchers to investigate the causes of injury in the cervical spine using

these approaches. The ability to analyze complicated structures, material properties and boundary conditions, whether linear or nonlinear, makes these methods more attractive tools in the investigation of cervical injuries in real life. Taking advantage of fast processor computers, the multi-body dynamic analysis approach is faster and cheaper than experimental techniques.

The first step in investigating the causes of neck injury using the multi-body dynamic analysis method is to develop a CAD model of the cervical spine and validate the model via quasi-static and dynamic analysis. Dynamic analyses can be performed on the validated model to obtain the forces and moments in every element in the model. Experts in the area of neck injury can study the results and locate the regions at risk of injury or they can feed this information into FEA model to get stress distribution in discs, bones or ligaments.

1.1 Helicopter pilot helmets and the loads on the cervical spine discs

The helicopter pilots are increasingly using helmet mounted devices to enhance their operational military capabilities. Night vision goggle (NVG) is one of those devices that are used at nights to perform a mission irrespective of visibility condition. The majority of the NVG mass is concentrated in the display (Knight and Barbar, 2007) and some pilots counteract this imbalance by using a counterweight (CW) situated posteriorly at the base of their helmets [Ford et al. 2011]. NVG and CW increase the mass of the helmet from 14 N to 36 N. This added mass can lead to spinal degeneration disc in cyclic loading in different flight conditions considering the head position relative to the cervical spine. A report reveals that 19.8 percent of total 232 Indian helicopter aircrews had

cervical disc degeneration [Sharma, Agarwal, 2008]. Therefore, it is very useful to develop a multi-body dynamic model of the cervical spine to extract the loads exerted on the discs in different situations and long time spans. This load can be later on used solely to predict the level of injuries on the discs or to be fed into a finite element model for calculating the maximum stress in a disc. The current model is created in MD ADAMS and then validated against the published data under flexion, extension, torsion and lateral bending load configuration [Panjabi, Oda et al. 1992, Moroney et al. 1988 and Panjabi et al. 1993]. To understand better the loading on the discs, three case studies are done to simulate a moving head without helmet in extension/flexion, axial rotation and lateral movements. Finally helmet data are incorporated into the model and variation of discs loadings due to different helmet weight are investigated.

1.2 Creating the cervical spine geometry

The original geometry of vertebras which is used for this study was created by Farsa, 2005. The following explain how he has extracted the information in order to develop a 3D model. The anatomy of the cervical spine has been qualitatively documented in various textbooks and research [Dvorak et al., 1991, Sherk et al. 1989, Johannes, Verlag 1993, Goel 1990, Lowery 2001, Panjabi et al 1992]. Because of the existing complication in the geometry of the cervical spine vertebrae, it is not possible to find all of the necessary parameters defining geometry of vertebrae in a single research. Therefore, to model the vertebrae it is essential to obtain the missing parameters from other reports [Panjabi et al. 1993, Xu et al. 1999]. Although the cervical spine contains seven vertebrae, no research has reported the quantitative parameters for all seven

vertebrae in a single work. This is because the first two vertebrae of the cervical spine, Atlas and Axis, are completely different from the rest of vertebrae. Some quantitative studies have reported the required parameters to model Atlas and Axis [Doherty, Heggeness 1994 and 1995, Dong et al. 2003, Naderi et al. 2004, Schaffler 1992].

The last parameter that has a significant contribution in the modeling of cervical spine is the height or relative location of the intervertebral discs to the adjacent vertebrae. In the simplified model of the intervertebral discs presented by Nissan et al. 1986, the required parameters to locate adjacent vertebrae of the cervical spine can be found.

Then Farsa's vertebra CAD data was re-created and simplified so that it suites for importing into MD ADAMS.

1.3 Material data

The geometry of C1 to T1 is fairly close to the size of real vertebra. Therefore, in ADAMS model, only the right density was defined for each vertebra to have the right mass as presented by Jager, Johannes 1998. To define ligaments force-deflection properties, results of those experiments presented by Pintar et al. 2001 are used. All ligaments have damping factor of 300 N.s/m which is defined by Jager, Johannes 1998. Also, their stiffness is zero when they are in compression. Material properties of the inter-vertebral discs are required for multiple directions of loading, i.e. flexion, extension, tension, compression, anterior and posterior shear, lateral shear, axial rotation, and lateral bending [Acar , Loptic 2007].

1.4 Multibody Dynamic Model in ADAMS

For the first step to make the model in ADAMS, the CAD data of the vertebras were imported into ADAMS using step format. Then the ligaments and discs insertion point's CAD data were added in igs format. Spring-dashpot element and bushing type spring-dashpot were used for ligaments and discs respectively.

1.5 Validation of the model

To validate the model, three reference papers were used. In these literatures, the results of experimental tests on different parts of the cervical spine were presented. The model of upper cervical spine segment, C0-C2 was validated against the experimental data of Panjabi, Oda et al. 1992. The models of lower cervical spine vertebra pairs, C2-C3, C3-C4, C4-C5, C5-C6, C6-C7 and C7-T1 were validated under the results of experiments published by Moroney et al. 1988. Finally, the complete model of cervical spine was validated against the research work of Panjabi et al. 1993 for extension and flexion load conditions.

1.6 Case studies

In this study, three cases were investigated. These cases cover simulation of extension/flexion, later and torsional movements. They actually simulate some basic movements of the cervical spine which can be happened every day. Therefore, the speed is not high for these conditions. For all of them, a load, which can be a displacement or a force in different directions, is applied to the center of mass of the head and also T1 is fully constrained. Then, resultants loads on the discs versus simulation time are demonstrated.

1.7 Sensitivity

The goal of this activity is to examine different weights of helicopter helmets for demonstrating the effect on cervical spine loads and moments in different directions. The NVG equipped helmet has the maximum weight of 3.7 kg [Ford et al. 2011].

Chapter 2

Anatomy of cervical spine

2.1 Introduction

The cervical spine includes the first seven vertebrae in the spine. They are located between the skull and the thoracic spine (Figure 2.1).

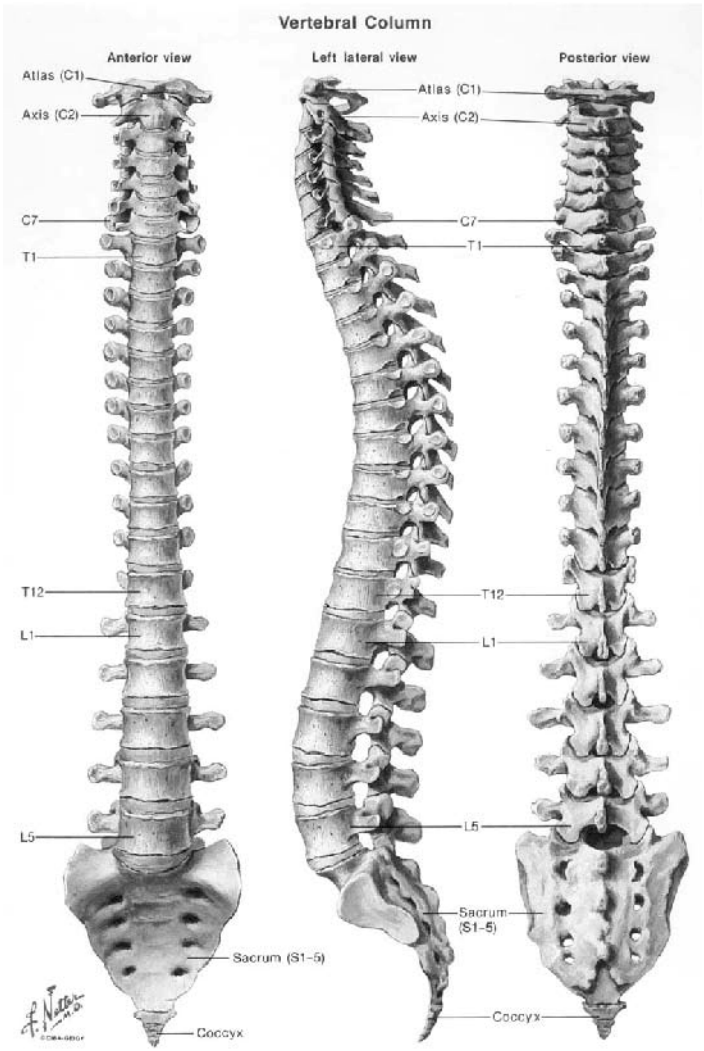

Figure 2.1: The spine with the cervical spine starting from C1 to C7, the thoracic spine from T1 to T12, the lumbar spine from L1 to L5 [Atlas of human body Frank H. Netter]

The cervical spine has a backward C-shape curve; in this regard it is similar to the lumbar spine. The cervical spine is not as stiff as the other part of the spine. Therefore, It can move much easier in different directions. There is a main hole on each vertebra which is for passage of spinal cord and similarly there are such these holes in other spine vertebras. However, there are smaller holes which is for the arteries and they are specific to just cervical spine area. The ligaments and intervertebral discs connect the skull and vertebrae with flexibility in movement while the neck structure is still stable [Sherk et al., 1989].

2.2 Vertebrae of the cervical spine

Due to the difference in shape of the vertebra, the cervical spine can be categorized into upper, which include the vertebra from occiput to C2, and lower which is from C3 to C7 (Figure 2.2).

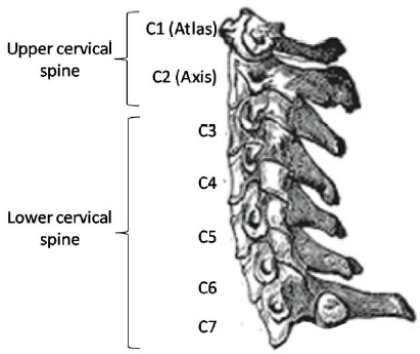

Figure 2.2: Upper and lower cervical spine [Gray's Anatomy, 2000]

The first vertebra at the top is called atlas (C1) and looks like a ring. This vertebra joins to the occiput bone of the skull with ligaments. The next cervical spine vertebra is the axis (C2), and it has a special bony extension, called dens, that acts as axis of rotation

for the atlas. There are ligaments on this extension that connect occiput directly to this vertebra. The other ligaments join this vertebra to the atlas and C3 (Figure 2.3).

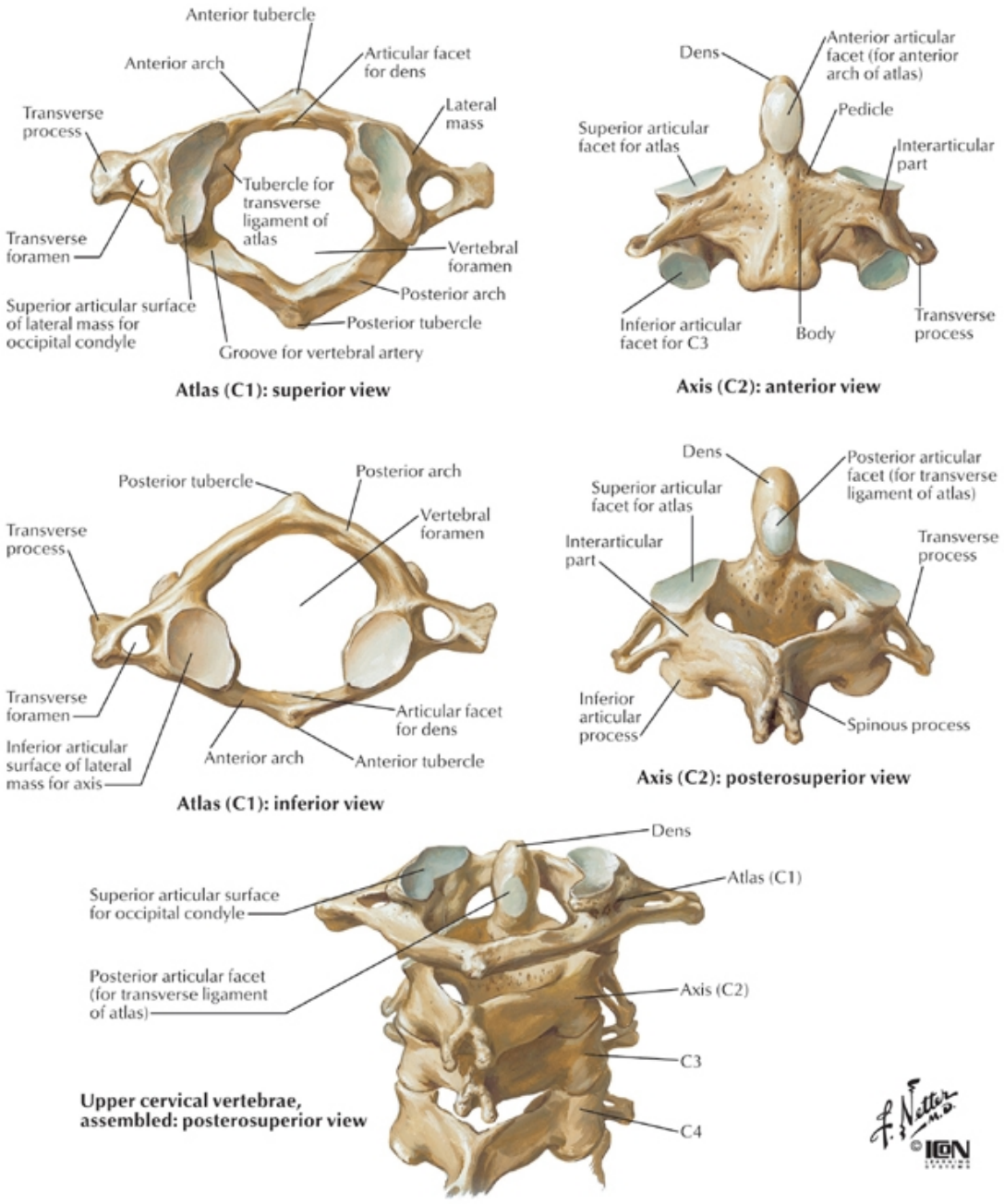

Figure 2.3: C1, C2 and upper cervical spine assembly [Atlas of human body Frank H. Netter]

The atlanto-axial joint, where the C2 dens is, is very important as the most of the cervical spine rotation happens at this joint [Penning and Wilmink, 1987]. Figure 2.4 shows a vertebra in the lower part of the cervical spine. These vertebras at the lower look more similar to each others. They have anterior body as the main bulk of the vertebra and a ring at the back, which called the neural arch. This ring includes two laminas and pedicles. The lamina has two superior and two inferior, two transverse processes, and one spinous process (Figure 2.4).

The ligaments and muscles attachment points are at the place of the transverse and spinous processes. The main bulk of vertebra bone and the lamina are joined at pedicles, which form an enclosed area for spinal cord. The enclosed area isolates the spinal cord and mostly it protects the cord at the neck area. There are two articular processes at the superior and two at inferior side of the vertebra. These surfaces are in contact with similar ones which belong to the adjacent vertebrae. They make a joint at these places, called the zygapophysial or facet joints. To reduce the friction, there is hyaline cartilage between a pair of joint surfaces.

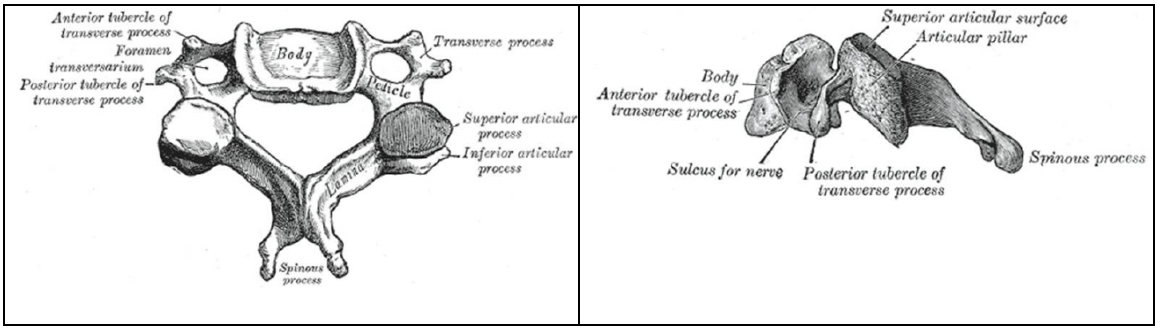

Figure 2.4: Anatomy of the cervical vertebrae [Gray's Anatomy, 2000]

The lower spine vertebra has some specific features in both anatomy and geometry point of view. The superior surface of the vertebra main body has a seat shape. There is a bony lip which can be seen on the front side of the inferior surface of the main body,

(lateral view in Figure 2.4). In addition, the facet surface has an angle of 45 degree from the transverse plane. These features are the reasons for having the largest range of motion in flexion and extension movements at the lower part of the cervical spine [Bogduk and Mercer, 2000]. Also, there is an opening in each vertebra transverse process which is a passage for the veins, nerves. These openings are called foramen transversarium. There is a primary structural tissue, called osseous tissue, which carry the some compressive loads exerted on the vertebrae. The main body of the vertebrae, the posterior arch and the facet joints take the majority of the loads. The main body of the vertebrae is made of cancellous bone and the bone itself is covered by a thin cortical shell (Figure 2.5). Cancellous bone is spongy and there is vascular in it. The cortical shell is thicker on the posterior arch and there is less cancellous bone in comparison to the main body.

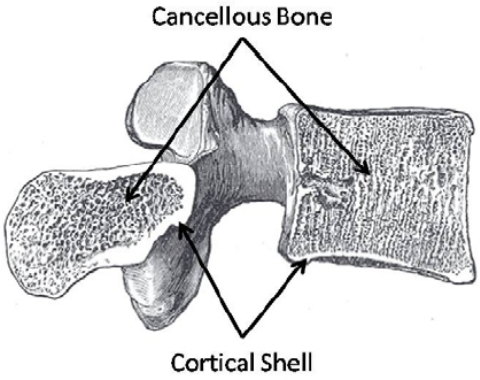

Figure 2.5: Cervical spine vertebra cancellous bone and cortical shell [Gray's Anatomy, 2000]

2.3 Intervertebral disc

Cervical intervertebral disc are positioned between the superior surface of a vertebra main body and the inferior surface of the body on the adjacent. The most upper disc is positioned between C2 and C3 and the last lowest one is between C7 and T1. They are

flexible and let the vertebrae to have translational and rotational movements relative to each other at each level. They can carry loads and moments in different directions. The loads can be tensile, compressive and shear. The moments are torsional, flexion, extension and lateral bending. When there is relative movement between adjacent vertebrae, multiple loading conditions are applied to the discs while they share the loads with facet joints in compression and the ligaments in tension [Augustus, M.M.P., 1990]. Then the load is transferred to the main body of the vertebrae over the surfaces which are in touch with the discs [Adams and Roughley, 2006]. Cervical spine discs are made of an inner nucleus pulposus, wrapped by the annulus fibrosis. There is a thin cartilaginous endplates which is on top and bottom of each disc and these endplates connect to main body of the adjacent vertebrae (Figure 2.6).

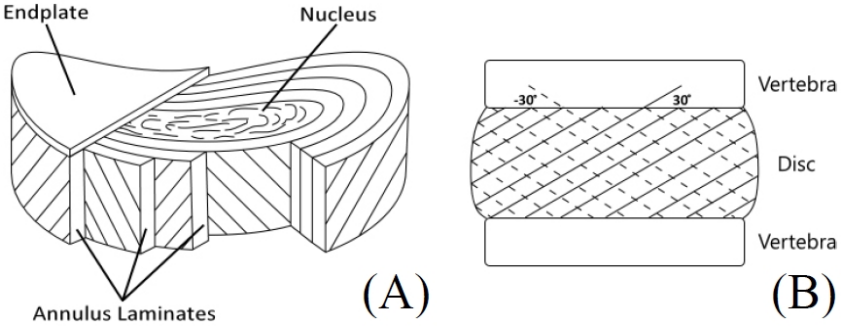

Figure 2.6: Schematic of the human intervertebral disc. (A). Layers of fibrous annulus tissue enclose an inner gelatinous nucleus (B). Adjacent layers of annular lamellae contain aligned collagen fibers alternate between ±30° with respect to the disc plane. [Kevin L. Troyer, 2010]

The nucleus is composed of suspended cells in an extracellular matrix which include water, proteoglycan macromolecules, elastin fibers type II and collagen fibers [Adams and Roughley, 2006]. The level of hydration is high and it the amount of the water is ranging from 70 to 90% [Augustus, M.M.P., 1990]. This hydration causes the nucleus to

behave hydrostatically when it is under compressive load, and it distributes the pressure uniformly to the annulus and endplates [Urban, J.P.G. et al., 2000]. The annulus fibrosis surrounds the nucleus and it is composed of fibrous tissue concentric layers (lamellae) which are made of type I collagen fibers that span the disc space. As a result, disc can resist against bending and rotational movements with tension in these fibers (Figure 2.6). The fibers have ±30° angle to the transverse disc plane, and so that there is 120° between fibers of adjacent lamina (Figure 2.6 B) [Augustus, M.M.P., 1990]. Ground substance which contains water and mucopolysaccharide protein complexes encloses these fibers [Wu et al., 1976]. Vertebral main bodies are connected to these fibers ends at the outer periphery of the annulus to resist better against torsion and tensile loads, while the fibers which are poistioned more interiorly are connected to the endplates [Augustus, M.M.P., 1990].

Also, the endplates take hydrostatic pressure from the disc during and prevent the nucleus from protruding into the vertebral body [Moore, R.J., 2000]. In addition, the endplates provide the disc with nutrients from vasculature of the vertebral bone through diffusion [Urban et al. 2000].

2.4 Ligaments

Ligaments are made of elastic dense fibers, water, collagen, cells and proteoglycans [Walsh, W.R., 2006]. Their stiffness makes the spinal column stable. They can absorb energy during trauma, and are flexible enough to let the spine to move safely; while preventing excessive motion that could hurt the spinal cord [Augustus, M.M.P., 1990]. The ligament can carry the load as the most when the direction of the load is parallel to

the fiber axis. They can resist against tension and buckling. When a spinal column moves, those ligaments which are in tension keep the structure together and they share the loads with discs.

Figure 2.7 present the ligaments in both the lower and upper parts of cervical spine. The lower cervical spinal ligaments include the inter spinous ligaments (ISL), the super spinous ligaments (SSL), the ligamentum flavum (LF), the posterior longitudinal ligament (PLL), the anterior longitudinal ligament (ALL) and the capsular ligaments (CL). Most of these ligaments are extended to the upper parts of the cervical spine too. Those ligaments which are existed just in the upper cervical spine (axis, atlas and occiput) are the posterior atlanto-occipital membrane (PAOM), the anterior atlanto-occipital membrane (AAOM), the apical ligament, the transverse ligament (TL), the alar ligament and the tectorial membrane (TM), and. The shape of PLL changes at the upper and it is called TM from C2 to the occiput and similarly it happens for the ALL too and it is the AAOM from Cl to the occiput [Myklebust et al., 1988]. Table 2.1 shows the list of the lower and upper cervical spinal ligaments.

Table 2.1: Upper and lower cervical spine ligaments

	Ligamen	Mnemonic
The Lower Cervical Spinal Ligaments	Posterior Longitudinal Ligament	PLL
	Anterior Longitudinal Ligament	ALL
	Capsular Ligaments	CL
	Ligamentum Flavum	LF
	Interspinous Ligaments	ISL
	Superspinous Ligaments	SSL
The Upper Cervical Spinal Ligaments	Alar Ligament	AL
	Transverse Ligament	TL
	Tectorial Membrane	TM
	Anterior Atlanto-Occipital Membrane	AA-OM
	Posterior Atlanto-Occipital Membrane	PA-OM
	Vertical Cruciate Ligament	CLV

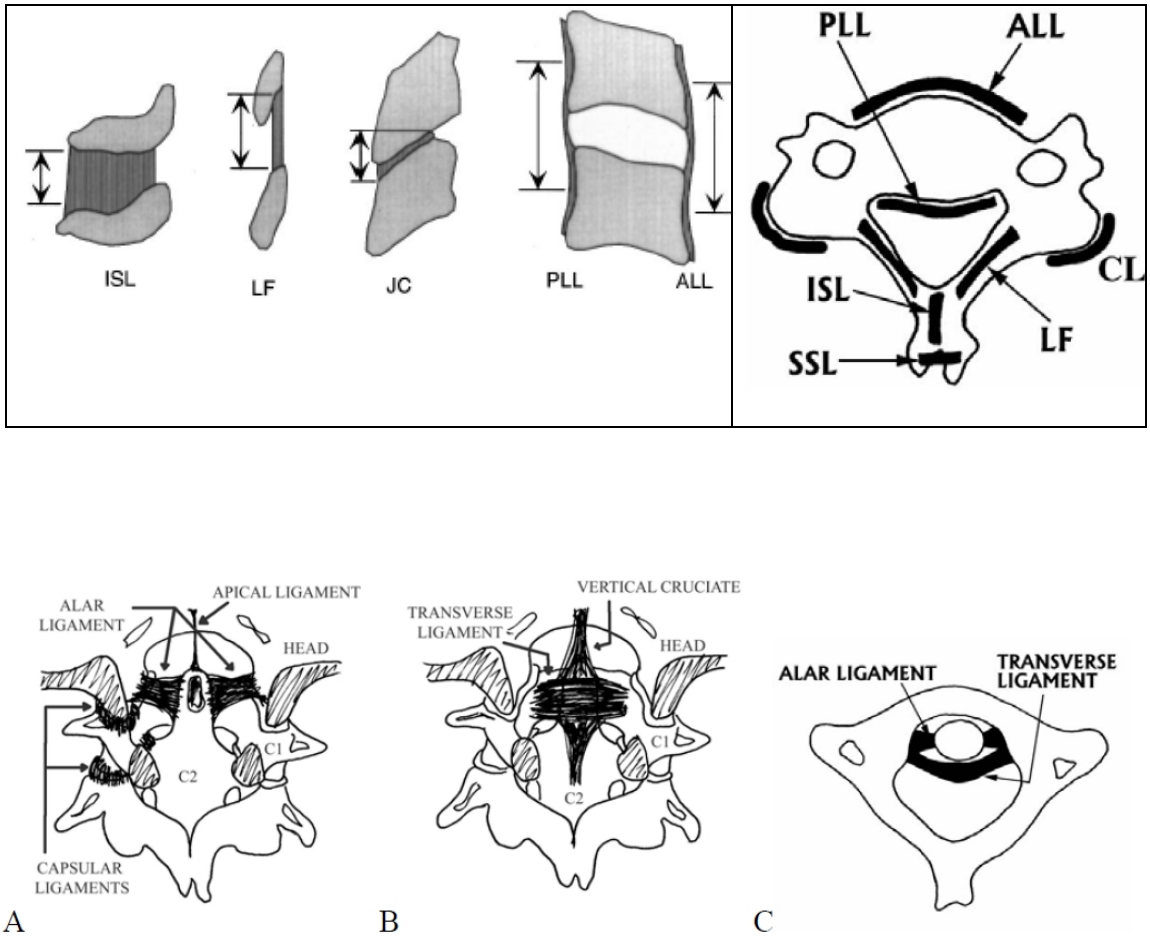

Figure 2.7: Upper cervical spine ligaments. A) Posterior view of occiput to C2 with apical and alar ligament. B) Posterior view of occiput to C2 with transverse membrane and vertical cruciate. C) Superior view of C1 with alar and transverse ligaments. [Karin Blorin, 2002]

2.4.1 The Apical Ligament

The apical ligament is a V-shaped tissue that connects the occipital formamen to the superior surface of the dens. The ligaments fibers are mainly positioned at the middle of the ligament. This ligament is relatively thin and can limit the motion of the cervical spine in flexion.

2.4.2 The Alar Ligament

This ligament connects the upper portion of the dens and the occiput [Panjabi et al., 1991]. Mainly, they are made of collagen, so, their stiffness is high and the ligaments do not behave very flexible. The purpose of this ligament is to limit the axial rotation of the occipito-atlantal joint

2.4.3 The Transverse Ligament and Vertical Cruciate

The transverse ligament is mainly composed of collagen, similar to the alar ligaments [Saldinger et al. 1990]. The transverse ligament is originated on one side of atlas inner surface and it is inserted on the other side of that, while it is passing on the posterior surface of the dens. It constrains the fore and aft movement of the dens, and it keeps the dens against the inner surface of the atlas at the front. As a result it prevents the dens to move toward the spinal cord. Two extensions come out from the middle of the transverse ligament; one is upward which connects to the occiput and the other one is a downward ligament and connect to the lower area of the axis. These ligaments are called the vertical cruciate and limit the motion of the head in the flexion (Figure 2.7).

2.4.4 The Anterior Longitudinal Ligament and the Anterior Atlanto-occipital Membrane

The ALL connects the anterior surface of main body of the vertebrae and the discs which are between them. This is a flat ligament which its thickness reduces at the C1-C2 level. The ALL is extended to the skull and changes its name to the anterior atlanto-occipital membrane at the CO-Cl level [Myklebust al. 1988].

2.4.5 The Posterior Longitudinal Ligament and the Tectorial Membrane

The PLL connects the posterior surface of the vertebral bodies and the disc which are between them. The PLL is extended from T1 to C2 vertebra. The continuation of PLL which is between C2 and the occiput, is called tectorial membrane.

2.4.6 The Ligamentum Flavum and the Posterior Atlantooccipital Membrane

The ligamentum flavurn connects the posterior surface of vertebrae arc within the spinal canal. The density of elastin fibers is high in this ligament and so, it behaves very stiff. The Posterior Atlantooccipital Membrane is similar to the ligamentum flavum where it is positioned between C1 and C0.

2.4.7 The Supraspinous and Interspinous Ligament

Both the SSL and ISL connect the spinous part of adjacent vertebrae. The SSL exists only in lower of the cervical spine, but the ISL is extended to the top at C1-C2 level. Their purposes are to limit the motion of the cervical spine in extension.

2.4.8 The Capsular Ligament

This ligament connects the two facet joint surfaces which are in neighborhood. The capsular ligament is thin and loose. This condition is more dominant at occipito-atlantal (C0-C1) and atlatoaxial (C1-C2) joints. The CL can carry the tension load while it keeps the synovial fluid inside the capsular joint.

Chapter 3

Biomechanics of Soft Tissue

3.1. Background on the structure of soft tissues – collagen and elastin

The tissue that connects and protects the other body parts is called soft connective tissue. This group of tissue has wide range of biological materials. The extracellular material in this tissue separates the cells from each other [Holzapfel G. A., 2000-a].

Connective tissues are different than hard tissues which have mineral materials like bones. They have soft material properties and are very flexible. Tendons, skins, blood vessels, articular cartilage and ligament are the soft tissues in human body. Tendon connects a muscle to a bone, to make it possible to move the skeleton. Ligament connect a bone to the another one to limit the relative motion and to keep the structure stable. Blood vessels are very flexible tissues which swell as the local blood pressure increases to store more blood and return back to their original shape when the pressure decreases and as a result they release the stored blood. The skin has the sixteen percent of the human weight, so it is largest body part. They protect the body part by isolating them from outside. At the place of a joint, there is soft tissue between two contact surfaces of bones, called articular cartilage, which has a thickness of a few millimeter and its role is to reduce the friction and distribute the load uniformly across the joint.

The soft connective tissues are composed of fibers which give stiffness to the tissue. The density and the arrangement of the tissue components affect directly on mechanical behaviour of the tissue. Some of these components are elastin, collagen and the hydrated

matrix of proteoglycans. The extracelluar matrix of connective tissues is made of a protein which is called collagen. Collagen is the main components of a soft tissue which carry the highest load. In addition, in human physiology point of view, collagen is important too. As an example, achilles tendon has twenty times more collagen than that of elastin.

Collagen has a length of 280 nm as a macromolecule. Collagen fibrils are composed of many Collagen molecules which are attached to each other by covalent bonds. The diameter of collagen fibrils varies based on the required strength and its primary function. Its length is in the order of 1.5 nm [Nimni, Harkness, 1988]). Collagen fibers are oriented parallel to each other in ligaments and tendons [Betsch, Baer, 1980], but they look to be scattered in many other tissues. In these tissues, collagen fibers are positioned in a proteoglycans gelatinous matrix.

There are more than twelve 12 types of collagen [Nimni, Harkness, 1988]. Type I is the most common collagen which any tissue can have. The blood vessels are mainly composed of this material. Collagen molecules have a rod-shape due to three polypeptide chains. Majority of the collagen molecule is composed of three amino acids, hydroxyproline (15%) , proline (15%), glycine (33%), which improve the stability of the molecule [Ramachandran, 1967].

There is an intra-molecular cross link in a collagen which strengthens the connective tissue. This strength is affected by age, pathology, etc. Table 3.1 present tensile strength, amount of collagen and elastin in the different tissues. Collagen fibers can carry tension loads and the stretched collagen can keep the integrity and function of organs. If collagen is heated, they shrink due to breakdown of the crystalline structure. As an example, if a

mammalian collagen gets heated to 65 degree centigrade, its length reaches to about one-tens of its original size [Fung, 1993].

Elastin is a kind of protein too which connective tissue extracellular matrix is mainly composed of. Elastin can be found in lung, skin, ligamenta flava of cervical spine. Some of the soft tissues have five times more elatin than collagen.

Elastin has long flexible molecules which are built in a three-dimensional network like rubbers. This feature lets elastin to be stretched around two and half times of its original length where it is not under a load. Similar to Elastin, glycine comprises one third of the elastin total amino acids. But, collagen molecules have more hydroxyproline and proline than elastin.

Entropic elasticity of elastin affects directly on its mechanical behavior. The entropy of elastin changes due to deformation as a result random molecular positioning like rubbers. In elastin, as the entropy decreases, the internal energy gets increased [Holzapfel, 2000-b]. Elastin shows linear elastic behavior while it exposes a small amount of relaxation when the stress does not change with time. Collagen shows more relaxation behavior.

Table 3.1: Mechanical properties [Fung, 1993] and associated biochemical data [Woo et al. 1985] of some representative organs mainly consisting of soft connective tissues [Holzapfel, 2000-a].

Material	Ultimate tensile strength (Mpa)	Ultimate tensile strain (%)	Collagen (%dry weight)	Elastin (% dry weight)
Tendon	50-100	10-15	75-85	<3
Ligament	50-100	10-15	70-80	10-15
Aorta	0.3-0.8	50-100	25-35	40-50
Skin	1-20	30-70	60-80	5-10
Articular Cartilage	9-40	60-120	40-70	-

3.2. General mechanical characteristic of soft tissues

Fibers in soft tissues are lined up in different directions, so soft tissue shows anisotropic behavior. In addition, their material composition is not same at different locations. Therefore they are non-homogeneous materials too. The soft tissues exhibit nonlinear properties when they are under tension load. Also, their stiffness changes with variation in strain rate too. Big deformation without failure can be seen on soft tissue. This is a significant difference of the soft and hard tissues.

A typical stress-strain curve of a soft tissue in tension can be seen on figure 3.1. The figure shows how the fibers inside the soft tissue get straightened as the strain increases.

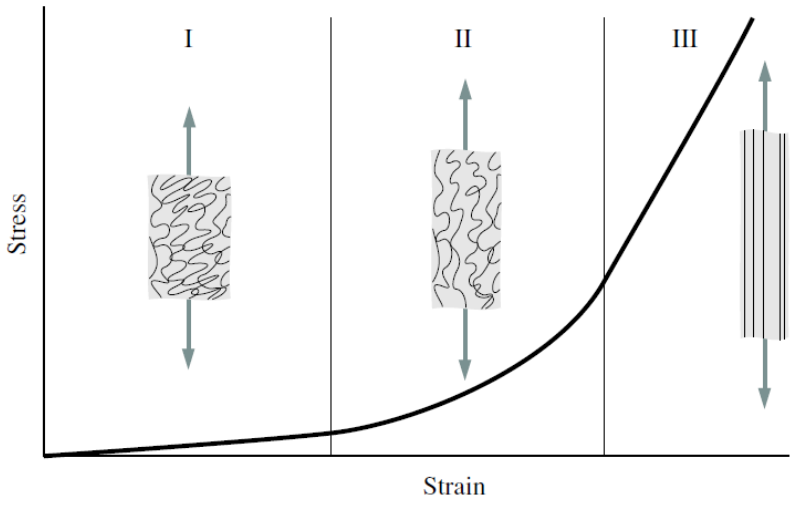

Figure 3.1: Schematic diagram of a typical (tensile) stress-strain curve for skin showing the associated collagen fiber morphology [Holzapfel, 2000-a].

To better understand the behavior of the soft tissue, the stress-strain curve can be divided in to three zones.

In the first zone of the stress-strain curve, the amount of the stress is very low, and collagen fibers look wavy and still are in un-stretched condition. The soft tissue exhibits approximately isotropic behavior. Significant deformation is resulted from small amount of stress while the collagen fibers are not stretched yet. The stress-strain curve is nearly linear in this area and modulus of elasticity is around 0.1Mpa to 2.0 Mpa. Also, they behave relatively isotropic and very soft.

In the second zone of the stress-strain curve, the fibers are aligning themselves with the load direction while they show resistance against the loads. The wavy fibers are stretched and due to that, they have interaction with the hydrated matrix of proteoglycans. As the stress increases, the fibers tend to change to smoother shapes. The stress-strain relationship is completely non-linear in this area and much more load is necessary to stretch the soft tissue in comparison to the condition in the first zone.

In the third zone, the wavy pattern of the fibers replaced with stretched nearly straight fibers which are aligned with the high loads. In this zone, the collagen can carry more loads and so, the stiffness of the soft tissue is higher at theses level of stresses. The stress-strain curve is nearly linear in this zone and applying more loads beyond the zone causes the failure of fibers and rupture of the soft tissue.

Some soft tissue like articular cartilage can carry the compressive load [Ethier and Simmons, 2007]. The compressive modulus of elasticity is ranging from 0.1Mpa to 2.0MPa similar to the tensile one. As the cartilage is a non-homogeneous material, this elasticity varies even in different locations of a small single joint cartilage. Many tests have been done and the results show that the elasticity are affected by the proteoglycan content and there is no role with amount of collagen. Proteoglycans can link

electromechanically the water inside the soft tissue together and so, they make the soft tissue capable of resisting against the compressive forces.

Another important material property of connective tissues is that they behave as a viscoelastic material. Connective tissue viscoelastic material can exhibit one of time-dependant responses, history dependant responses and hysteresis responses [Ethier and Simmons, 2007].

Time dependant responses: This is a creep behavior type response, where the deformation increases over the time while the load is constant, or the stress relaxes over the time while the deformation is constant [Figure 3.2]. The material behavior of these kinds of tissues is time dependent too. Their responses are different as the rate of stress or strain changes [Figure 3.2].

History dependant responses: If different stress paths are applied separately to a tissue while the final stress level at time T1 is same on the tissue for all of the stress paths, the relevant strains at time T1 are different as the result of different load history [Figure 3.3].

Hysteresis responses: If a load is applied to a viscoelastic tissue and then the load is removed, the stress-strain curve does not follow the same curve and this feature indicates that internal energy of the system is decreased when unloading is happened. The loading-unloading stress strain curves look as a hysteresis loop [Figure 3.2].

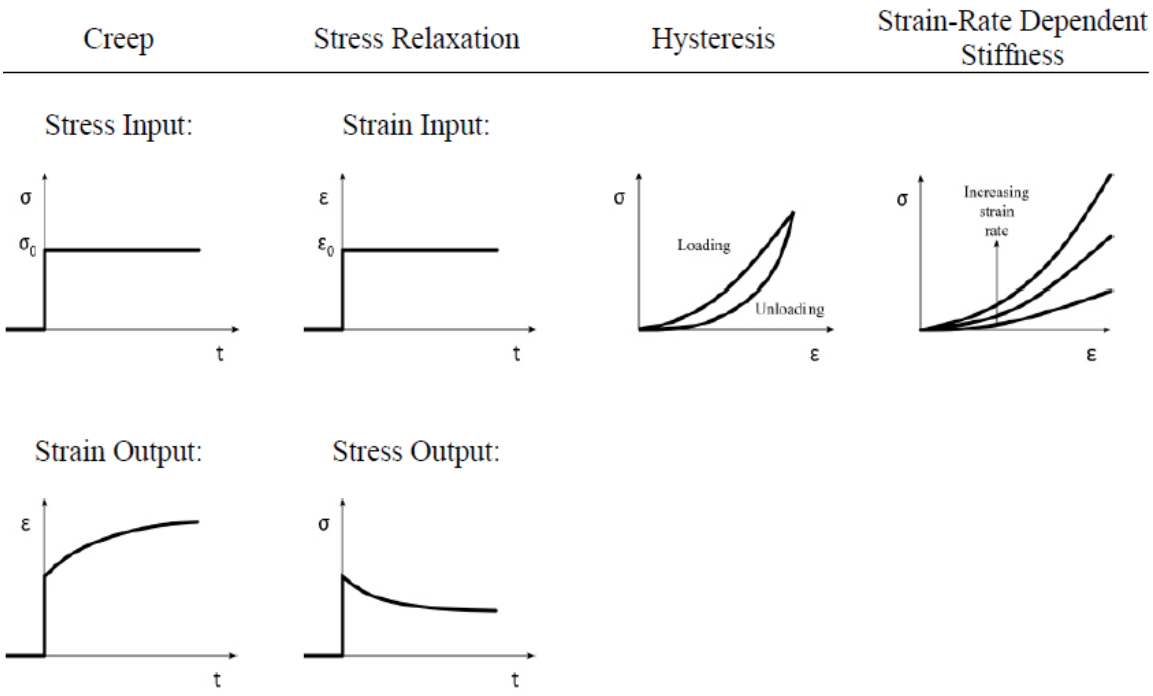

Figure 3.2: Different visco-elastic material behaviors attributed to the soft tissues [Troyer 2010]

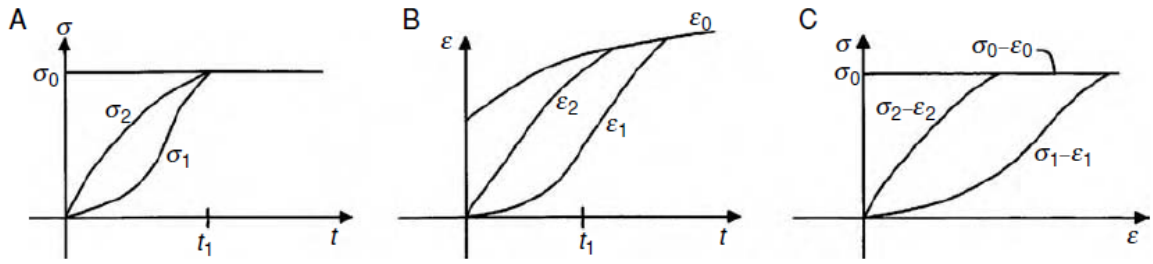

Figure 3.3: Another visco-elastic material behavior attributed to the soft tissues which is a stress history dependent material behavior: A shows three different stress paths where all have the same amount at time t1, B shows the strains are not same at t1, C presents the stress-strain curves are different for the three stress paths [Ethier and Simmons, 2007]

Chapter 4

Multibody dynamic analysis definitions and MD ADAMS ©

4.1 Introduction

A mechanism as a mechanical system can be very simple like a four bar linkage or relatively complex like a robot [Zwiers 2001]. In every kind of mechanical system, there are a series of bodies which all or some of them are able to have a relative motion to another one. To analyze this system, it is important how the bodies are joined together and how the forces are applied to the system elements. In simplest way, a multi-body system does not have flexible bodies and the assumption is that they are all rigid. Also, this ideal system comprises of ideal joints too. To perform dynamic analysis, equation of motions should be used to explain the system. These equations will define the displacement, velocity and acceleration of the system elements.

4.2 Basic definitions

4.2.1 Rigid bodies

A rigid body can not deform or change the shape. This kind of body can have rotational and translational movements. Creation of rigid bodies requires formulations based on ordinary differential equations. But for flexible bodies, there is a need for higher order of these equations and one of the methods which is suitable for solving the equations is finite element analysis.

In reality there is no rigid body, however for some applications this assumption is

acceptable like robots. This simplification can help a lot to create the model easier.

4.2.2 Degree of freedom

To analysis a mechanical system, at first it is necessary to identify the number of degree of freedom of the system. This system has many elements which are connected together by different kind of joints, springs and/or dampers elements. The number of independent coordinates that explain the configuration of a system is call degree of freedom. For a 3 dimensional system, each body has six degree of freedom. Therefore, a system which is composed of n bodies has 6n, called n_v, coordinates. However some of these coordinates are dependant and they are constrained by joints. The constraint equations define mathematically these conditions.

The number of degree of freedom for a system which has n_c independent constraints and n_v total coordinates is equal to [Zwiers 2001]:

$$n_{Dof} = n_v - n_c \qquad (1)$$

If number of degree of freedom is less than zero, the system is over constrained. If it is zero, the system is called a non-movable system and if it is bigger than zero, the system is a resolvable mechanism.

Based on the above definition, the number degree of freedom has the same meaning as the number of independent coordinate which can explain the configuration of the system.

4.2.3 Type of joints

As mentioned before, joints and force elements connect the bodies of a mechanism. The joints constrain the motion of the element in certain directions and so, they reduce the

degree of freedom of the system. However, force elements such as dampers or springs impose some limitations on the movement and they do not decrease the degree of freedom of the system.

On figure 4.1 some of the joints are presented.

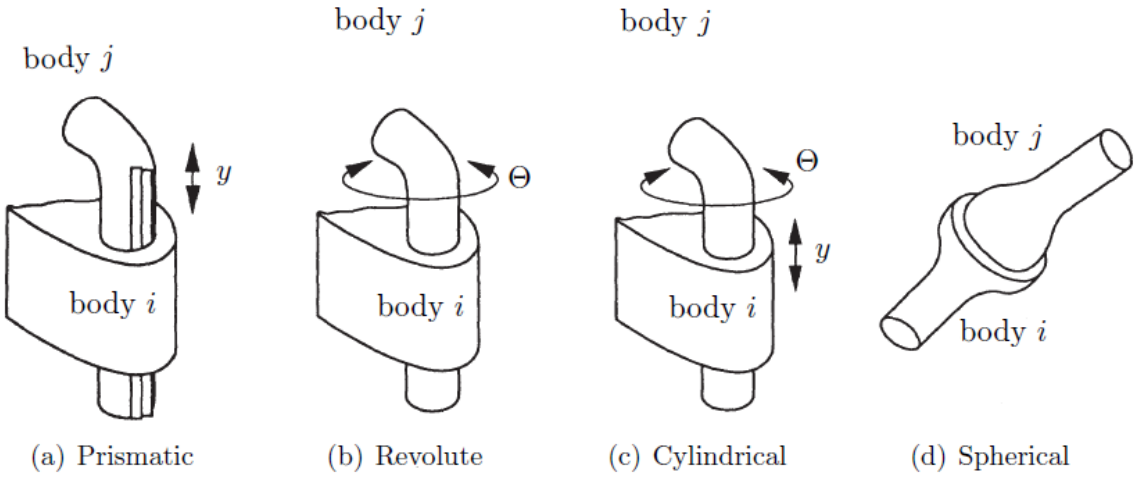

Figure 4.1: Some types of joints [Shabana, 1994]

4.3 Analysis of Mechanical Systems

4.3.1 Type of Analysis

The analysis can be conducted in static condition which is for a stationary system or in dynamic situation where the system is moving and its behavior is time dependant. For the moving system, two kinds of analysis are desired, kinematic and kinetic analysis. In kinematic analysis, the path of the motion of each element is the main concern of the analysis; and the forces, velocities and accelerations are not calculated for any of the system components. In contrary, the kinetic analysis which is much more complex to perform, and the goal is to calculate displacements, velocities, accelerations and forces. To perform kinetic calculation, mathematically second order differential equations should

be used to represent the system. There are two different types of analysis to investigate kinetic of a system, the first one is forward dynamic and the second one is inverse dynamic. In forward analysis, the motion of the system components, as the unknown of the system, is calculated using the differential equations with incorporating the external forces where they are the known parameters. In reverse dynamic, there is an assumption for the motion of the system and then the loads are calculated in order the system to follow that motion.

4.3.2 Newton-Euler equation

In general there are three groups of forces in a system, as internal, external and inertia forces. Inertia forces are the function of mass, shape of the system elements, velocity and acceleration. In static analysis, these forces are equal to zero. The definition of a joint makes it possible to calculate the internal forces between two bodies which are connected together. The external forces are imposed forces or torques, gravity forces, spring and damper forces, and actuator forces.

Newton-Euler equations for a constrained system can be written as [Zwiers 2001]:

$$M\ddot{q} = g + g_c \qquad (2)$$

In equation (2), $\ddot{q}$ is a 6n x 1 matrix including the translational and rotational accelerations of the system components where n is the number of the components. g_c and g are internal and external forces respectively. Matrix M refers to mass matrix which includes mass and mass moment inertia of the system components. Mass matrix can be written as the following with the assumption of local coordinate systems are positioned at the mass center of the components [Zwiers 2001]:

$$M = blockdiag[M_1, M_2, ..., M_n] \qquad \text{With} \qquad M_i = \begin{bmatrix} m_i I & 0 \\ 0 & J_i \end{bmatrix} \qquad (3)$$

In equation (3), where M_i is the mass of component *i*, *I* is a three by three identity matrix, *Ji* is the global moment of inertia of component *I*.

By applying the Lagrange multipliers principle, it can be induced that the internal forces which are result of the reaction forces at the joints are as follows [Zwiers 2001]:

$$g_c = D^T \lambda \qquad (4)$$

In equation (4), *D* is the Jacobian constraints matrix and λ is a vector which its content is the Lagrange multipliers.

The equation of the motion can be written as [Zwiers 2001]:

$$M\ddot{q} - D^T \lambda = g \qquad (5)$$

The equation (5) can be mentioned in matrix form which is called complete set of motion equations and is written as the following one [Zwiers 2001]:

$$\begin{bmatrix} M & -D^T \\ D & 0 \end{bmatrix} \begin{bmatrix} \ddot{q} \\ \lambda \end{bmatrix} = \begin{bmatrix} g \\ \gamma \end{bmatrix} \qquad (6)$$

In more generalized case, when bodies are flexible, rather than rigid, the equation of the motion can be written as [Shabana, 2005]:

$$M\ddot{q} + Kq + C_q^T \lambda = Q_e + Q_v \qquad (7)$$

In equation (7), k is the system stiffness matrix, *Cq* is equivalent to *D* at the above, *Qe* and *Qv* are external and coriolis forces respectively. This equation can be written in matrix form as the following one [Shabana, 2005]:

$$\begin{bmatrix} m_{rr} & m_{rf} \\ symmetric & m_{ff} \end{bmatrix} \begin{bmatrix} \ddot{q}_r \\ \ddot{q}_f \end{bmatrix} + \begin{bmatrix} 0 & 0 \\ 0 & K_{ff} \end{bmatrix} \begin{bmatrix} q_r \\ q_f \end{bmatrix} + \begin{bmatrix} C_{qr}^T \\ C_{qf}^T \end{bmatrix} \lambda = \begin{bmatrix} (Q_r)_v \\ (Q_f)_v \end{bmatrix} \qquad (8)$$

The subscripts r is the reference coordinate system and f is the elastic coordinate system. Figure 4.1 shows a system of two bodies which are connected together using a spring, actuator and a damper. R and u refer to displacement vector from global and local coordinate systems respectively, and p is the insertion points of those parallel force elements.

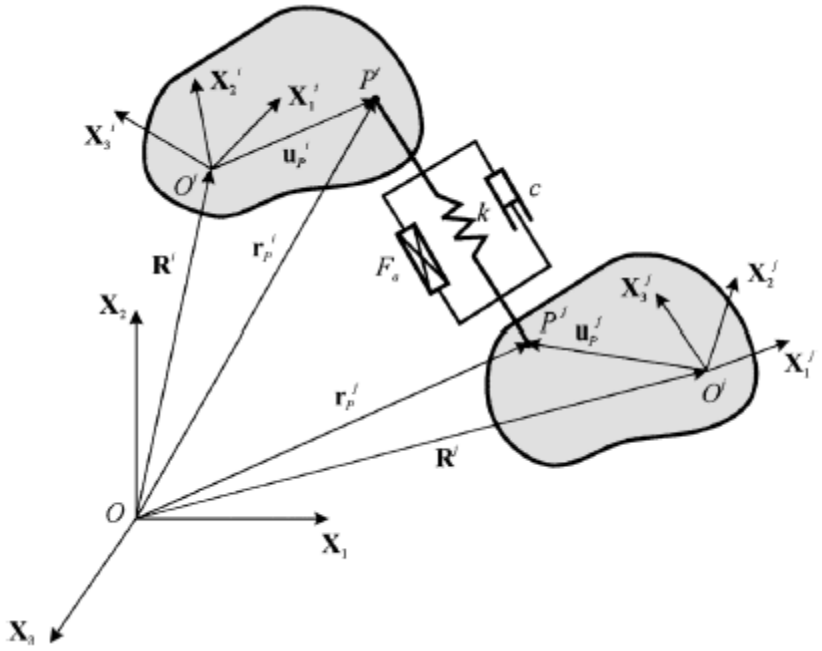

Figure 4.2: Force elements such as spring, damper, actuator [Shabana, 2005]

4.4 MD ADAMS ©

MD ADAMS is protected by copyright and licensed from MSC.Software suppliers. This software is an advanced software which is capable of solving complex multibody

problems for static, quasi-static and dynamic conditions. It helps to investigate the moving parts dynamics and also to improve the performance of the mechanical system.

The main features of ADAMS are as follows:

- The virtual model can be created inside the software environment or imported from the other software
- It has a strong library of different joints and constraint to define the connectivity of the system bodies
- Internal and external forces can be defined in order to represent the mechanical system operating environment
- Both 2D and 3D contact can be defined
- It is possible to create parametric variable and to optimize the function of the system by defining the targets
- Non-linear results can be obtained for complex problems with long time spans.

4.5 How ADAMS solves the dynamic problems?

Adams has a predictor-corrector type solver [Madsen 2007]. Time steps are calculated by estimation of the next step based on the number which is used in previous step, and then it corrects this estimation based on a set of extended equations. Adams follows four phases for each solver step when it is simulating a dynamic problem. The first phase is called predictor phase. At this phase, the system state at the next time-step is estimated. The second one is corrector phase. The estimated state is corrected during this phase. Third one is an error checking phase. At this phase, ADAMS finds the solution of the set of equations which is closest to the previous solution. The last phase is preparation phase

which make the solver ready for the next time step estimation.

Chapter 5

Creating the cervical spine multibody dynamic model

5.1 Introduction

Qualitative information about anatomy of the cervical spine can be found in many papers and books [Dvorak et al., 1991, Sherk et al. 1989, Johannes, Verlag, 1993, Goel, 1990, Lowery, 2001, Panjabi et al 1992]. However, the cervical spine vertebra has many details in the geometry and just some of these features in geometry of the vertebra have been measured in a single paper till now. So, all of the reports have been put together to extract the missing geometry parameters [Panjabi et al. 1993, Xu et al. 1999]. There is no research that has quantified the geometry information for all of the vertebrae which are from C1 to C7 in a single paper. One reason could be that the two upper most vertebrae, C1 and C2, have different shapes in comparison to the other vertebrae. To create a CAD data for atlas and axis, there are some paper which have presented the necessary measurements [Doherty, Heggeness, 1994 and 1995, Dong et al., 2003, Naderi et al. 2004, Schaffler, 1992]. The height of intervertebral discs and their relative positions to the connecting vertebrae are two parameters which are very important to model the cervical correctly. The parameters which are required to position the adjacent cervical spine vertebrae can be found in a research done by Nissan et al., 1986. This research depicts the major information about modeling the cervical spine discs.

5.2 Parameters Defining Vertebrae in Cervical Spine

5.2.1 Parameters Defining Atlas

Since obtaining the required information from a single paper which presents the measurements of the vertebrae is not possible, so, several research works in this area have been put together to extract the crucial information. In addition to the parameters which are required to model facet joints, six other parameters (ARH, ART, PRH, PRT, ODS and FDL) should be defined too. This information is presented completely by Doherty et al., 1994.

Dong et al., 2003 has performed a measurement study which more defines the atlas lateral mass geometric parameters. As a result, Dong et al., 2003 and Panjabi et al., 1993 research studies are chosen to obtain the atlas facet joint geometry parameters for modeling.

Atlas and the rest of the vertebrae have inferior articular facets which their CAD data are created as elliptical shapes. Panjabi et al., 1993 has illustrated all the parameters which identify the geometry of the cervical spine facet joints. The required parameters which explain the atlas geometry are present on figure 5.1. Also, table 5.1 shows all of the reported measurements for defining the geometry of atlas.

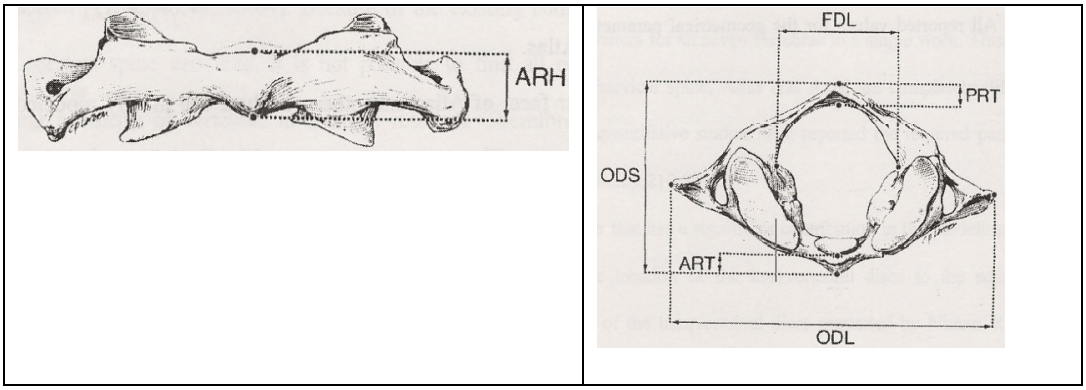

Figure 5.1: Atlas dimensioning parameters [Dong et al., 2003]

Parameter	Mnemonic	Value (mm)
Anterior Ring Height (mm)	ARH	16.74
Posterior Ring Height (mm)	PRH	11.09
Anterior Ring Thickness (mm)	ART	11.84
Posterior Ring Thickness (mm)	PRT	12.77
Foramen Diameter Lateral (mm)	FDL	30.99
Overall Diameter Sagittal (mm)	ODS	47.98
Superior Facet Width (mm)	FCWS	14.30
Superior Facet Height (mm)	FCHS	25.25
Superior Facet Depth (mm)	FCDS	6.78
Superior Facet CAX (degree)	CAXS	32.65
Superior Facet CAY (degree)	CAYS	-59.41
Lateral Mass Height (mm)	LMH	18.82
Inferior Facet CAX (degree)	CAXI	-37.1
Inferior Facet CAY (degree)	CAYI	49.4
Inferior Facet Width (mm)	FCWI	16.4
Inferior Facet Height(mm)	FCHI	17.85

Table 5.1: The parameters of Atlas [Dong et al., 2003]

5.2.2 Parameters Defining Axis

Three regions can be distinguished on the second cervical spine vertebra as the main body, dens and the posterior part of the vertebra. Axis looks similar posteriorly to the other vertebra from C3 to C7, but it has a unique feature anteriorly. The front part of axis can be considered in two sections, the first is the main body of the vertebra and the second one is the dens. To define the inferior endplate of axis, those parameters which are used for the other vertebrae can be considered here too due to similarity. But some

other parameters are required to define dens geometry and the main body of the vertebra. There is another research which is done by Schaffler et al., 1992 and it includes enough information to model the front part of the vertebra. All parameters which are used to create the CAD data of the anterior part of the axis are presented in figure 5.2 and table 5.2. As the posterior parts of the vertebra and its inferior endplate have similarity with the rest of the lower vertebrae, their information is shown in the next sections.

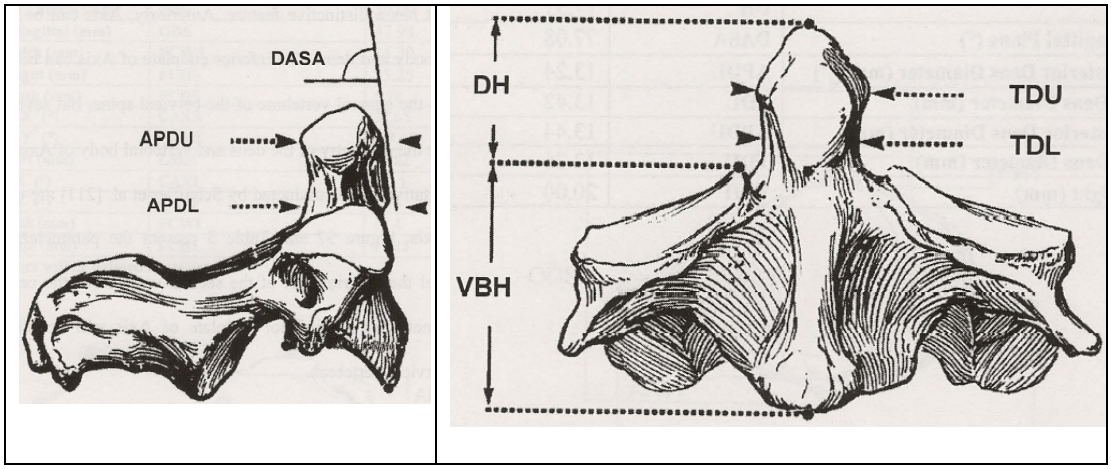

Figure 5.2: Axis dimensioning parameters [Schaffler et al., 1992]

Table 5.2: The parameters of Axis [Schaffler et al., 1992]

Parameter	Mnemonic	Value (mm)
Dens Height (mm)	DH	17.31
Angles of Dens in Sagittal Plane (degree)	DASA	77.08
Lower Anterioroposterior Dens Diameter (mm)	APDL	13.24
Lower Transverse Dens Diameter (mm)	TDL	13.42
Upper Anterioroposterior Dens Diameter (mm)	APDU	13.44
Upper Transverse Dens Diameter (mm)	TDU	12.26
Vertebral Body Height (mm)	VBH	20.00

5.2.3 Parameters Defining Vertebrae of the Middle and Lower Regions (C3-C7)

The vertebrae C3 to C7 look very similar to each other. Each of them has a main vertebral body and is connected to the adjacent one where there is an intervertebral disc

between a pair of joined vertebrae. The upper surface of the main body is concave from side and convex from the front. The lower surface of the main body is convex from side and concave from the front. The posterior area of the spinal disc is thinner than the anterior area. Some of the researches have illustrated the result of measurements of C3 through C7 [Francis, 1995, Liu et al. 1982, Panjabi et al. 1992, Tan et al. 2004]. The research which is done by Panjabi et al. 1992 has many details and is the latest one in this regard. However, the measurements in the area of facet joints and posterior region are not complete because of complexity of the vertebrae in these places. Figure 5.3, table 5.3 and table 5.4 present the results of Panjabi's work.

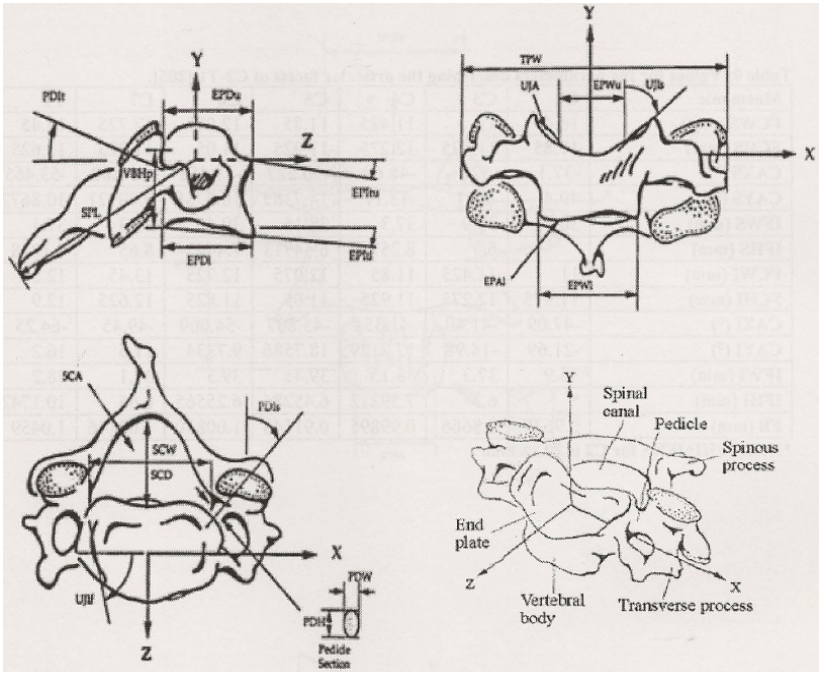

Figure 5.3: Different views of a cervical spine vertebra [Panjabi et al. 1992]

Table 5.3: Parameters describing the vertebral body of C2-T1 [Farsa, 2006]

Parameter	Mnemonic
End Plate Depth Upper	EPDU
End Plate Width Upper	EPWU
Uncovertebral Joint Inclination Frontal Plane Upper	UJIFU
Uncovertebral Joint Inclination Sagittal Plane Upper	UJISU
Uncovertebral Joint Area Upper	UJAU
End Plate Anterior Radius Upper	EPARU
End Plate Depth Lower	EPDL
End Plate Width Lower	EPWL
Uncovertebral Joint Inclination Frontal Plane Lower	UJIFL
Uncovertebral Joint Inclination Sagittal Plane Lower	UJISL
Uncovertebral Joint Area Lower	UJAL
End Plate Anterior Radius Lower	EPARL
Vertebral Body Height	VBHP

Table 5.4: Values for the parameters describing the vertebral body of C2-T1 [Panjabi et al. 1992, Panjabi et al. 1991-b]

Mnemonic	C2	C3	C4	C5	C6	C7	Tl
EPDU(mm)	-	15	15.45	15.55	17.15	18.3	18.5
EPWU(mm)	-	15.8	17.2	17.25	18.95	21.9	24.5
UJAU (mm^2)	-	43.6	38.95	42.85	53.45	42.15	28.34
UJIFU (degree)	-	76.6	78.9	83.1	94.45	110.9	113.40
UJISU (degree)	-	38.7	40	34.5	40.8	47.3	0
EPARU (mm)	-	17	17	17	17	17	17
EPDL(mm)	15.3	15.45	15.55	17.15	18.3	17.65	19.7
EPWL(mm)	16.65	17.2	17.25	18.95	21.9	23.4	27.8
UJAL (mm^2)	18.75	22.45	24.5	28.85	24.7	21.2	32.55
UJIFL (degree)	77.5	78.9	83.1	94.45	110.9	113.4	113.40
UJISL (degree)	63.7	47.8	47.8	45	49.2	59.8	0
EPARL(mm)	17.16	17	17	17	17	17	17
VBHP(mm)	-	11.6	11.4	11.4	10.9	12.8	14.1

Panjabi et al., 1993 did a similar research to quantify the geometry of the cervical spine facet joints. Table 5.4 and table 5.5 present the result of this work.

Table 5.4: Parameters describing the articular facets of C2-T1[Farsa, 2006]

Parameter	Mnemonic
Facet Width Superior	FCWS
Facet Height Superior	FCHS
Card Angle about X-axis Superior	CAXS
Card Angle about Y-axis Superior	CAYS
Interfacet Width Superior	IFWS
lnterfacet Height Superior	IFHS
Facet Width Inferior	FCWI
Facet Height Inferior	FCHI
Card Angle about X-axis Inferior	CAXI
Card Angle about Y-axis Inferior	CAYI
lnterfacet Width Inferior	IFWI
Interfacet Height Inferior	IFHI
Facet Line Distance to Vertebral Wall	FB

Table 5.5: Parameters describing the articular facets of C2-T1 [Panjabi et al. 1993]

Mnemonic	C2	C3	C4	cs	C6	C7	Tl
FCWS(mm)	16.4	11	11.425	11.85	12.075	12.725	13.45
FCHS(mm)	17.85	11.975	12.275	11.925	11.05	11.825	12.625
CAXS (degree)	-37.1	-52	-48.60	-50.227	-53.453	-59.880	-53.465
CAYS (degree)	49.4	-20.1	-13.17	14.7385	16.6788	9.09921	10.8672
IFWS (mm)	30.3	35.9	37.3	38.15	39.45	39.3	37.1
IFHS(mm)	*	6.3	8.25787	6.54713	7.44434	8.65	8.1258
FCWI(mm)	11	11.425	11.85	12.075	12.725	13.45	12.55
FCHI(mm)	11.975	12.275	11.925	11.05	11.825	12.625	12.9
CAXI (degree)	-47.09	-41.40	-41.354	-45.807	-54.009	-49.45	-64.25
CAYI (degree)	-21.69	-14.98	17.2129	18.7586	9.7334	11.5	16.2
IFWI(mm)	35.9	37.3	38.15	39.45	39.3	37.1	28.2
IFHI (mm)	*	6.3	7.59212	6.45286	6.25565	8.65	10.1742
FB (mm)	0.9637	0.8666	0.99895	0.91548	1.00830	1.09146	1.0459

Figure 5.4 illustrates card angles and linear dimensions to clarify size, positioning and angular orientation of the facet joints.

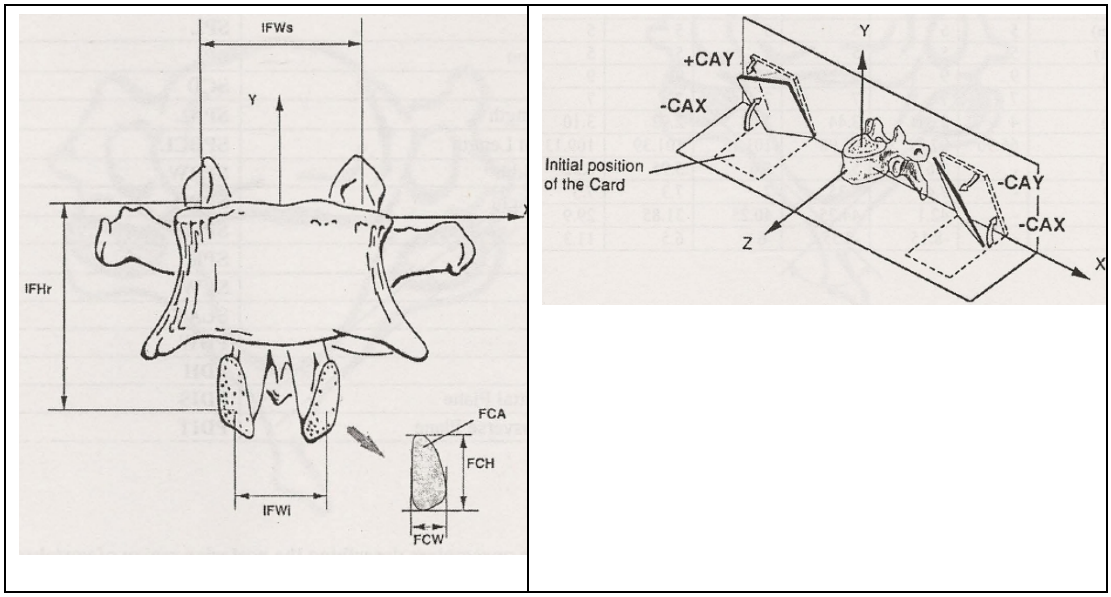

Figure 5.4: Facet joint measurements, orientations, in terms of planar and card angles [Panjabi et al. 1993]

The study which is done by Xu et al., 1999 presents the geometrical dimensions of the cervical spine laminas (Figure 5.5). This information, which is shown on table 5.6 and table 5.7, with the previously mentioned ones give sufficient data of lower and middle regions of cervical spine vertebrae geometry. As mentioned earlier, the posterior area of these vertebrae has the similar shape as the same area on axis (C2).

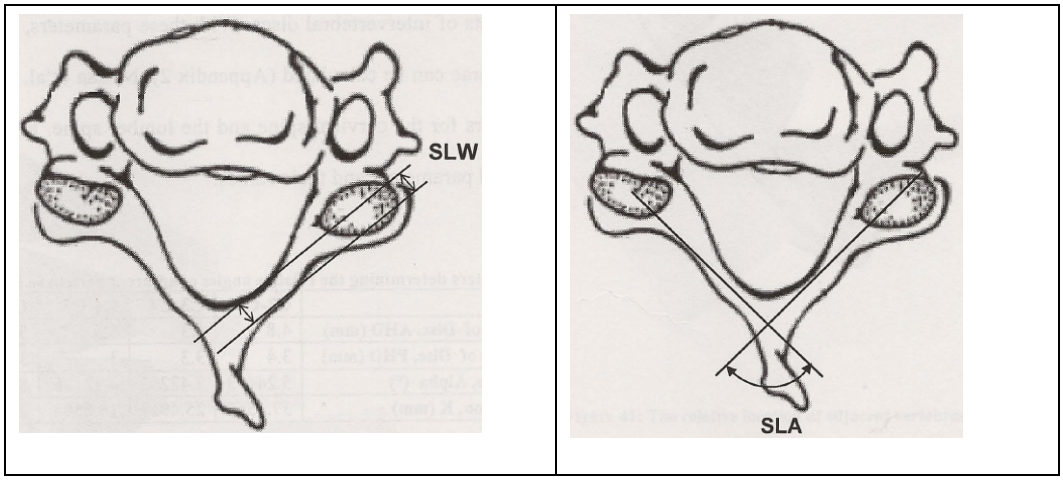

Figure 5.5: Parameters describing the posterior region of vertebra C2-T1 [Xu et al. 1999]

Table 5.6: Parameters describing the posterior region of vertebra C2-T1 [Farsa, 2006]

Parameter	Mnemonic
Spinal Process Length	SPL
Spinal Process Inclination	SPI
Spinal Canal Depth	SCD
Spinal Process Back Length	SPBL
Spinal Process Back Cut Length	SPBCL
Spinal Process Back Width	SPBW
Spinal Process Back Height	SPBH
Spinal Process Width	SPW
Spinal Process Height	SPH
Spinal Lamina Width	SLW
Spinal Lamina Angle	SLA
Pedicle Width	PDW
Pedicle Height	PDH
Pedicle Inclination Sagittal Plane	PDIS
Pedicle Inclination Transverse Plane	PDIT

Table 5.7: Values of parameters describing the posterior region of vertebra C2-T1 [Xu et al. 1999, Panjabi et al. 1992]

Mnemonic	C2	C3	C4	C5	C6	C7	T1
SPL(mm)	33.7	34.4	33.6	35.4	41.5	49.6	50.1
SPI (mm)	16.88	27.39863	25.27285	21.23229	17.02374	21.138	25.55
SCD (mm)	21	16.2	17.7	17.4	18.1	15.2	16.4
SPBL(mm)	1	1	1	1	1	1	1
SPBCL (mm)	4	4	4	4	4	4	4
SPBW(mm)	5	5	5	5	5	5	5
SPBH(mm)	5	5	5	5	5	5	5
SPW(mm)	9	9	9	9	9	9	9
SPH(mm)	7	7	7	7	7	7	7
SLW(mm)	4	3.31	3.44	3.08	2.92	3.10	3.44
SLA(degree)	66.90	97.32	95.98	101.13	101.39	109.13	104.03
PDW(mm)	-	5.6	5.4	5.6	5.95	6.55	8.45
PDH(mm)	-	7.4	7.35	7	7.3	7.5	9.6
PDIS (degree)	-	42.1	44.25	40.25	31.85	29.9	27.05
PDIT(degree)	-	-8.15	-7.55	-6	6.5	11.3	7.55

In addition to extracting the required the geometry data to model C1 to C7, it is necessary to find a paper which has enough parameters to describe completely the first thoracic spine vertebra (T1). Panjabi et al., 1991 literature has quantified these parameters for T1.

The previous data have illustrated only the dimensions of each vertebra, however it is crucial to identify to relative position of vertebrae in translational and rotational relative to each other, to create the model as an assembly while it helps to determine the thickness of the cervical spine discs at the back and at the front. These measurements have been done for the lumber and cervical spine by Nissan et al., 1986. The required parameters are shown on figure 5.6 and table 5.8

Table 5.8: Parameters determining the relative angles of adjacent vertebra [Nissan, Gilad, 1986]

Parameter	C2-C3	C3-C4	C4-C5	C5-C6	C6-C7	C7-Tl
Anterior Height of Disc, AHD (mm)	4.8	5.3	5.5	5.4	5.2	4.7
Posterior Height of Disc, PHD (mm)	3.4	3.3	3	3	3.3	3.5
Calculated Angle, Alpha (degree)	5.2	7.4	9.2	8.0	5.95	4.09
Radius of Rotation, K (mm)	37.2	25.5	18.7	21.4	31.78	49

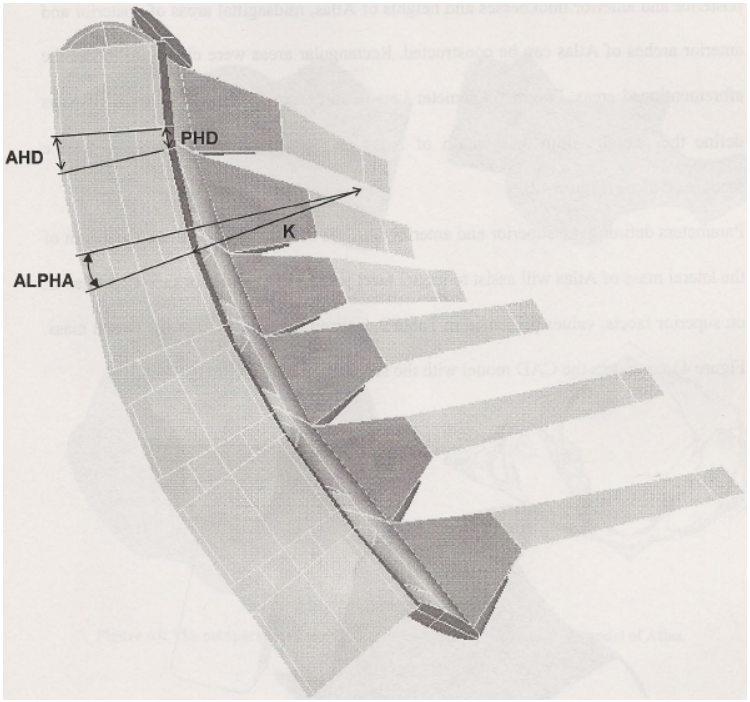

Figure 5.6: The relative location of adjacent vertebrae [Farsa, 2006]

5.3 Geometry in ADAMS

Farsa has used the above information to create the cervical spine CAD data. Then, this data was imported into ANSYS for his study. To perform this study, the CAD data in ANSYS was exported in igs format. However, this data could not be imported into ADAMS for the following reasons:

1- poor quality of surfaces in igs file

2- complexity in curvature of several surfaces

As a result, the whole CAD data was recreated again in CATIA software to solve the above problems. Then, the CAD data was imported into ADAMS. Figure 5.7 and Figure 5.8 demonstrate the original and regenerated CAD data.

5.4 Material data

In the ADAMS model, all vertebrae act as solid materials, so to perform the analysis, only mass, center of mass and moment of inertia should be defined for each vertebra. The ligaments and discs were modeled as spring-dashpot and six degrees of freedom bushing type spring-dashpot respectively, and their force-deflection characteristics and the damping ratio were the input for this model.

5.4.1 Vertebra data

The geometry of C1 through T1 is fairly close to the size of real vertebra. Therefore, in ADAMS model, only the right density was defined for each vertebra to have the right mass as presented by Jager, Johannes, 1998.

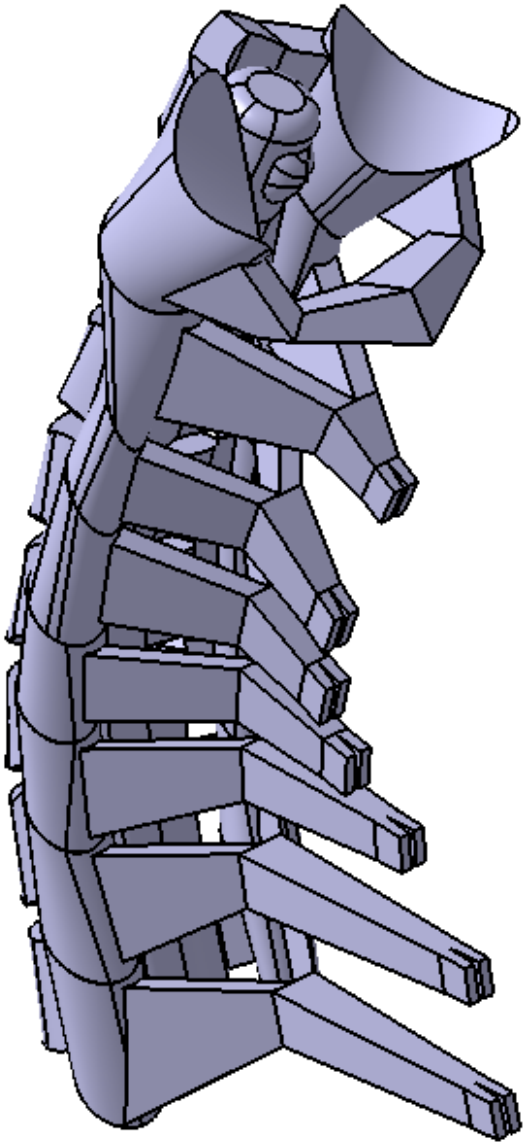

Re-created CAD data

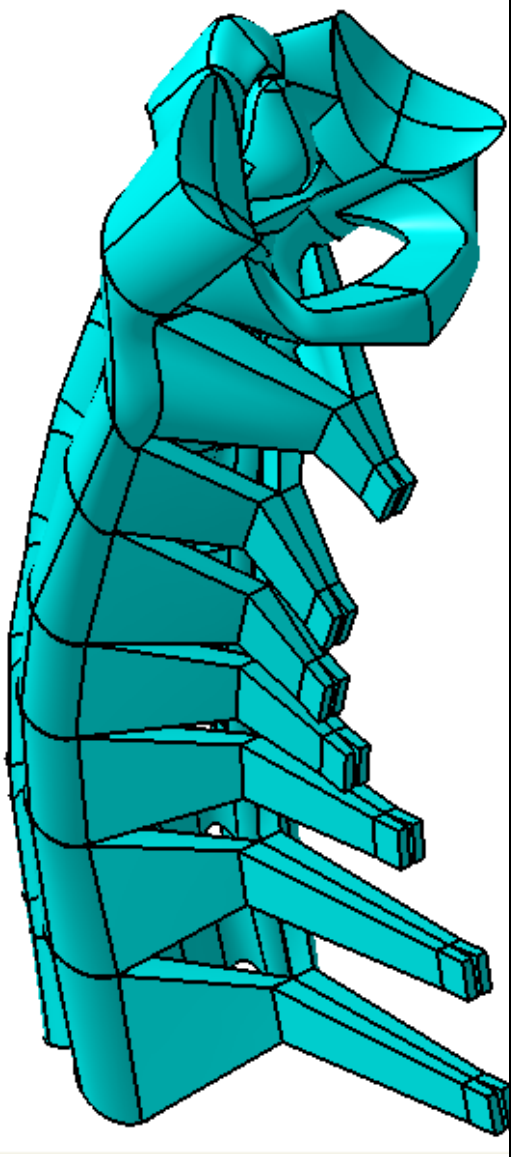

Original CAD data

Figure 5.7: Comparison of re-created and original CAD data

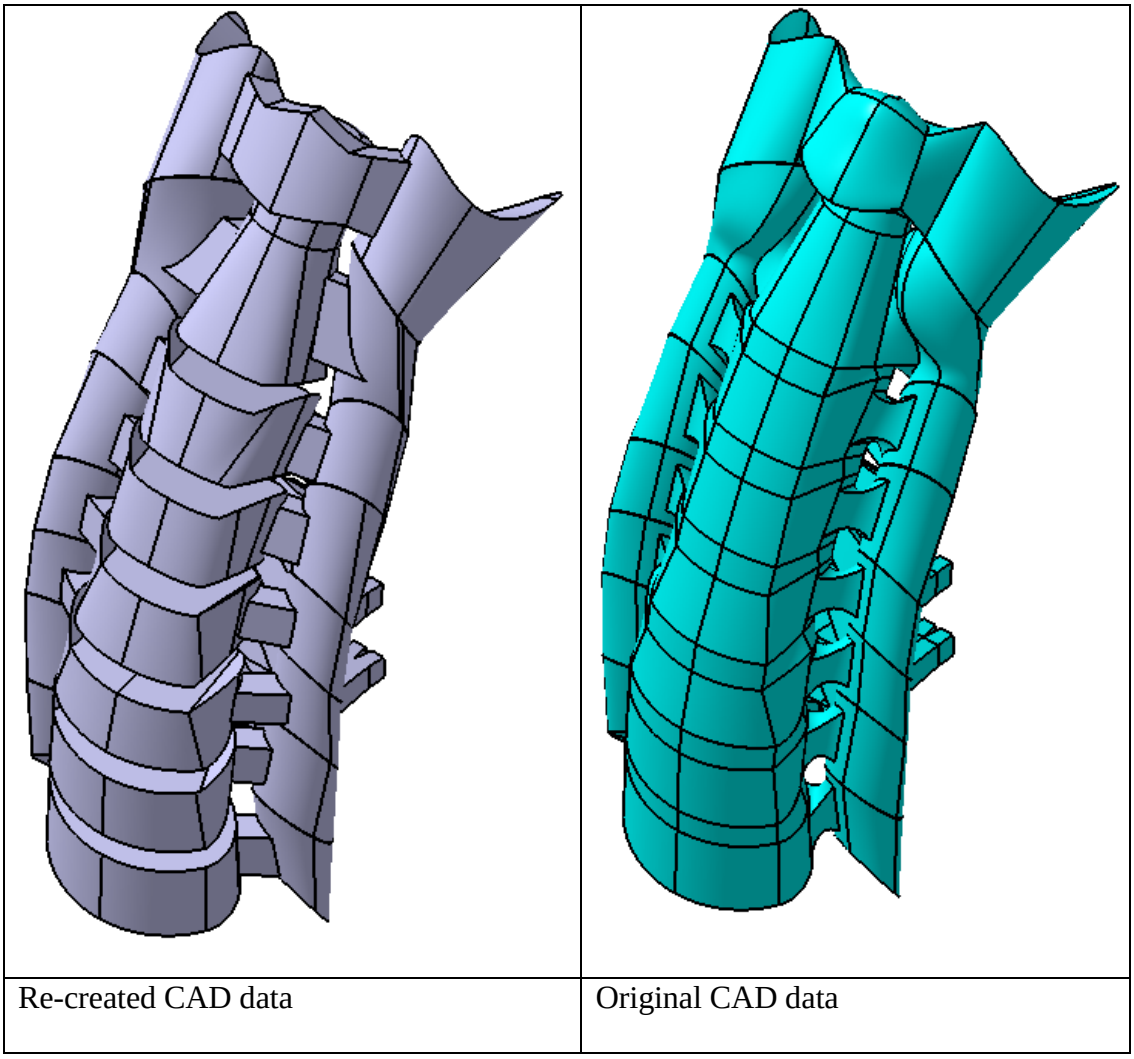

Re-created CAD data	Original CAD data

Figure 5.8: Comparison of re-created and original CAD data (back view)

The moment of inertias and mass centers were calculated by Adams software internally during the analysis. However, as there is no representative CAD data for skull; the mass, mass center and moment of inertia were input in the model. Table 5.9 shows these quantities [Jager, Johannes, 1998].

A local cording system which is right handed is designated to each cervical spine vertebra body to identify the relative orientation and position of each body to its adjacent lower vertebra body (Figure 5.9).

Table 5.9: Inertial and geometric data of cervical spine vertebrae [Jager, Johannes, 1998]

			moment of inertia (kg. cm2)				coordinate system origin (mm)		gravity center position (mm)	
no.	name	mass (kg)	I xx	I yy	I zz	I xz	S x	S z	g x	g z
1	T1	-	-	-	-	-	0	0	-	-
2	C7	0.22	2.2	22	43	-	6.4	16.8	-8.2	0
3	C6	0.24	2.4	2.4	4.7	-	-2	18.4	-8.3	0
4	C5	0.23	2.3	2.3	4.5	-	-2.8	17.4	-8.1	0
5	C4	0. 23	2.3	2.3	4.4	-	-3.3	17.2	-1.9	0
6	C3	0.24	2.4	2.4	4.6	-	-4	17.8	-7.8	0
7	C2	0.25	2.5	2.5	4 8	-	-3.3	18.7	-7.7	0
8	C1	0.22	22	2.2	4.2	-	0	16.5	-7. 7	0
9	CO	4.69	181	236	173	71	-4	20	27	43 .0

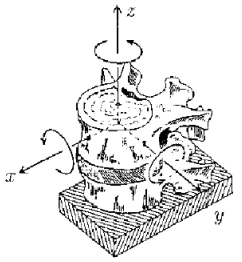

load	displ.	name	abbr.
$+F_x$	$+t_x$	anterior shear	AS
$-F_x$	$-t_x$	posterior shear	PS
$\pm F_y$	$\pm t_y$	lateral shear	LS
$+F_z$	$+t_z$	tension	TNS
$-F_z$	$-t_z$	compression	CMP
$\pm M_x$	$\pm \phi_x$	lateral bending	LB
$+M_y$	$+\phi_y$	flexion	FLX
$-M_y$	$-\phi_y$	extension	EXT
$\pm M_z$	$\pm \phi_z$	axial rotation	AR

Figure 2.4: Definition of coordinate system, loads and displacements. Drawing adapted from White and Panjabi [110].

Figure 5.9: Definition of local coordinate system [Jager, Johannes, 1998]

The global coordinate system of this model is the local coordinate system which is assigned to T1, where x, y and z are pointing forward, left and upward respectively. The origin of the lower vertebra local coordinate system is the reference to define the origin

of upper one by defining the parameters Sx, Sy, Sz which are measured using the lower vertebra coordinate system (Figure 5.10 and Table 5.9).The origin of each local coordinate system coincides with the mass center of the vertebra main body. This rule is for the vertebrae from C2 to T1. C1 does not have a main body like the lower vertebrae, so, its origin is positioned at the upper part of the dens. The origin of the local coordinate system of C0 is located above and a little back to the occipital condyles where it is apparently the rotation center of the head around C1.

The angle φ_y defines the relative angular orientation of each body about the y axis of lower cervical spine vertebra body. These relative positions illustrate the backward C shape of the cervical spine. Figure 5.10 presents how the cervical vertebrae, T1 and the head are positioned relative to each other.

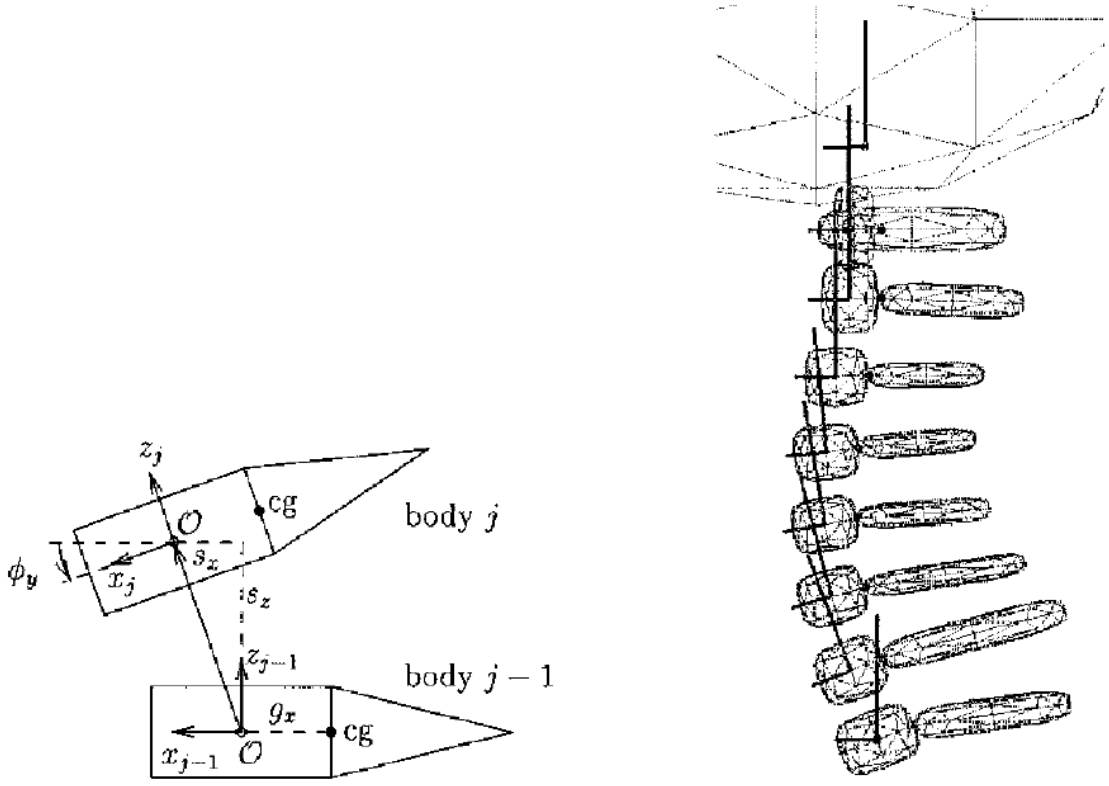

Figure 5.10: Definition of local coordinate system for each vertebra and its origin [Jager, Johannes, 1998]

5.4.2 Ligaments data

To create a mathematical model, it is necessary to extract the data of stiffness, elastic modulus and stress-strain curve as the important material properties. The tensile test has been done by Pintar et al 2001 to grab these properties. Human cadaver cervical spine samples are used to perform the tensile tests. They include isolated ligaments and bone-ligament-bone samples. To provide the ligament test sample, the ligaments should be removed from the spinal column and often it leads to damaging the structure and as a result the sample can not be mounted on the test fixture. However bone-ligament-bone samples are less likely to be damaged as there is no need for isolation from the other areas.

To perform the tests generally for a specific cervical spine vertebral level, all ligaments are separated carefully in order to measure accurately their resistances against the tension. There are some difficulties with providing the samples like separation of ligaments from the disc. It should be done by differentiating the ligaments fibers from the oblique positioned disc fibers. The vertebrae at the two ends of the ligaments are fixed and a six axis load cell is mounted at the distal end [Pintar et al 2001].

Finally the tensile test is conducted to obtain the load-deformation characteristic of the sample. Table 5.10 illustrates the stiffness of the upper cervical spine ligaments.

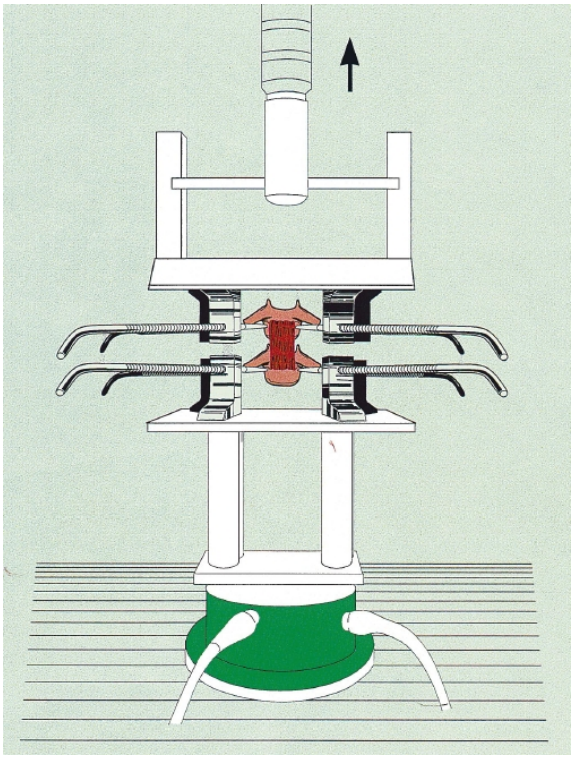

Figure 5.11: Schematic of an in situ bone-anterior longitudinal ligament-bone preparation for tensile tests. A six-axis load cell is placed below the specimen to ensure the uniaxial nature of force application [Pintar et al 2001].

Table 5.10: Upper cervical spine ligaments stiffness [Pintar et al 2001]

Biomechanical data of upper cervical spine ligaments (Mean SD)		
Spinal level	Type	Stiffness (N/mm)
OC-C1	JC	32.6 (28.0)
OC-C1	AA-OM	16.9 (32)
OC-C1	PA-OM	5.7 (0.4)
C1-C2	ALL	24.0 (11.7)
C1-C2	JC	23.3 (23.5)
C1-C2	LF	11.6 (11.0)
OC-C2	TM	7.1 (2.3)
OC-C2	APICAL	28.6 (29.0)
OC-C2	ALAR	21.2 (15.7)
OC-C2	CLV	19.0(0.2)

Pintar et al. 2001 has provided non-linear force-deflection data of all of C2-T1 ligaments which are incorporated into the current dynamic model. Also, for more accurate data of C1-C2 ligaments, the relevant C2-C5 ligaments force deflection curves were scaled by a suitable factor and then the new curves were used for C1-C2 ligaments in the multibody dynamic model. This scale factor is calculated by dividing the average stiffness of a ligament at C1-C2 level by this stiffness at C2-C5 level (Table 5.11). The average stiffness of C2-C5 ligaments can be seen on Table 5.11 [Pintar et al. 2001].

Table 5.11: Lower cervical spine ligaments stiffness [Pintar et al 2001]

Cervicsl spine ligaments material properties	
C2-C5	Stiffness (N/mm)
ALL	16.0 (2.7)
PLL	25.4 (7.2)
LF	25.0 (7.0)
ISL	7.74 (1.6)
C5-T1	
ALL	17.9(3.4)
PLL	23.0 (2.4)
LF	21.6 (3.7)
ISL	6.4 (0.7)

There is an important point about CF joints at C1-C2 and C0-C1 levels. The CF is often described as thin and loose, especially in the occipitoatlantal (C0-C1) and atlantoaxial (C1-C2) joints, but they function in restraining rotation of the joints [Brolin K., 2002]. However, this looseness is not quantified in any paper, so they were adjusted as 4mm, 0.5mm for C1-C2 and C0-C1 levels respectively.

All ligaments have visco-elastic behavior, and damping factor of 300 N.s/m is defined for them [Jager, Johannes, 1998]. Also, ligaments stiffness is zero when they are in compression.

In this study, the insertion points of ligaments are similar to the ones that farsa, 2006 has used in his FEA model for C1 to T1. However, some ligaments are added to this model to join the head to the cervical spine. Table 5.13 present the complete insertion points of upper cervical spine ligaments [Jager, Johannes, 1998].

Table 5.12: Ligaments insertion points [Jager, Johannes M. K. , 1998].

	origin (mm)				insertion (mm)			
ligament	body no.	x	y	z	body no.	x	y	z
Cl-C2 AM	7	6.3	0	0	8	7.8	0	0
Cl-C2 PM	7	-28.6	0	-0.7	8	-37.8	0	0
Cl-C2 CL	7	-4.1	±14.3	4.1	8	-3.9	±16.1	-5.5
C0-C1 AM	8	7.8	0	0	9	4.3	0	-2.6
C0-C1 PM	8	-37.8	0	0	9	-32.6	0	-4.3
C0-C1 CL	8	-8	±19.4	3.8	9	-4	±20.6	-9.3
C0-C2 ALAR	7	-1.2	±3.0	26.5	9	2.8	±13.3	-5.8
TL-left part	7	-6.7	0	15.6	8	-5.5	10.3	-0.9
TL -right part	8	-5.5	-10.3	-0.9	7	-6.7	0	15.6
TM-lower part	7	-7.7	0	0	7	-6.7	0	26.6
TM-upper part	7	-6.7	0	26.6	9	1.7	0	-2.1

The method of defining the coordinate system was explained in earlier pages.

The optimized force-deflection characteristics of ligaments data shown on Tables 5.13 are used in the multi-dynamic model. The units of force and deflections are N and mm respectively.

Tables 5.13: Ligaments force-deflection data for the dynamic model

C2-C5									
JC		ALL		PLL		LF		ISL	
def.	force	def.	force	def.	force	def.	force	def.	force
0	0	0	0	0	0	0	0	0	0
1.97	58.62	1.2	32	1.2	28	1.8	30	1.3	8.5
3.97	123.03	2.5	60	2.2	50	3.5	55	2.8	10
5.9	171.74	3.7	81	3.2	66	5.1	71	4.1	23
7.87	207.25	4.8	100	4.3	79	6.9	95	5.5	28
9.7	240.28	6	115	5	88	8	105	7	32

C5-T1									
JC		ALL		PLL		LF		ISL	
def.	force	def.	force	def.	force	def.	force	def.	force
0	0	0	0	0	0	0	0	0	0
1.95	61.23	1.31	26.96	1	18.75	1.84	28.60	1.34	10.08
3.84	112.75	2.71	49.96	2.01	39.06	3.70	61.79	2.68	17.43
5.76	156.80	4.05	78.11	3.03	60.94	5.57	98.55	4	23.65
7.71	198.61	5.40	103.08	4.07	82.19	7.48	123.06	5.32	30
9.63	226.24	6.76	120.13	5.09	94.69	9.34	146.55	6.68	34.98

OC-C2					
ALAR		TM		APICAL	
deflection	force	deflection	force	deflection	force
0	0	0	0	0	0
1	5.51	1	7.1	1	2.86
2	11.02	2	14.2	2	5.72
3	16.54	3	21.3	3	8.58
4	22.05	4	28.4	4	11.44

OC-Transvers Ligament	
CLV deflection	force
0	0
1	19
2	38
3	57
4	76

OC-C1					
JC		AA-OM		PA-OM	
deflection	force	deflection	force	deflection	force
0	0	0	0	0	0
1	4.89	1	13.689	1	5.7
2	9.78	2	27.378	2	11.4
3	14.67	3	41.067	3	17.1
4	19.56	4	54.756	4	22.8

5.4.3 Disc Properties

Intervertebral discs can carry loads and moments in different directions such as tension, compression, axial shear, lateral bending, anterior and posterior shear. Therefore, it is required to obtain the material properties in these directions [Acar, Loptic, 2007].

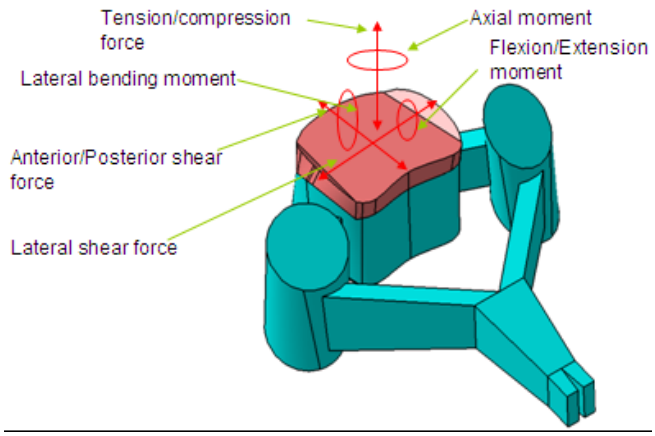

Figure 5.12: Illustration of force and moment vectors applied on a cervical spine disc

Cervical spine has a mid-sagittal symmetry plane, so the material behaviors are same for the left and right sides such as lateral shear, lateral bending and torsinal moments. The tests are conducted by applying external loads on motion segment which is a vertebra-disc-vertebra and on disc segment which is composed of body-disc-body in order to find out the disc responses.

Moroney et al., 1988 has presented the stiffness of the discs where the investigations were done along with the tension and compression results illustrated by Pintar et al. 2001. Moroney et al., 1988 induced that stiffness of the disc depends on the disc level. Also, Pintar et al., 2001 has presented that stiffness of the discs in compressions raises from 6737.5 N/mm at the upper most disc level (C2-C3) to 973.6 N/mm at the disc where it is

located between C7 and T1. There is no other information to obtain the disc stiffness. Therefore, Acar, Loptic, 2007 has used the Moroney's test results for calculating the material behavior in axial rotation, lateral bending, and all shear stiffness coefficients. Camacho et al. 1997 performed a research to illustrate the response of the complete pair of vertebrae at different levels in flexion and extension as non-linear load-displacement curves.

Based on test results of Moroney on discs and intact segments, half of the load is carried by the ligaments and the rest by the disc in extension and flexion. Therefore, Acar assumed that the flexion/extension load-displacement curves which are provided by Camacho et al., 1997 can be divided by 2 to obtain the approximate intervertebral disc non-linear behavior. The translational and rotational damping coeficients are set to 1000 Ns/m and 1.5 Nms/rad respectively [Acar et al. 2007] as an estimation which was used before by De Jager. Till now, there has been no research to measure these values. The stiffness of the cervical spine discs are presented on table 5.14 [Acar et al., 2007].

Table 5.14: Biomedical stiffness data for the inter-vertebral discs [Acar et al. , 2007]

	stiffness (N/mm)					
Loading direction	C2-C3	C3-C4	C4-C5	C5-C6	C6-C7	C7-T1
Anterior shear	62	62	62	62	62	62
Posterior shear	50	50	50	50	50	50
Lateral shear	73	73	73	73	73	73
Tension	63.5	69.8	66.8	68	69	82.2
Compression	637.5	765.3	784.6	800.2	829.7	973.6
Flexion	Load curve from Camacho et al. /2					
Extension	Load curve from Camacho et al. /2					

Flexion and extension of discs can be calculated using the following formula:

$$M = A\left(e^{\theta B} - 1\right)$$

Where M is moment in N.m, θ is deformation angle in radian. Coefficients A and B can be found on Table 5.15.

Table 5.15: Flexion and extension stiffness of the inter-vertebral discs [Acar et al., 2007, Camacho et al., 1997]

	Flexion		Extension	
Disk	A_F	B_F	A_E	B_E
C2C3	0.0515	27.0092	−0.0019	−58.080
C3C4	0.0109	42.9889	−0.0034	−65.408
C4C5	0.0565	22.5115	−0.0014	−94.022
C5C6	0.0309	32.0111	−0.0063	−54.895
C6C7	0.0703	32.1257	−0.0063	−70.851
C7T1	0.3042	22.6261	−0.1553	−37.179

Similar to the method which was used by Acar et al., 2007, average lateral bending and axial rotation disc stiffness were recalculated in this study using the test results of Moroney et al. 1988 as 9.5 Nm/rad and 24 Nm/rad respectively. Damping value is 1.5 Nm/rad for these two rotational directions.

5.5 Model in ADAMS

The first step to make the model in ADAMS is that the CAD data of the vertebrae were imported into ADAMS using step format. Then the ligaments and discs insertion point's CAD data were added in igs format. Spring-dashpot element and bushing type spring-dashpot were used for ligaments and discs respectively. Many SP-lines, functions and global variables were created for definition of material properties for ligaments and discs. All vertebras behave as solids; so, just their mass, mass center and moment inertia were

involved in the simulations. Since the geometry of the vertebras were close to the real ones, only the density was defined for each vertebra in order to adjust the mass with the one mentioned in Jager, Johannes M. K., 1998 literature. Contact elements were defined between adjacent vertebras using impact method. Also, the CAD data of skull was imported in stl format and acts as a dummy part in this model. In this model, the units of force, moment, mass, length, angle, time are Newton, N.mm, Tone, mm, radian and second respectively.

Figure 5.13 shows the complete model in ADAMS.

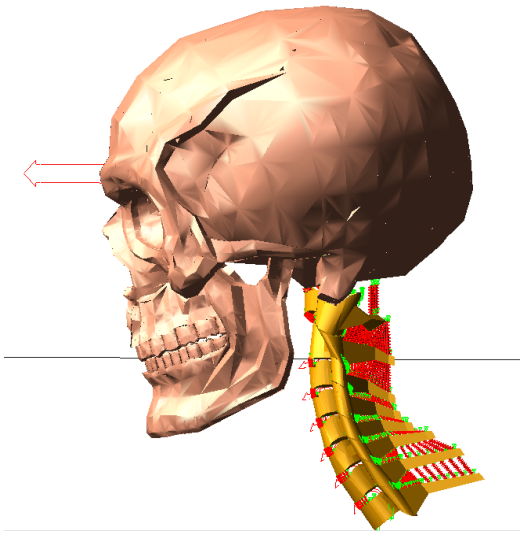

Figure 5.13: Completed multi-dynamic model in ADAMS

The numbers of the elements of the ligaments at each level in the model are as follows:

A) C2 to T1: numbers of JC, ALL, PLL, LF and ISL elements are 16, 13, 13, 20, and 7 respectively.

B) OC to C1/C2: numbers of JC, AA-OM, PA-OM, ALAR, TM, APICAL and CLV are 16, 5, 5, 1, 1, 1 and 1 respectively.

Clearly, the loads shown on the previous force-deflection tables for these ligaments should be divided by number of the elements as mentioned at the above in order to represent the required force versus the deflection data for each element.

Chapter 6

Validation of the cervical spine multi-body dynamic model

6.1 Introduction

To validate the model, three literatures were used. In these literatures, the results of experimental tests on different parts of the cervical spine were presented. In general, they have fixed the lowest vertebra and applied a load on the vertebra which is at top, to generate flexion, extension, lateral or torsion moments. Then, the relative rotation of adjacent vertebras was measured. First, the model of upper cervical spine segment, C0-C2 was validated by the experimental data of Panjabi, Oda et al. 1992. then, the models of lower cervical spine vertebra pairs, C2-C3, C3-C4, C4-C5, C5-C6, C6-C7, C7-T1 were validated by the results of experiments published by Moroney et al. 1988. Finally, the complete model of cervical spine was validated by the research work of Panjabi et al. 1993 for extension and flexion load conditions.

6.2 Upper cervical spine test method

Five samples where each is composed of C0 to C3 were provided to conduct the test [Panjabi, Oda et al. 1992]. The sample was fixed to the test machine at C3 and loading jig was connected to C0. Special markers were fixed to C0, C1 and C2 for measuring the movements of the vertebrae in three directions. Then the torque was applied in three steps to a maximum of 1.5 N.m.

6.3 Upper cervical spine validation

Validation was performed using the above mentioned method by Panjabi, Oda et al. 1992. 1.5 Nm moment was applied in flexion, extension, lateral and torsion directions on occiput for conducting four separate simulations and C3 was fixed completely. Because of complexity of contact definition in the model, it was not possible to perform static analysis, so a quasi-static analysis was done for duration of five seconds while the moment was increased gradually and smoothly to a maximum of 1500 Nmm. Finally, the relative rotation of C0-C1 and C1-C2 were measured. Figure 6.1 demonstrates the results for these simulations and comparison with experimental data.

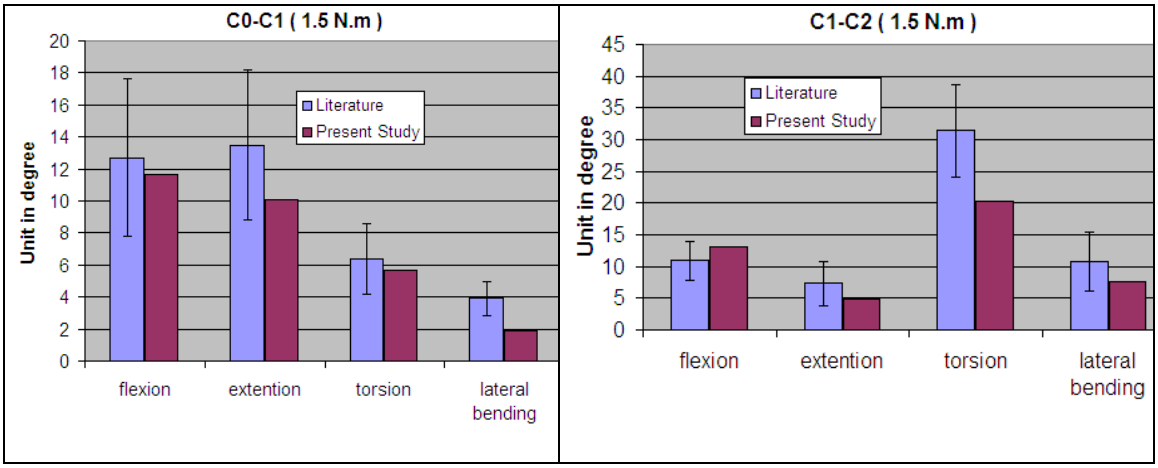

Figure 6.1: Validation of C0-C2 of the cervical spine model

6.4 Lower cervical spine test method

Moroney et al. 1988 performed the tests on 35 pair of vertebrae from 16 cervical spines. The pairs of vertebrae include C2-C3, C3-C4, C4-C5, C6-C7 and C7-T1. The lower vertebra of each sample was fixed to the test machine and the load was applied to the

upper one. Six mechanical dial gauges were used to measure all six components of segment motion. The tests were conducted by applying 1.8 Nm moment on the upper vertebra in different directions separately.

6.5 Lower cervical spine validation

Validation was performed using the above mentioned method by Moroney et al. 1988. 1.8 Nm moment was applied in flexion, extension, lateral and torsion directions on superior vertebra while the inferior vertebra was fixed.

These load conditions were applied on separate models for pairs of C2-C3, C3-C4, C4-C5, C5-C6, C6-C7 and C7-T1. Because of complexity of contact definition in the model, it was not possible to perform static analysis, so a quasi-static analysis was done for duration of five seconds while the moment was increased gradually and smoothly to the above mentioned values. Finally, the relative rotations of pairs of vertebra were measured. Figure 6.2 demonstrate the results for these simulations and comparison with experimental data.

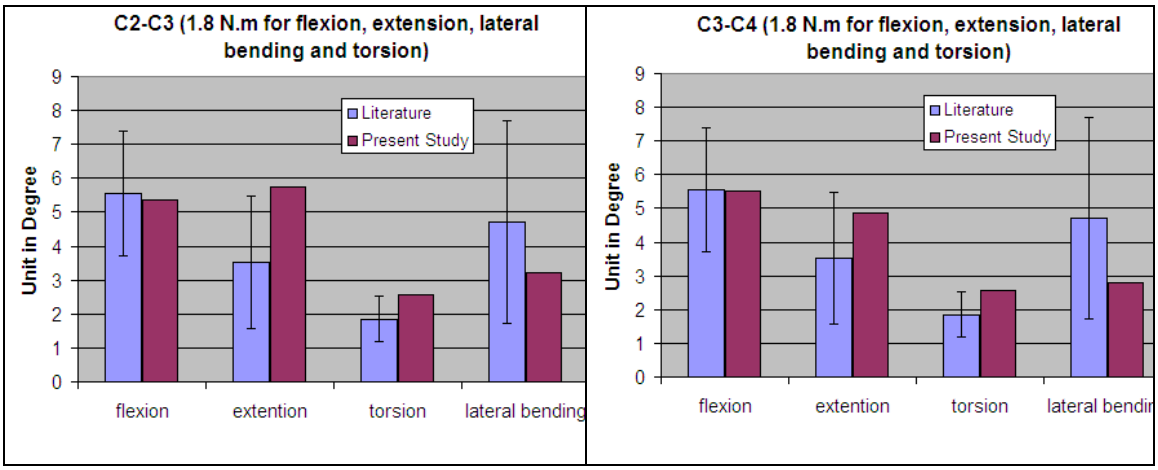

Figure 6.2: Validation of pairs of C2-T1 of the cervical spine model

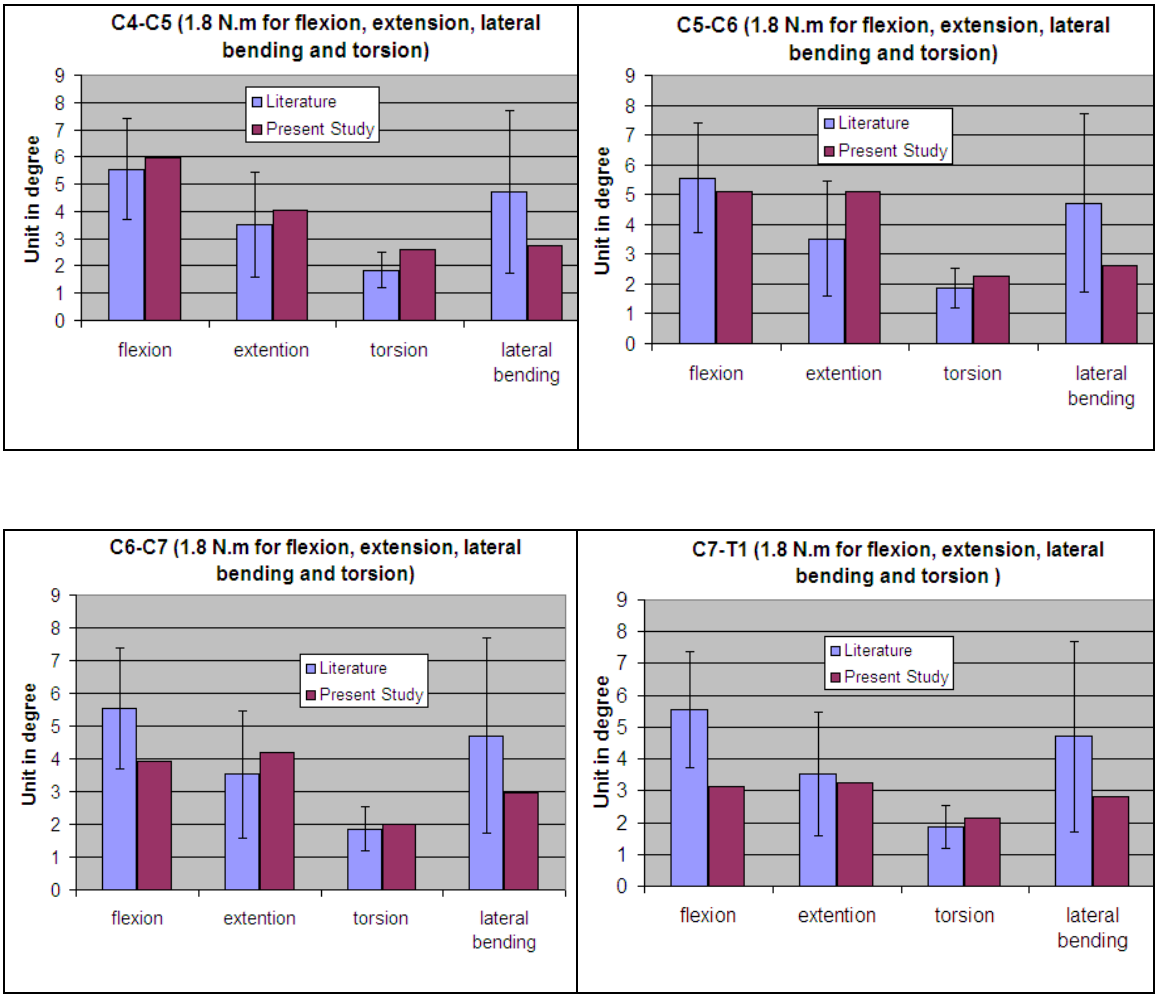

Figure 6.2: Validation of pairs of C2-T1 of the cervical spine model (continued)

6.6 Complete cervical spine test method

Panjabi et al. 1993 conducted the tests on sixteen samples which include C0-C5, C0-C6, C0-C7 and C2-C7. Markers were fixed to each vertebra body for the purpose of measuring the vertebra motions in different directions. The lowest vertebrae were mounted to the test machine and the load applied incrementally to C0 for a maximum of 1 Nm. During each test, both neutral zone (NZ) and range of motion (ROM) were measured.

The neutral zone is the total motion of the sample from zero position where the sample does not show any resistance against the load and the stiffness is very low. The range of motion depicts the total motion of the segment where the maximum load is applied. On this zone, the sample shows stiffness against applying the load. Figure 6.3 presents these two zones.

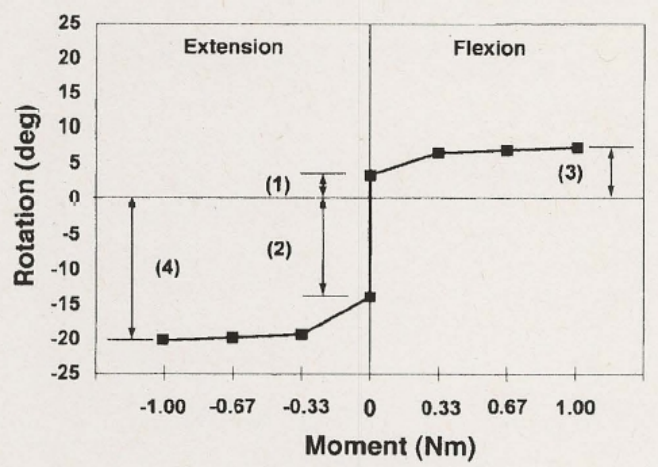

Figure 3. The neutral zone (NZ) and range of motion (ROM) using a load–displacement curve for flexion–extension rotation. In this example (1) = the NZ for flexion rotation, whereas (2) = the NZ for extension rotation. Likewise, (3) = the ROM for flexion rotation with a maximum load of 1.00 Nm, whereas (4) = the ROM for extension rotation with a maximum load of 1.00 Nm. The NZ and ROM were obtained for each of the 6 degrees of freedom of motion for all seven levels.

Figure 6.3: Neutral zone and range of motion [Panjabi et al. 1993]

6.7 Whole cervical spine validation

Validation was performed using the above mentioned method by Panjabi et al. 1993. 1.0 Nm moment was applied in flexion and extension direction on occiput while C7 was fixed. Because of complexity of contact definition in the model, it was not possible to perform static analysis, so a quasi-static analysis was done for duration of fifteen seconds while the moment was increased gradually and smoothly to the above mentioned value. Finally, the relative rotations of pairs of vertebra were measured. Figure 6.4 demonstrate

the results for these simulations and comparison with experimental data.

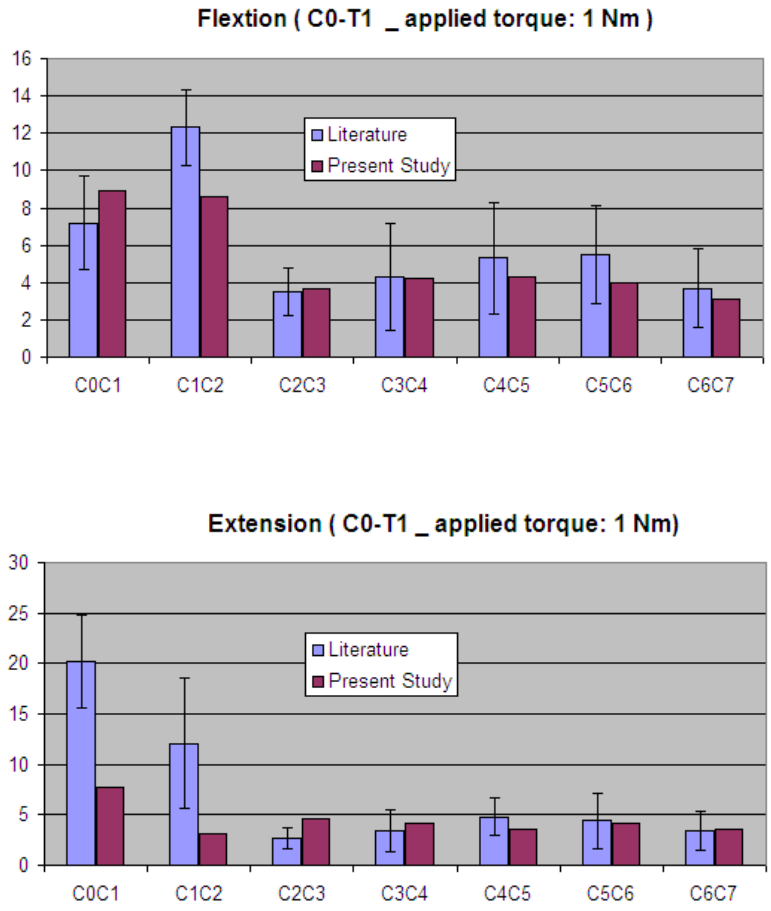

Figure 6.4: Validation of the whole cervical spine model in flexion and extension directions

The picture for extension result shows that there is a significant difference on relative rotation of C0C1 between current study and Panjabi's result while C0C1 extension result matches well with Panjabi, Oda et al. 1992 relevant test data as explained earlier. The reason is that a cervical spine does not have same amount of neural zone in different people and if the result is affected highly by this zone, probably the test results would not be similar in different research studies. Therefore, the current model can not be in good

agreement with both of the above mentioned literatures in extension mode at the same time.

6.8 Conclusion for validation of cervical spine model

The above results show that the model is reasonably in good agreement with the experimental test data. Therefore, this model can be used to evaluate the loads on the ligaments and the discs in different dynamic or static conditions.

6.9 Percentage of carried loads by the discs

It is useful to know how much of a load is taken by a disc when a moment is applied to the cervical spine. The results of above mentioned simulations which were done by conducting Moroney's test method can be used to demonstrate the capability of disc to resist against the moments in different directions (Tables 6.1).

These tables demonstrate that the discs can take the moments between 28% and 42% in flexion, between 32% and 65% in extension, between 46% and 61% in torsion, and between 24% and 30% in lateral bending directions.

Tables 6.1: Illustration of the percentage of the loads carried by discs

C2-C3	relative rotation in radian	relative rotation in degree	stiffness coefficient	stiffness coefficient	moment in disc (Nm)	applied moment (Nm)	percentage of carried moment by disc
flexion	0.094	5.379	0.052(A)	27.009(B)	0.598	1.800	33.219
extension	0.100	5.726	0.002(A)	58.081(B)	0.627	1.800	34.818
torsion	0.045	2.554	24.000		1.069	1.800	59.400
lateral bending	0.056	3.205	9.500		0.531	1.800	29.508

Tables 6.1: Illustration of the percentage of the loads carried by discs (continued)

C3-C4	relative rotation in radian	relative rotation in degree	stiffness coefficient	stiffness coefficient	moment in disc (Nm)	applied moment (Nm)	percentage of carried moment by disc
flexion	0.096	5.504	0.011(A)	42.989(B)	0.665	1.800	36.964
extension	0.085	4.852	0.003(A)	65.409(B)	0.859	1.800	47.734
torsion	0.045	2.558	24.000		1.071	1.800	59.507
lateral bending	0.049	2.811	9.500		0.466	1.800	25.882

C4-C5	relative rotation in radian	relative rotation in degree	stiffness coefficient	stiffness coefficient	moment in disc (Nm)	applied moment (Nm)	percentage of carried moment by disc
flexion	0.104	5.985	0.057(A)	22.512(B)	0.536	1.800	29.781
extension	0.070	4.035	0.001(A)	94.022(B)	1.047	1.800	58.148
torsion	0.046	2.608	24.000		1.092	1.800	60.667
lateral bending	0.048	2.728	9.500		0.452	1.800	25.112

C5-C6	relative rotation in radian	relative rotation in degree	stiffness coefficient	stiffness coefficient	moment in disc (Nm)	applied moment (Nm)	percentage of carried moment by disc
flexion	0.089	5.115	0.031(A)	32.011(B)	0.507	1.800	28.140
extension	0.089	5.088	0.006(A)	54.895(B)	0.817	1.800	45.376
torsion	0.040	2.274	24.000		0.952	1.800	52.880
lateral bending	0.045	2.596	9.500		0.430	1.800	23.898

C6-C7	relative rotation in radian	relative rotation in degree	stiffness coefficient	stiffness coefficient	moment in disc (Nm)	applied moment (Nm)	percentage of carried moment by disc
flexion	0.068	3.922	0.070(A)	32.126(B)	0.563	1.800	31.273
extension	0.073	4.186	0.006(A)	70.852(B)	1.106	1.800	61.442
torsion	0.035	2.003	24.000		0.839	1.800	46.587
lateral bending	0.051	2.947	9.500		0.488	1.800	27.133

Tables 6.1: Illustration of the percentage of the loads carried by discs (continued)

C7-T1	relative rotation in radian	relative rotation in degree	stiffness coefficient	stiffness coefficient	moment in disc (Nm)	applied moment (Nm)	percentage of carried moment by disc
flexion	0.055	3.148	0.304(A)	22.626(B)	0.750	1.800	41.653
extension	0.057	3.239	0.155(A)	37.179(B)	1.114	1.800	61.872
torsion	0.037	2.139	24.000		0.895	1.800	49.747
lateral bending	0.049	2.812	9.500		0.466	1.800	25.893

Chapter 7

Case studies

7.1 Introduction

Multibody dynamic analysis is capable of determining the force-deflection of the elements inside a structure. This kind of analysis can supersede many experimental tests. Experimentations are usually costly and time consuming. Also, in many cases, it is not possible to extract every kind of test data accurately. However, a validated multibody dynamic model of the cervical spine can be used to perform different kind of case studies, while the results are accurate enough and the process is fast and cheep. In addition, the output of this analysis can be as an input for FE analysis of the cervical spine to calculate stress and strain in the desired area. Therefore it assists the researchers to discover the main cause of pains or to quantify the level of injuries in this region.

In this study, three cases were investigated. These case cover simulation of extension/flexion, later and torsional movements. There are no literature references for the load conditions; they actually simulate some basic movements of the cervical spine which can be happened every day. Therefore, the speed is not high for these conditions. For all of them, a load, which can be a displacement or a force in different directions, is applied to the center of mass of the head and also T1 is fully constrained. Then, resultants loads on the discs versus simulation time are demonstrated.

In lateral and torsional directions, the load signs are not important, but for the rest, it’s necessary to know as the material behavior is different when the load direction changes to

opposite one. Each load and moment is presented based on its own local coordinate system which belongs to a specific disc. To define the local coordinate system, x direction is normal to mid-sagittal plane, z is on the mid-sagittal plane and normal to inferior surface of the disc toward up and y is normal to xz plane toward anterior wall of the disc. Therefore, the anterior shear, tension load and extension moment have positive sign and the others, which are in opposite directions, have negative sign. All of the imposed loads are defined by using the global coordinate system. Figure 7.1 demonstrates a new coordinate system which is parallel to the global one and its origin is on the head mass center. The gravity is aligned with "–Z" direction.

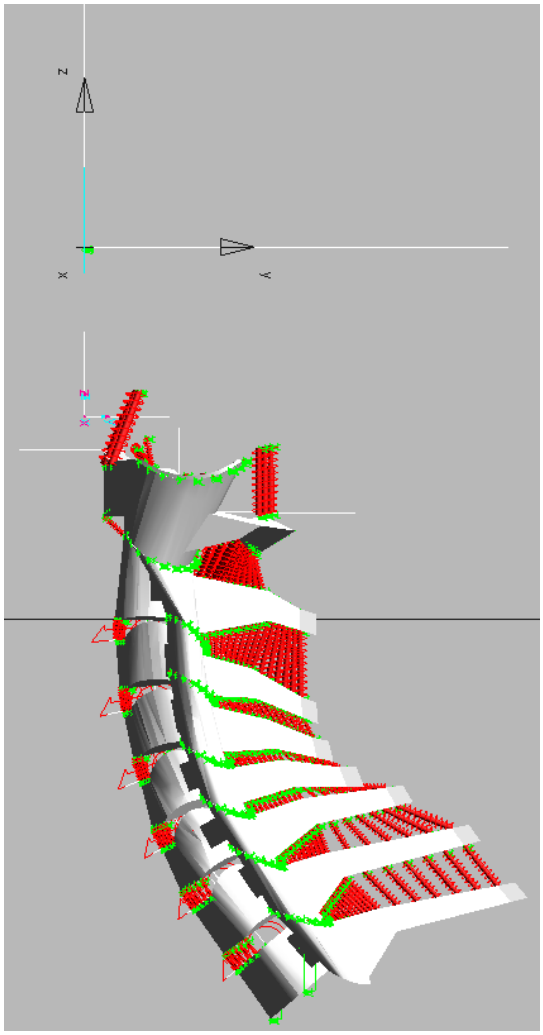

Figure 7.1: Cervical spine model and global coordinate system axis directions

In this report, X,Y,Z refer to the global coordinate system axes and x,y,z are for local coordinate system. The units are Newton and N.mm for loads and moments respectively. The units of force, moment, mass, displacement, rotation and time are N, N.mm, kg, mm, radian and second respectively in all of the following pictures.

7.2 Flexion/extension case study

This case study simulate the condition where the head goes to flexion and then move to back for extension position and finally it is back to its original location. A displacement type load is applied to the head mass center. The imposed load is parallel to Y axis. Also, this point is constrained in X, AY and AZ directions, so head movement and rotation is only in mid-sagittal plane. Figure 7.2 shows the profile of the load versus time.

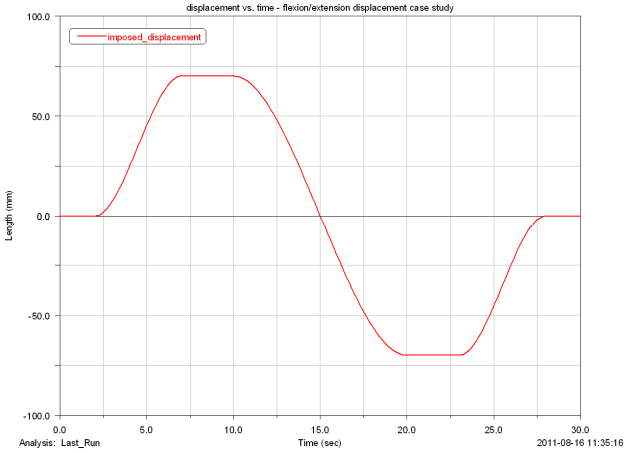

Figure 7.2: Variation of imposed displacement versus time (flexion/extension case study)

The above mentioned load is zero for two second to let the structure to reach a stable condition, then it takes 5 second to have a 70 mm displacement in "+Y" direction (it means the cervical spine is in extension), it stops in this location for 2 seconds, it starts moving in opposite direction for a 140 mm displacement in "-Y" direction in 10 seconds

(the cervical spine is in flexion), again it stops for two seconds, finally it has a 70 mm displacement in "+Y" direction in 5 seconds so that it is in its original position again, finally there is a two seconds rest to see its affect on the mount of disc loads. Figure 7.3 shows the resultant force at the point of imposed displacement.

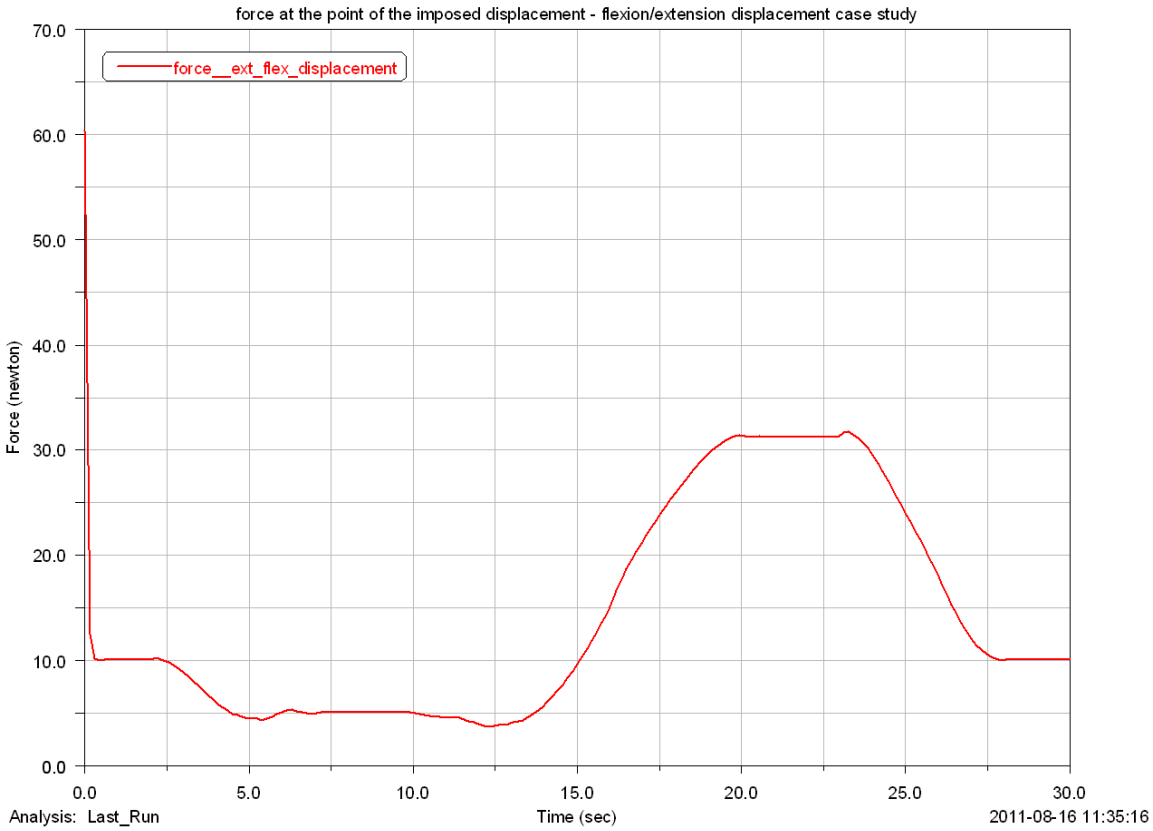

Figure 7.3: Resultant force versus time at the position of imposed displacement

Figure 7.3 shows that stiffness of the cervical spine is much more in flexion. The additional force which is needed to move the head in extension for 70mm from zero position is 10N, while this amount is 40N in flexion. Therefore, the stability of the structure is more in flexion movements. Also, the muscles should be stronger to move the head in this direction too.

Figure A.1 to Figure A.3 demonstrate the resultant loads on the discs.

The extension/flexion graph illustrates that C4C5 disc carry highest load in extension, while C7T1 take the highest moment in flexion. The difference between maximum and minimum moments in extension and flexion in the discs are 750Nmm and 350Nmm respectively. However, the maximum moments in extension and flexion are around 1550Nmm and 858Nmm. Therefore in both flexion and extension, the ratio of the difference of maximum and minimum moments to the maximum moment is about 0.5. The tension/compression graph illustrate that the average force acted on the discs after 70mm in extension and flexion are about 5N (in tension) and 110N (in compression). Therefore, the important feature of discs is to be resistant in compression loads rather than tension forces. Considering all of the graphs, in flexion/extension, c4c5 and c7t1 discs are carrying higher loads, so, they are in higher risk of injury relative to the other ones.

7.3 Lateral displacement case study

This case study simulate the condition where the head moves laterally to one side and then goes back to its primary position and then it continue its way to the other side and finally it returns back to its original position. A displacement type load is applied to the head mass center. The imposed load is parallel to X axis. Also, this point is constrained in Y, AX and AZ directions. Therefore, head rotates only in lateral direction and it does not move forward or backward as well. Figure 7.4 shows the profile of the load versus time. It has a same shape as the one which is in flexion/extension case study, except the maximum displacement which is 60 mm here.

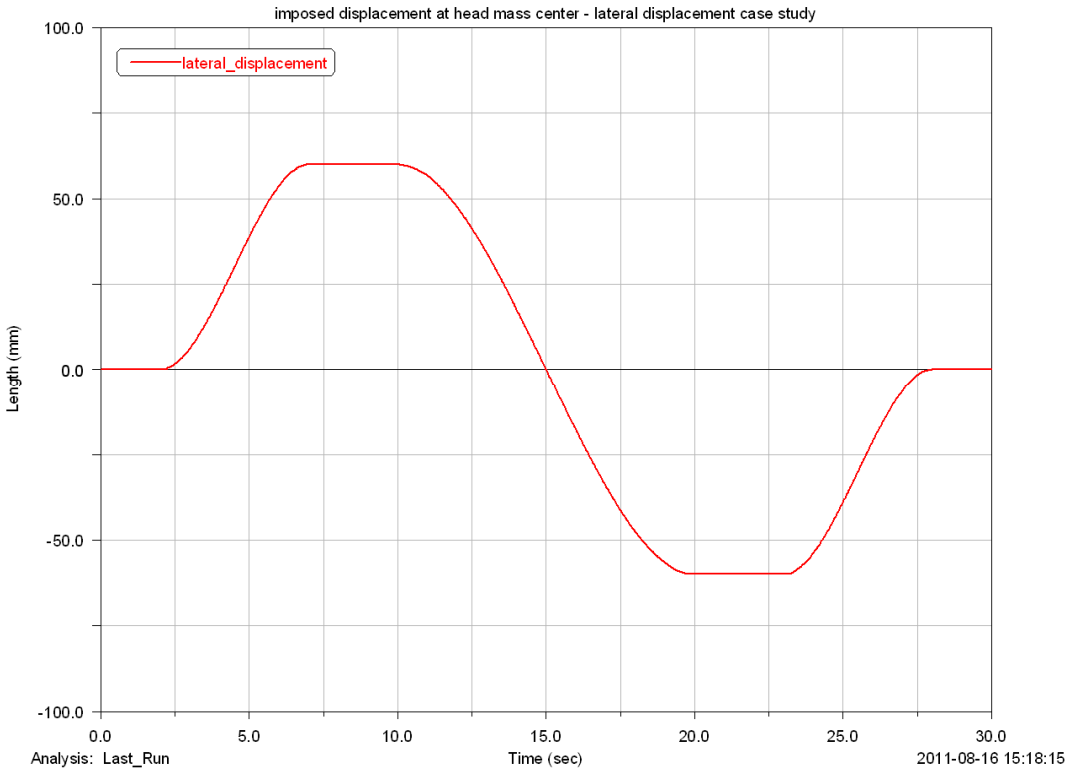

Figure 7.4: Variation of imposed displacement versus time (Lateral displacement case study)

Figure 7.5 shows the resultant force at the point of imposed displacement. Figure B.1 to Figure B.6 demonstrate the resultant loads on the discs.

The lateral bending moment graph depicts that C2C3 disc carry the highest moment, however the other discs take smaller moments, but, they are relatively close to the moment which is carried by C2C3. The tension/compression graph presents that compression force reduces on the discs as the head moves laterally. After 60mm move, all of the discs are under low tension forces. The maximum and minimum forces are 10N on C3C4 and 2N on C6C7.

All of the six resultant forces figures clarify that C7T1 is under the highest load in lateral displacement condition. The next discs that carry the high loads are C2C3 and C4C5.

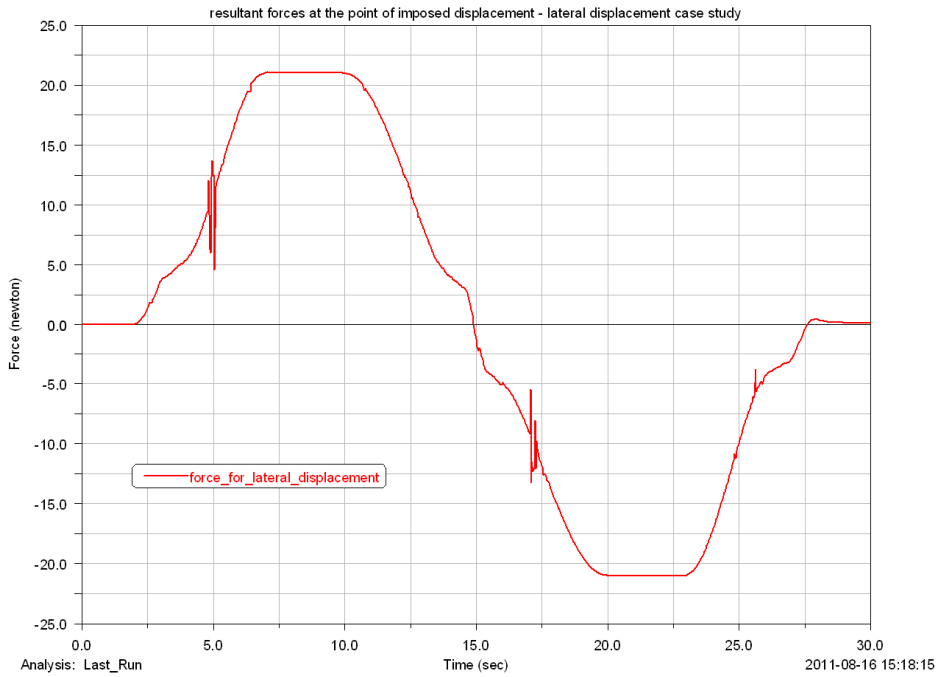

Figure 7.5: Resultant force versus time at the position of imposed displacement

Comparing figure 7.3 and figure 7.5, it can be seen that the lateral stiffness of cervical spine is similar to the stiffness in flexion direction.

7.4 Torsional moment case study

This case study investigates the situation where head rotates around normal axis and then it reverses the rotation until the absolute value of the moment in opposite direction is same as the one in the first move.

Also, head mass center is constrained in AX and AY. As a result, head rotates only around Z axis. A torsional moment is applied to head mass center. The imposed load is

parallel to Z axis. The moment is zero for 3 seconds; the zero load time lets the model to get into a stable position.

Because of the head weight and its relative position to the spine, the spine move 5.7 mm forward and it puts most of the discs in flexion condition at this step. Then, the imposed moment increases to 1850 Nmm in 7 seconds, this duration is big enough to consider the simulation in low or normal rotation speed. The moment remains constant for 3 seconds. Now, it decrease to -1850 Nmm in 14 seconds, again it remains constant for 3 second and following to that it backs to zero in 7 seconds and finally the simulation continues for 3 seconds while the moment does not change. Figure 7.6 shows the profile of the applied torque versus time.

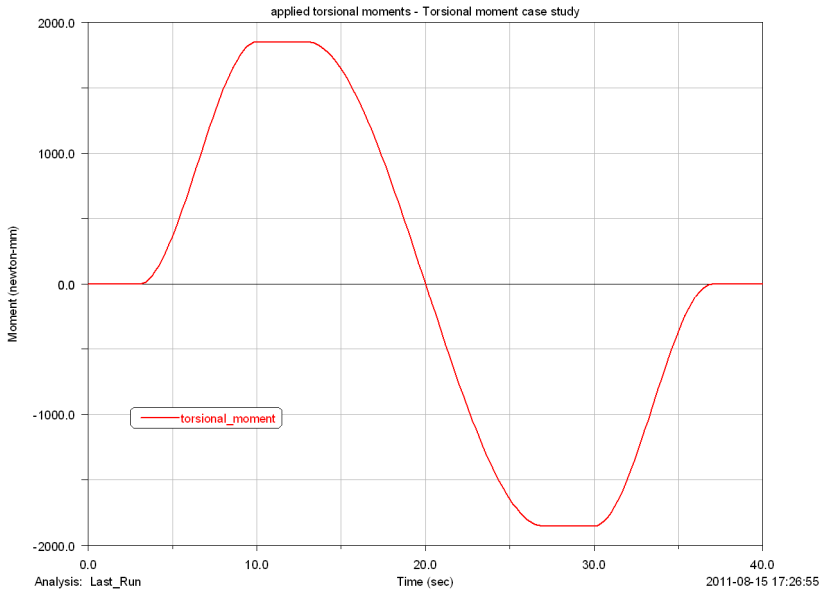

Figure 7.6: Variation of imposed torque versus time (torsional moment case study)

Figure 7.7 shows the rotation of head resulted from applying the above mentioned load. Figures C.1 to Figure C.6 demonstrate the resultant loads on the discs. The torsional loads graph present that the highest and lowest moments on the discs are about 950Nmm

(C4C5) and 550Nmm (C2C3). It means the discs carry 1/3 to 1/2 of the total applied torque on the head. Also, the tension/compression graph illustrate that after applying the torque, the highest level disc is in tension and as the disc is positioned closer to the bottom of the cervical spine, more compression is put on the disc. Therefore, the forces applied on the discs change from tension at the top to compression at the bottom. The tension on C2C3 is 10N and the compression on C7T1 is 65N.

The six resultant forces figures illustrate that the lower spine area, especially C7T1, is under higher loads. Therefore, the risk of C7T1 disc injury is higher than the other ones. Also, C4C5 is carrying the highest torsional moment.

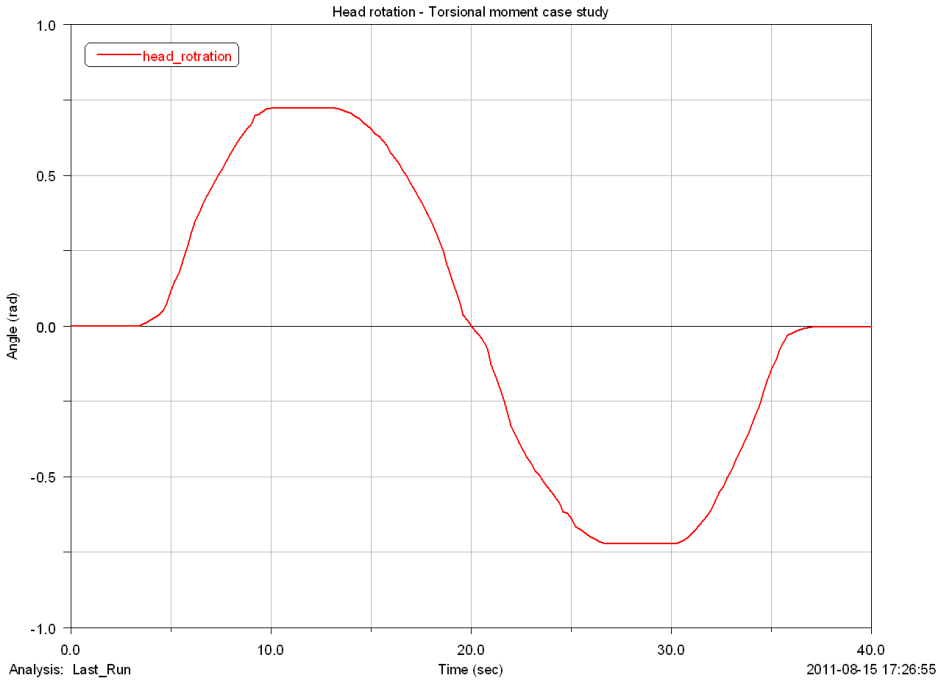

Figure 7.7: Variation of resultant head rotation versus time

7.5 Sensitivity

The goal of this section is to investigate the effect of helicopter pilot's helmet weight on the applied load on the cervical spine discs. As mentioned by Ford et al. 2011, the mass of helmet is from 14 N to 36 N. the heaviest one is equipped with NVG and counter weight (CW). As there was no other technical data available, it was assumed that the helmet is a 95mm radius hemisphere shell for calculating the mass moment of inertia in different directions. Also, It was assumed that the center of the hemisphere coincide with the head mass center. The definition of the problems is exactly same as the ones in the case study section, except that the displacement is 40 mm in flexion direction when solving for flexion/extension problem. The reason is when the head and helmet together becomes heavier than 6 kg, the C0-C1 joint can not hold rotationally this bulk of mass after a certain displacement, which is less than 70mm, in flexion direction and as a result, head start rotating at C0C1 joint while this joint does not show any rotational stiffness. The pictures D.1 to D.3 demonstrate the variation of loads versus helmet weight in flexion/extension, lateral bending and torsion studies.

The tension/compression graphs present that the rate of change of applied compression forces is highest in flexion position of the head as the weight of the helmet increases. The second highest rate of change of the compression loads is in axial rotation of the cervical spine. In extension position, all of the discs extension moments increase gradually as the helmet weight increases. But this is different when the head is in flexion position. The absolute value of the flexion moment increases on C2C3 disc as the helmet weight increases, while it decreases on C7T11 disc. This is due to more rotation of the head after 40 mm forward movement and this rotation applies more flexion moment on C1C2. In

lateral displacement study, both the lateral bending moment and its rate of change is highest on C2C3 disc. This disc carries much more moment relative to the other ones too. In torsional moment case study, all of the discs tortional moments increase gradually as the helmet weight increases, also C2C3 carries the highest moment in this situation.

Finally, these pictures clearly illustrate that C7T1, C4C5 and C2C3 discs carry the major loads in different load conditions.

Chapter 8

Conclusion and future work

Helicopter pilots carry the heavy helmets at nights which are equipped to NVG and CW. The helmet weight can be as maximum of 36N. Some reports reveal that cervical disc injuries are observed in these pilots due to use of these heavy helmets. To evaluate the loading on cervical spine affected by this excess of load in different moving positions of head, it is useful to develop a multi-body dynamic model of cervical spine. Then the resultant loads extracted from the simulations can be used directly to predict the injury level on a disc or to be as an input to a FE model of the cervical spine for calculating the stress on the discs. A 3D multi-body dynamic model of cervical spine is created in MSC ADAMS. It includes cervical vertebras, ligaments and discs. Non-linear properties of the ligaments and the discs are provided by Pintar et al. 2001 and Acar et al., 2007 respectively. The ligaments damping factor is defined by Jager, Johannes, 1998. The mass data of the vertebras is presented by Jager, Johannes, 1998. Then the model is validated under different loading conditions against the experimental data of Panjabi, Oda et al. 1992, Moroney et al. 1988 and Panjabi et al. 1993. The results of the simulations demonstrate a good agreement with experimental tests data. For the next step, 3 case studies are performed to understand better the loading on the discs while the pilot has no helmet on his head and the head is moving relatively slowly in extension/flexion, axial rotation and lateral directions.

The results of flexion/extension case study show that stiffness of the cervical spine is much more in flexion. The additional force which is needed to move the in extension for 70mm from zero position is 10N, while this amount is 40N in flexion. Therefore, the

stability of the structure is more in flexion movements. Also, the muscles should be stronger to move the head in this direction too. Also it can be induced that C4C5 disc carry highest load in extension, while C7T1 take the highest moments in flexion. The difference between maximum and minimum moments in extension and flexion in the discs are 750Nmm and 350Nmm respectively. However, the maximum moments in extension and flexion are around 1550Nmm and 858Nmm. Therefore in both flexion and extension, the ratio of the difference of maximum and minimum moments to the maximum moment is about 0.5. The tension/compression graph illustrate that the average force acted on the discs after 70mm in extension and flexion are about 5N (in tension) and 110N (in compression). Therefore, the important feature of discs is to be resistant in compression loads rather than tension forces. Considering all of the graphs, in flexion/extension, c4c5 and c7t1 discs are carrying higher loads, so, they are in higher risk of injury relative to the other ones.

In lateral displacement case study, the lateral bending moment graph depicts that C2C3 disc carry the highest moments, however the moments which is resisted by the other discs are relatively close to the moment carried by C2C3. The tension/compression graph presents that compression force reduces on the discs as the head moves laterally. After 60mm move, all of the discs are in low tension forces. The maximum and minimum tension forces are 10N on C3C4 and 2N on C6C7. Also, all of the six resultant loads graphs clarify that C7T1 is under the highest load in lateral displacement condition. The next discs that carry the high loads are C2C3 and C4C5. Comparing the resultant force graphs at the imposed displacement on the head for flexion/extension and lateral

displacement case studies, it can be seen that the lateral stiffness of cervical spine is similar to the stiffness in flexion direction.

In torsional moment case study, the torsional loads graph present that the highest and lowest moments on the discs are about 950Nmm (C4C5) and 550Nmm (C2C3). It means the discs carry 1/3 to 1/2 of the total applied torque on the head. Also, the tension/compression graph illustrate that after applying the torque, the highest level disc is in tension and as the disc is positioned closer to bottom of the cervical spine, more compression is put on the disc. Therefore, the forces applied on the discs change gradually from tension at the top to compression at the bottom. The tension on C2C3 is 10N and the compression on C7T1 is 65N. All of the six resultant loads figures illustrate that the lower spine area, especially C7T1, is under higher loads. Therefore, the risk of C7T1 disc injury is higher than the other ones. Also, C4C5 is carrying the highest torsional moment.

The results of above mentioned simulations demonstrate that C2C3, C4C5 and C6T1 carry the highest loads which depend on direction of moving head and its position at a specific time.

The last step is to consider the effect of helmet in the model and re-run the previous case studies simulations. However because of lack data, it is assumed that helmet is a 95mm radius hemisphere shell which its center located at the same position of head mass center. The resultant graphs illustrate trend of loads as the helmet weight increases.

The tension/compression graphs present that the rate of change of applied compression forces is highest in flexion position of the head as the weight of the helmet increases. The second highest rate of change of the compression loads is in axial rotation of the cervical

spine. In extension position, all of discs extension moment increases gradually as the helmet weight increases. But this is different when the head is in flexion position. The absolute value of the flexion moment increases on C2C3 disc as the helmet weight increases, while it decreases on C7T11 disc. This is due to more rotation of the head after 40 mm forward movement and this rotation applies more flexion moment on C1C2. In lateral displacement study, both the lateral bending moment and its rate of change is highest on C2C3 disc. This disc carries much more moment relative to the other ones too. In torsional moment case study, all of the discs tortional moments increase gradually as the helmet weight increases, also C2C3 carries the highest moment in this situation.

Finally, these pictures clearly illustrate that C7T1, C4C5 and C2C3 discs carry the major loads in different load conditions.

As a conclusion of the above mentioned studies, it can be observed that C2C3, C4C5 and C6T1 carry the highest loads. To see if the stresses reach to their maximum values on the discs, it is necessary to conduct a finite element analysis using these data.

As future works, all measurements and experiment test should be done again using similar cadaver samples in respect of race, age, gender, height and weight. Therefore, all the information which will be incorporated into the multi-body dynamic model would be consistent.

List of Appendices

Appendix A (flexion/extension case study)

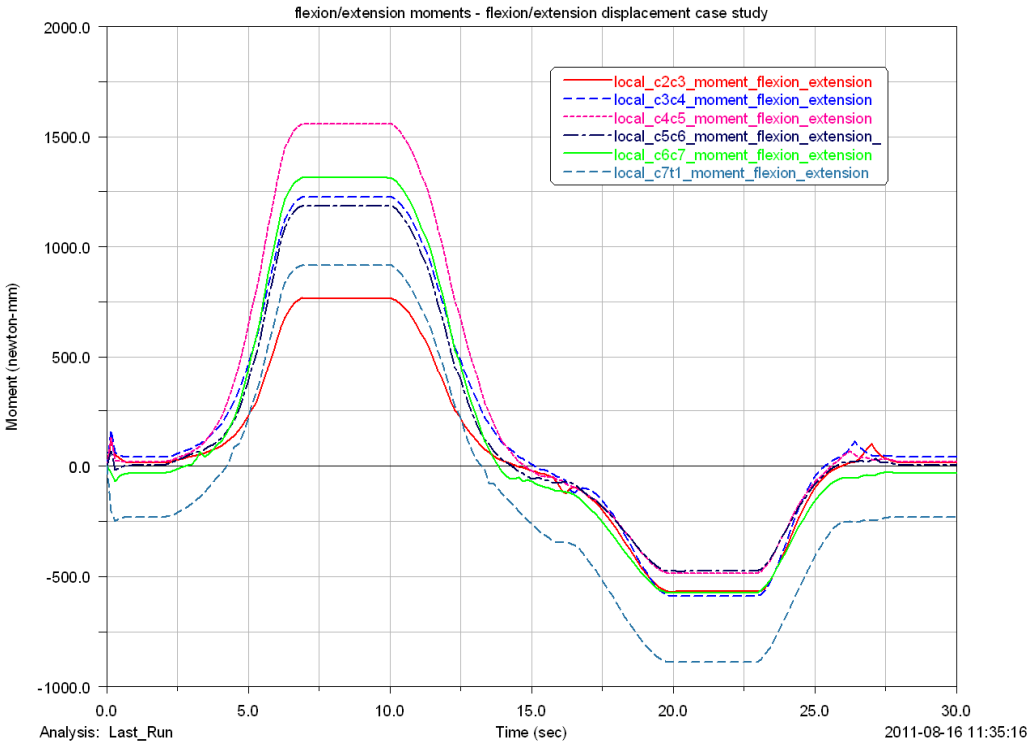

Figure A.1: Comparison of resultant flexion/extension moments on the discs

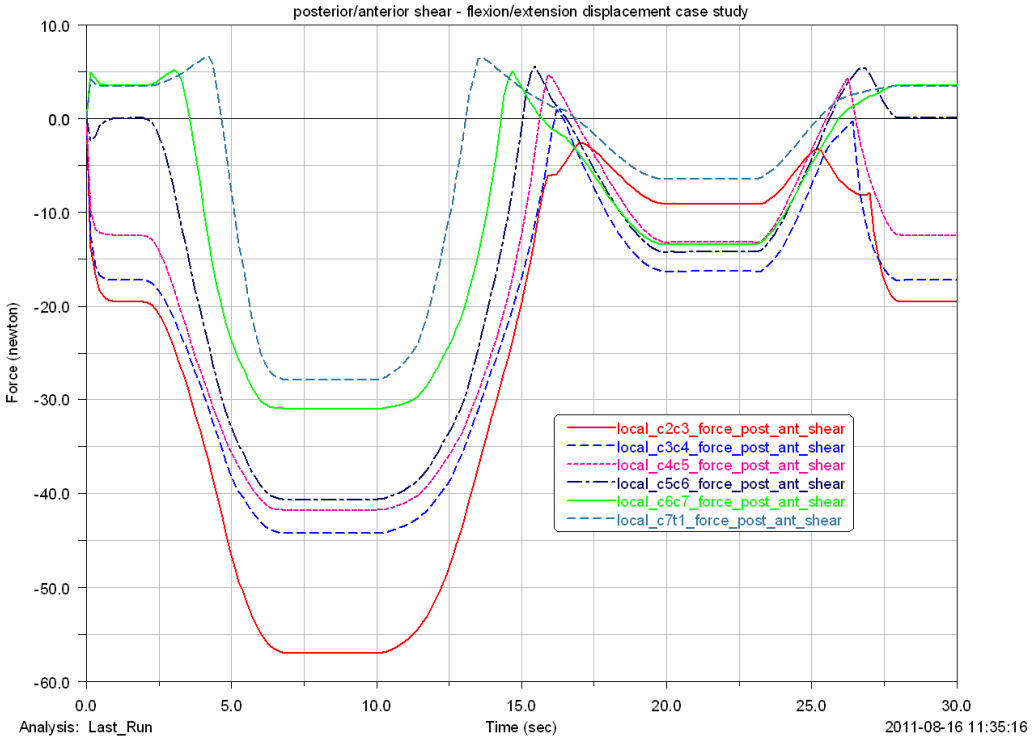

Figure A.2: Comparison of resultant posterior/anterior shear forces on the discs

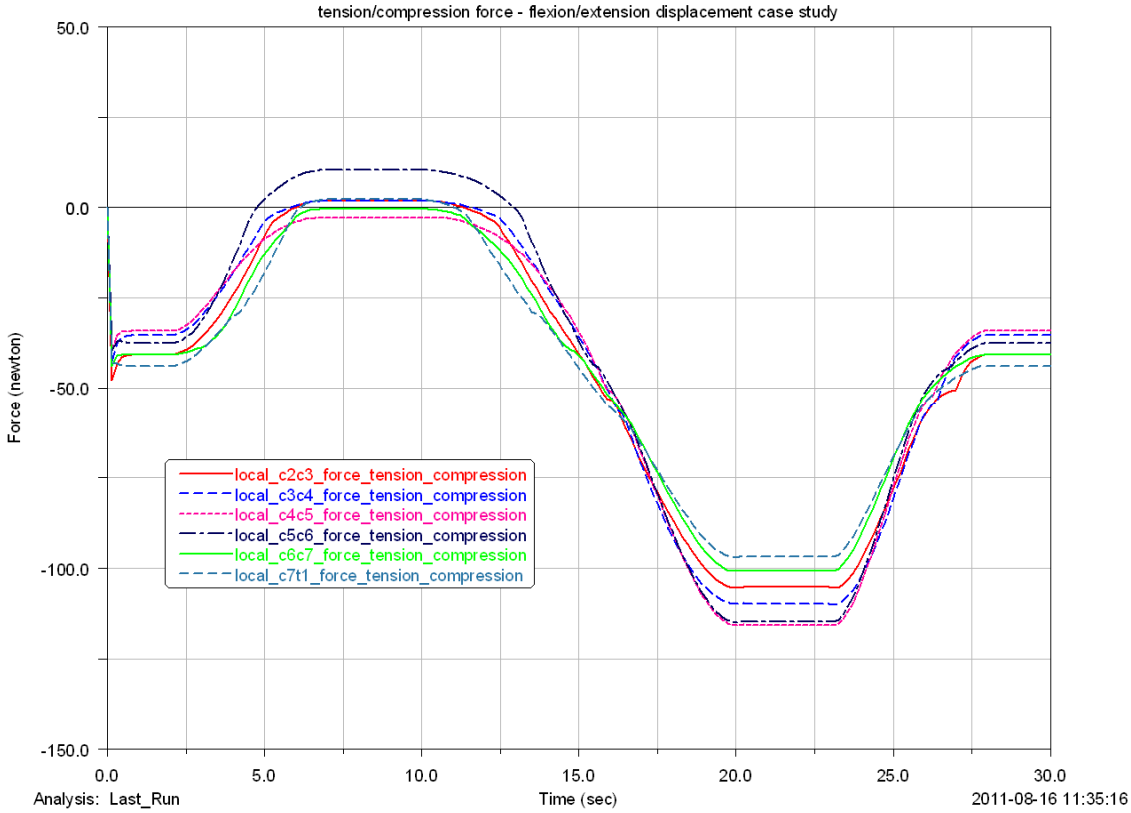

Figure A.3: Comparison of resultant tension/compression forces on the discs

Appendix B (lateral displacement case study)

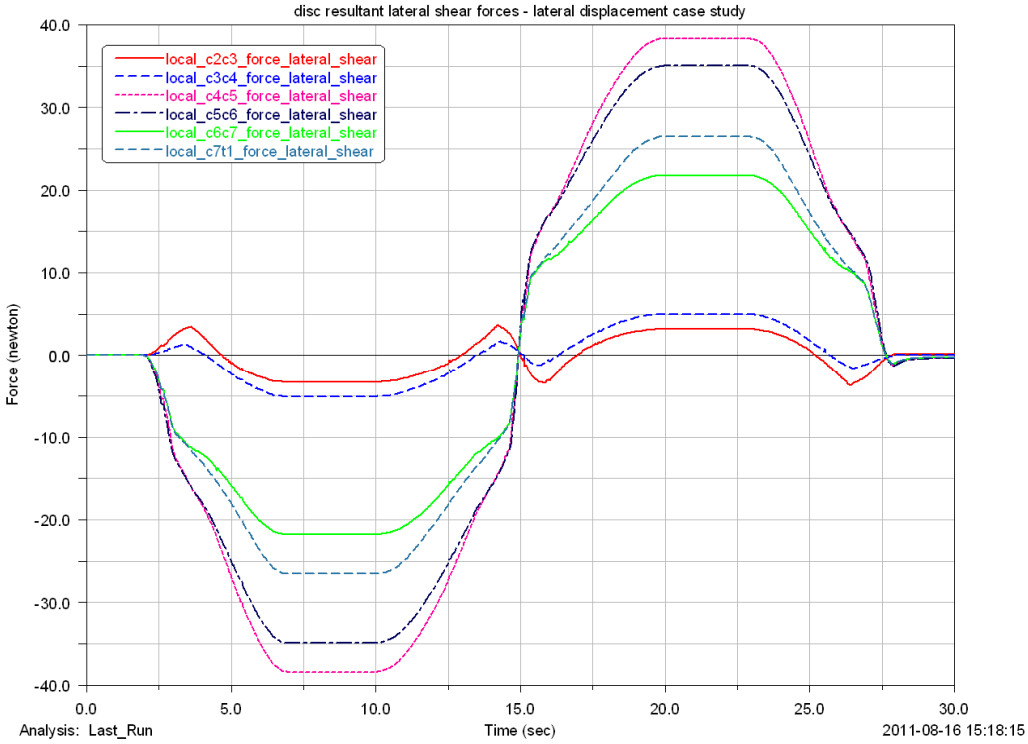

Figure B.1: Comparison of resultant lateral shear forces on the discs

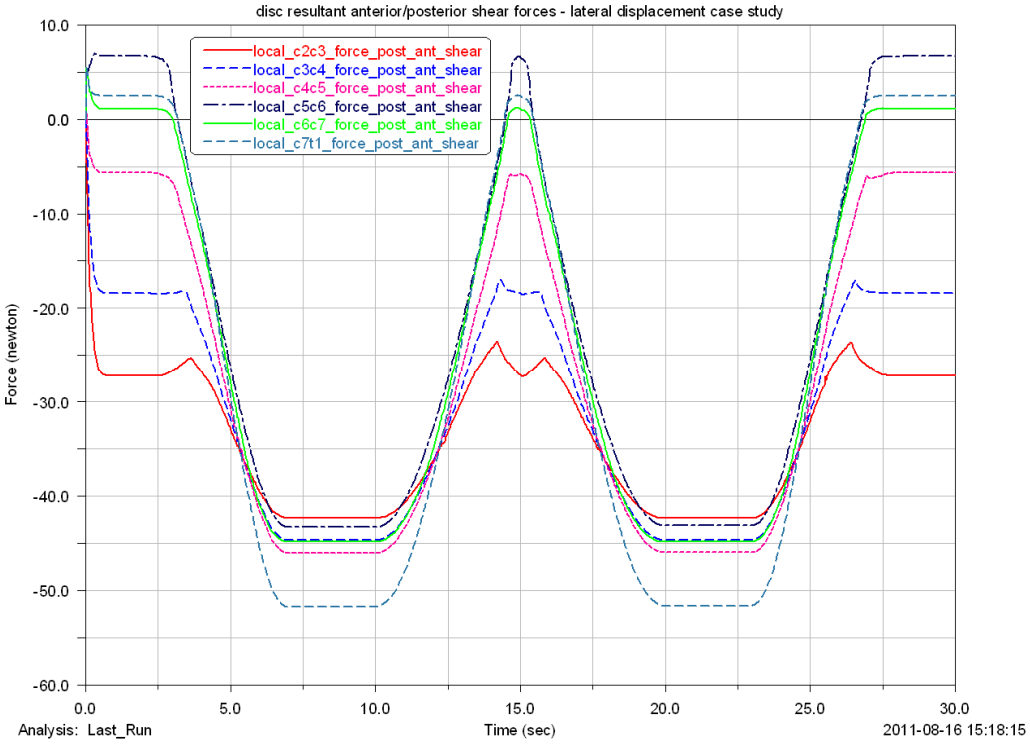

Figure B.2: Comparison of resultant posterior/anterior shear forces on the discs

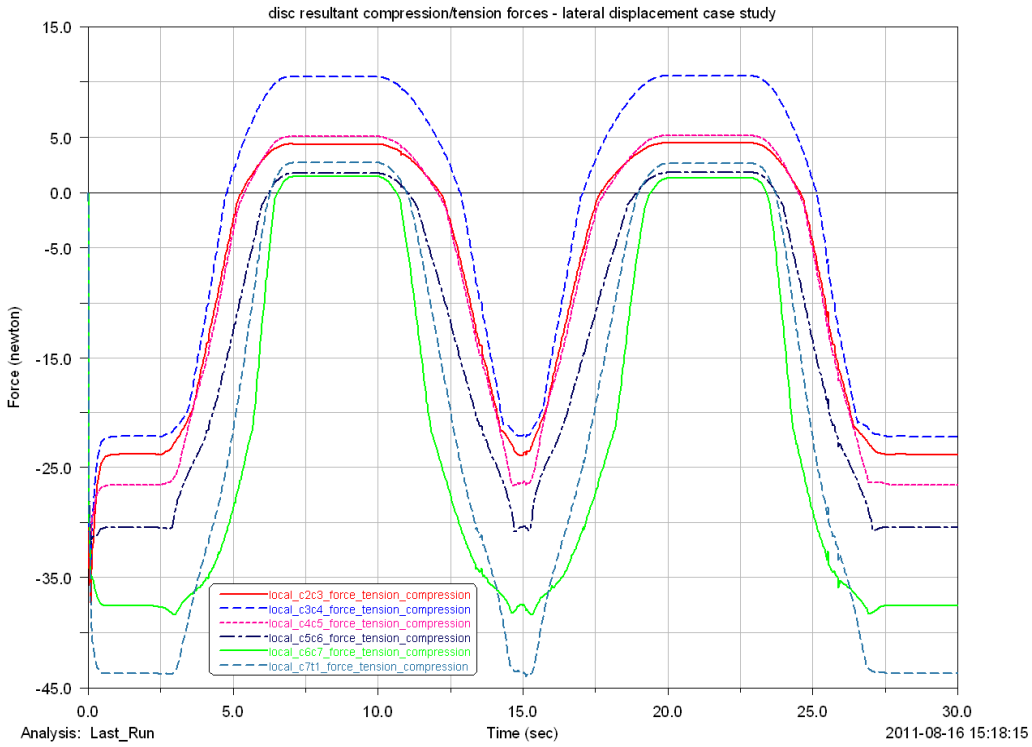

Figure B.3: Comparison of resultant tension/compression forces on the discs

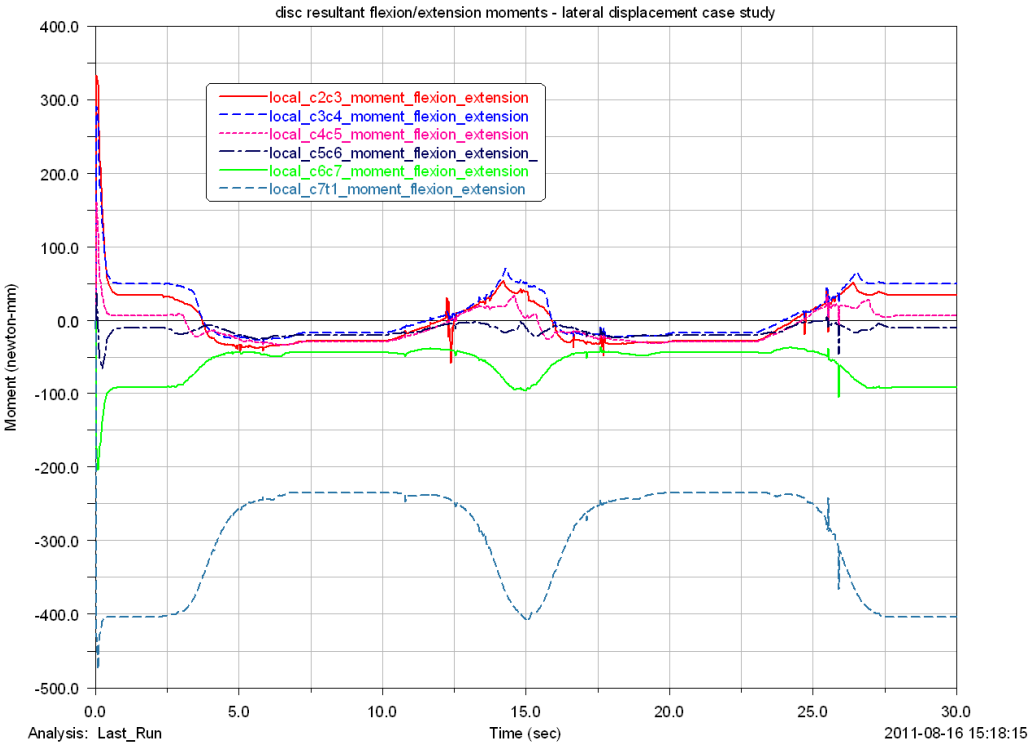

Figure B.4: Comparison of resultant flexion/extension moments on the discs

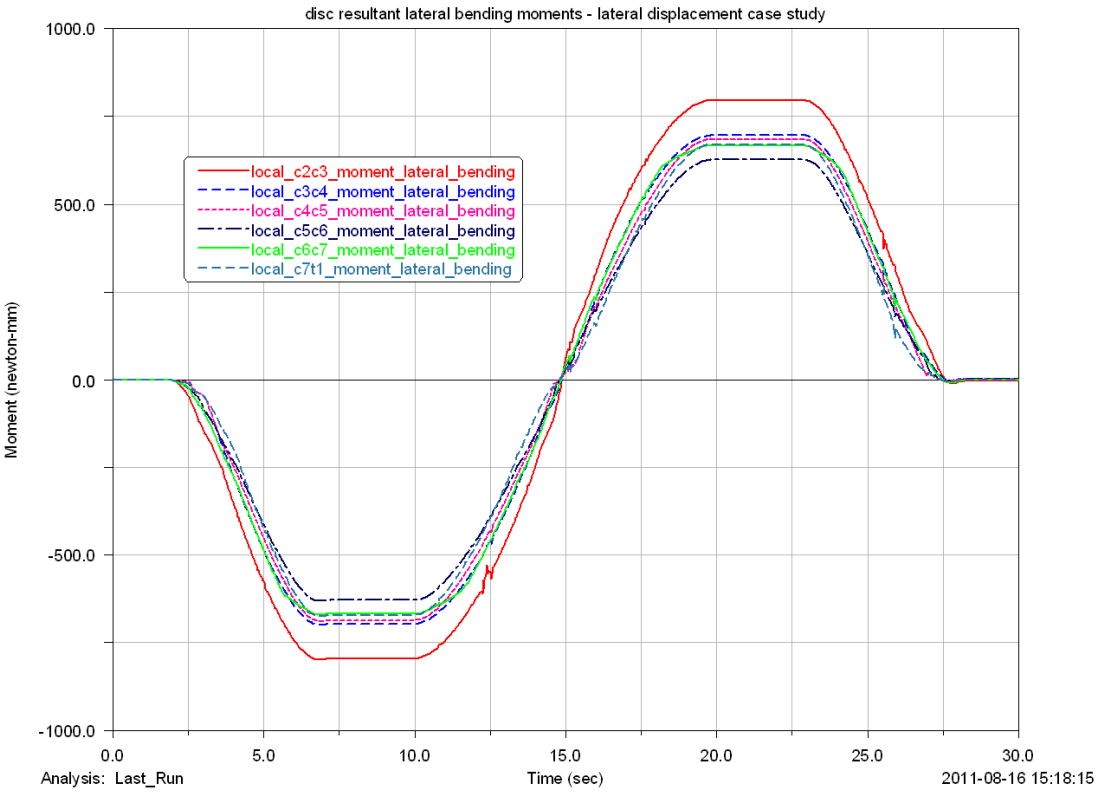

Figure B.5: Comparison of resultant lateral bending moments on the discs

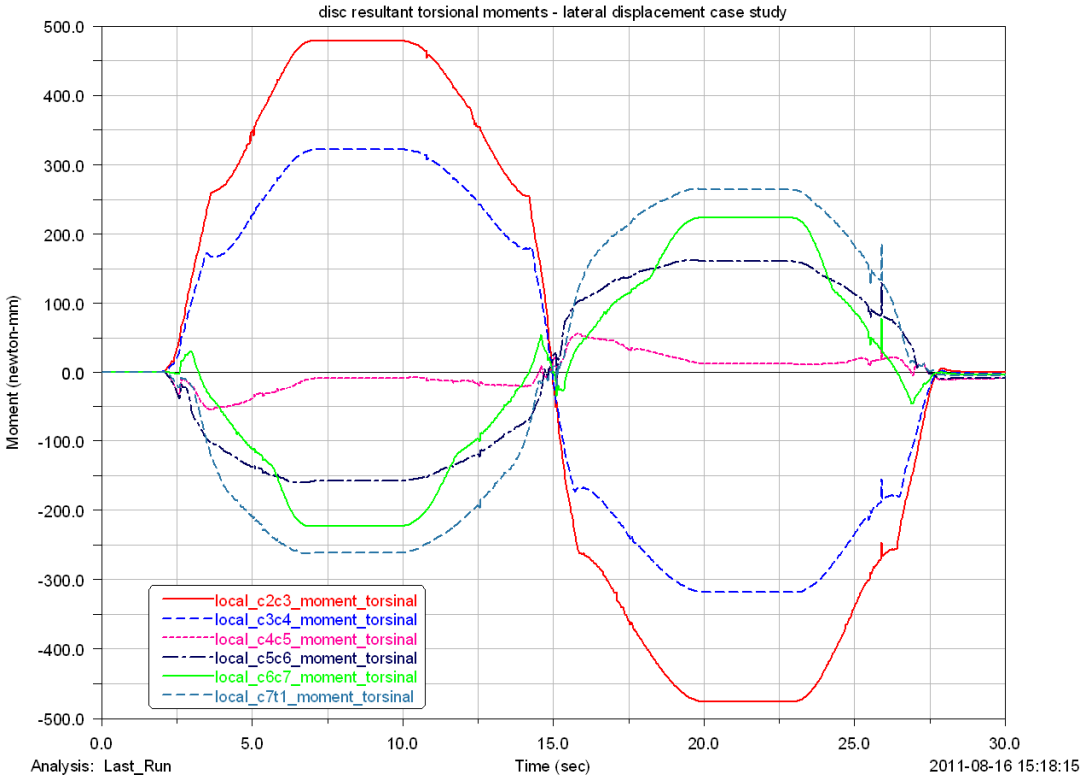

Figure B.6: Comparison of resultant torsional moments on the discs

Appendix C (torsional moment case study)

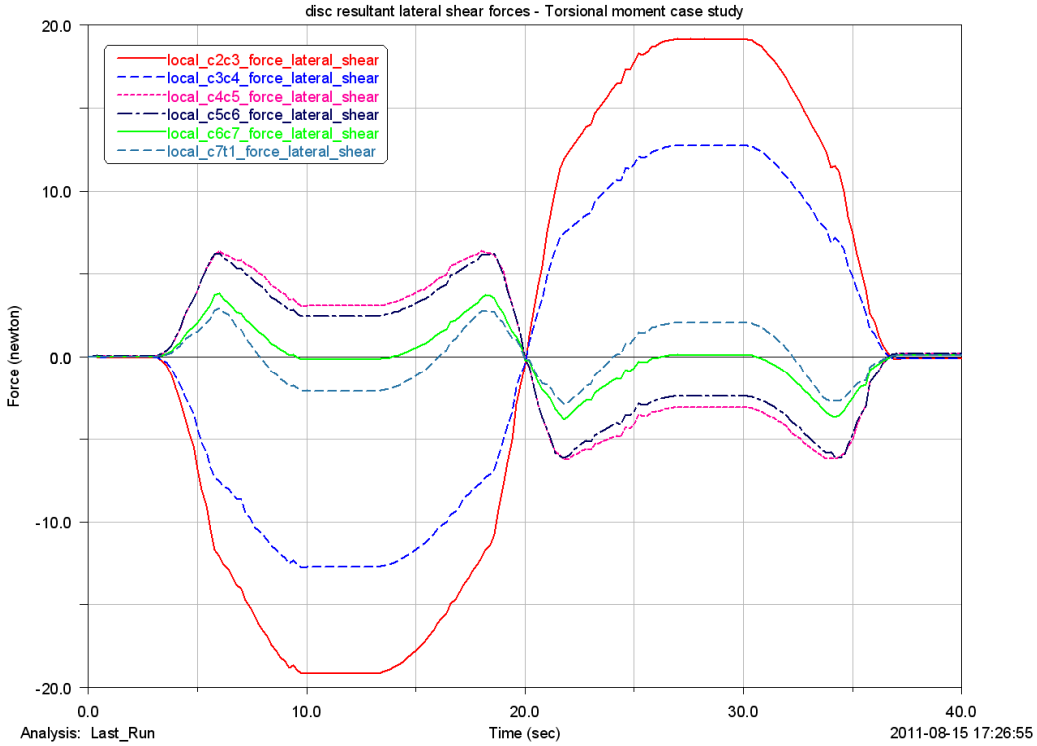

Figure C.1: Comparison of resultant lateral shear forces on the discs

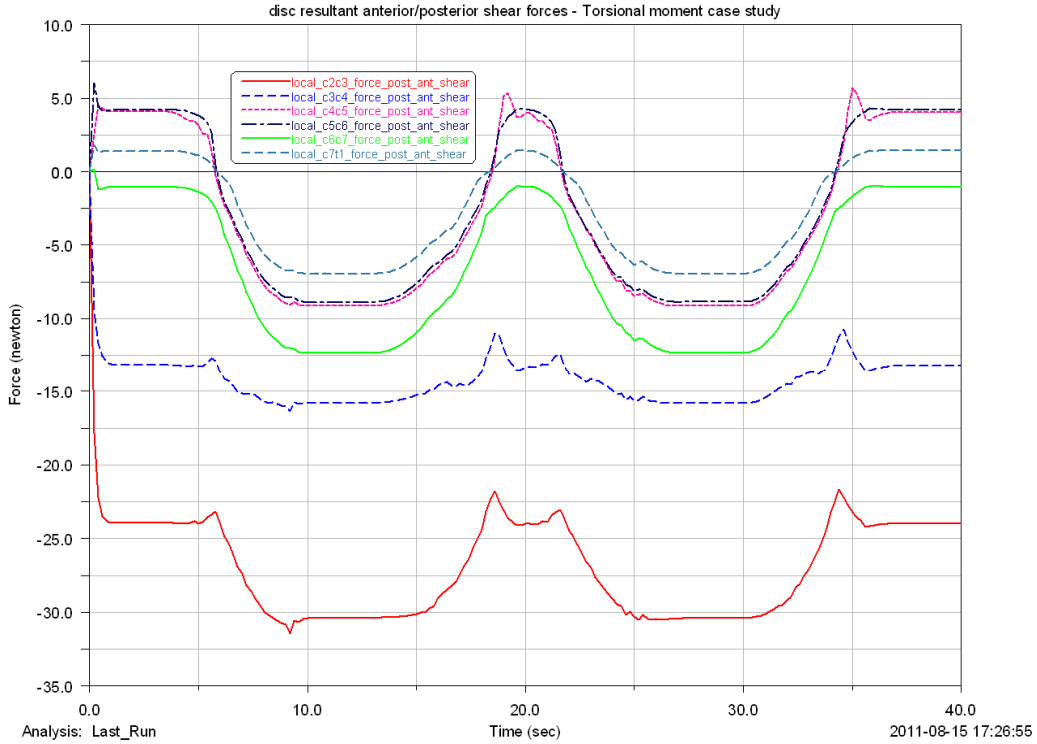

Figure C.2: Comparison of resultant posterior/anterior shear forces on the discs

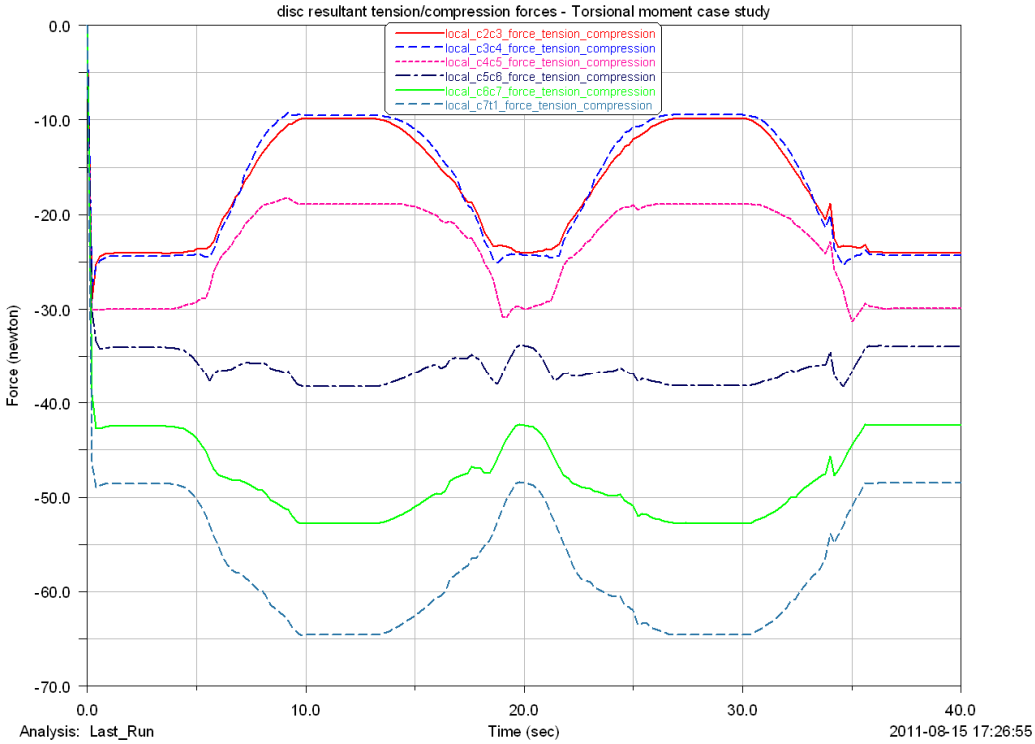

Figure C.3: Comparison of resultant tension/compression forces on the discs

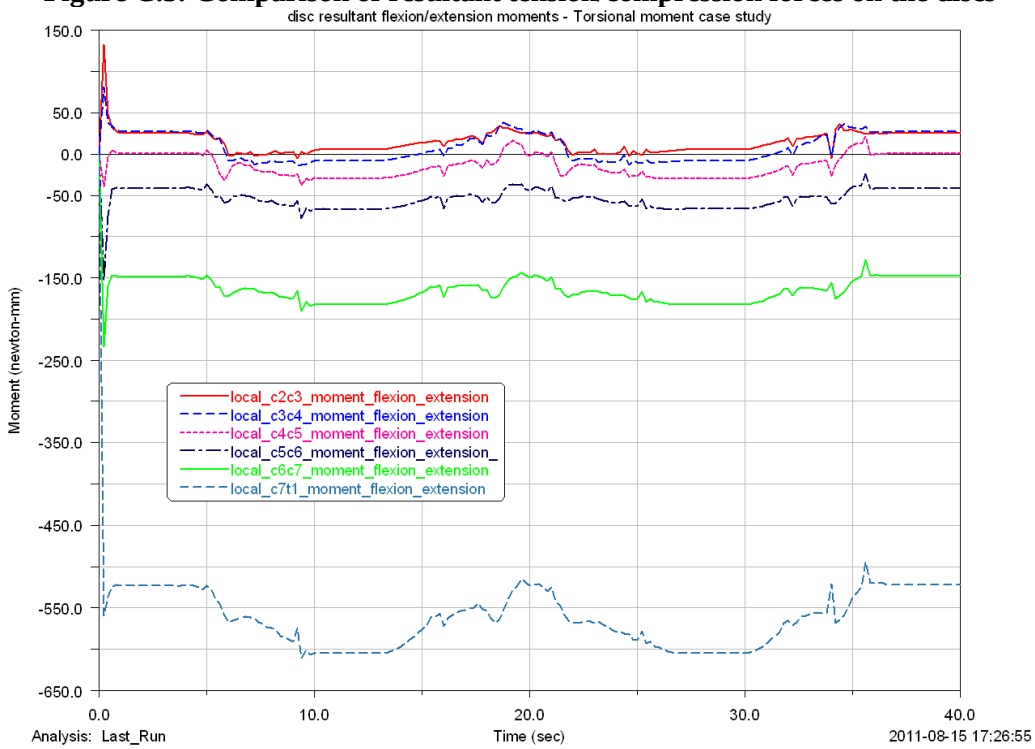

Figure C.4: Comparison of resultant flexion/extension moments on the discs

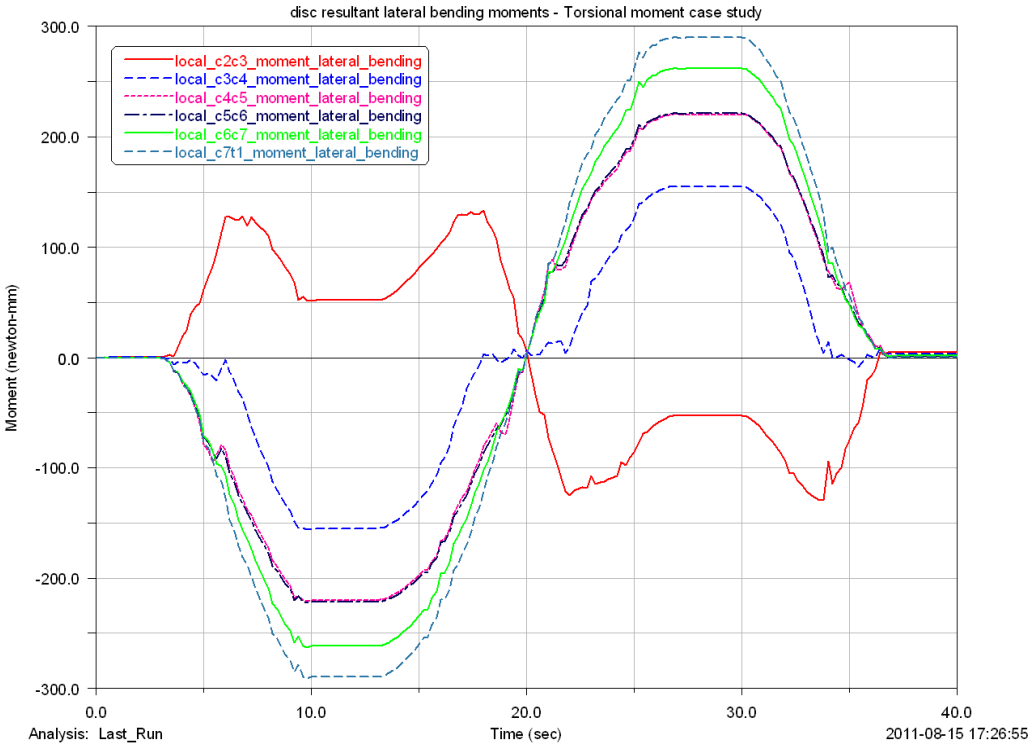

Figure C.5: Comparison of resultant lateral bending moments on the discs

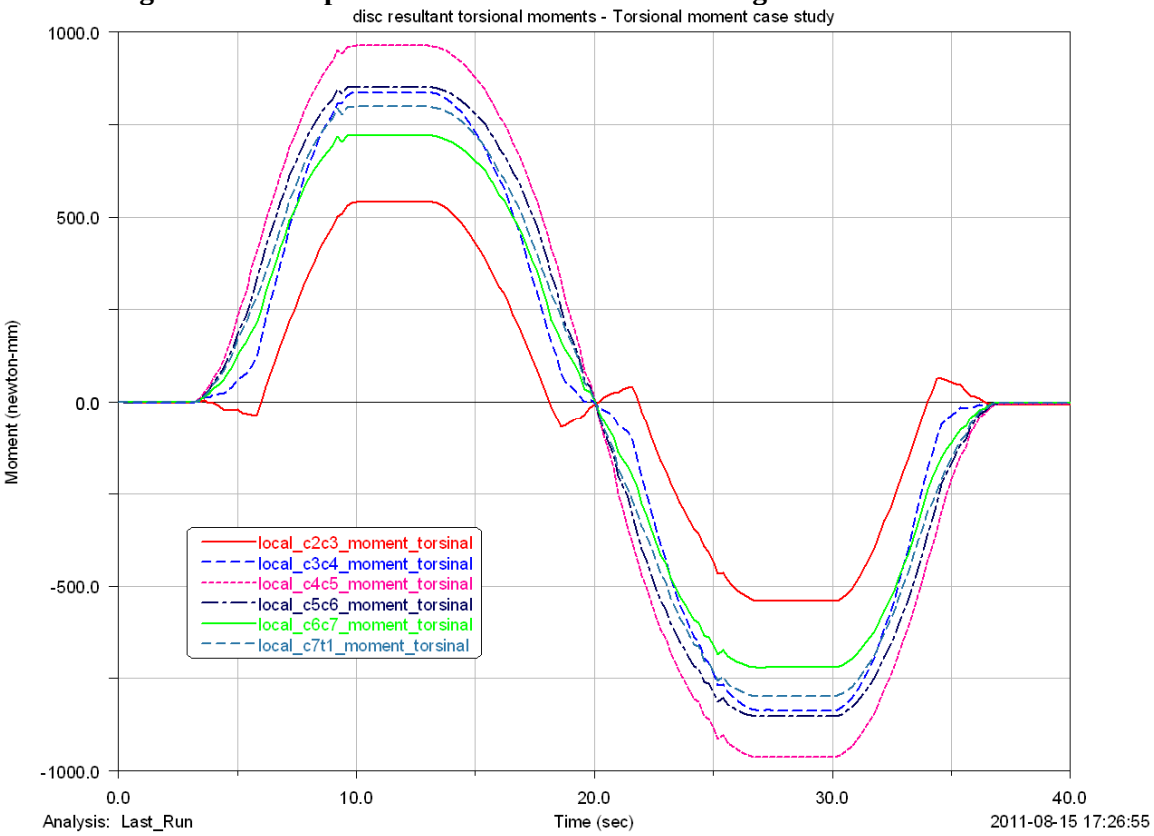

Figure C.6: Comparison of resultant torsional moments on the discs

Appendix D (sensitivity analysis)

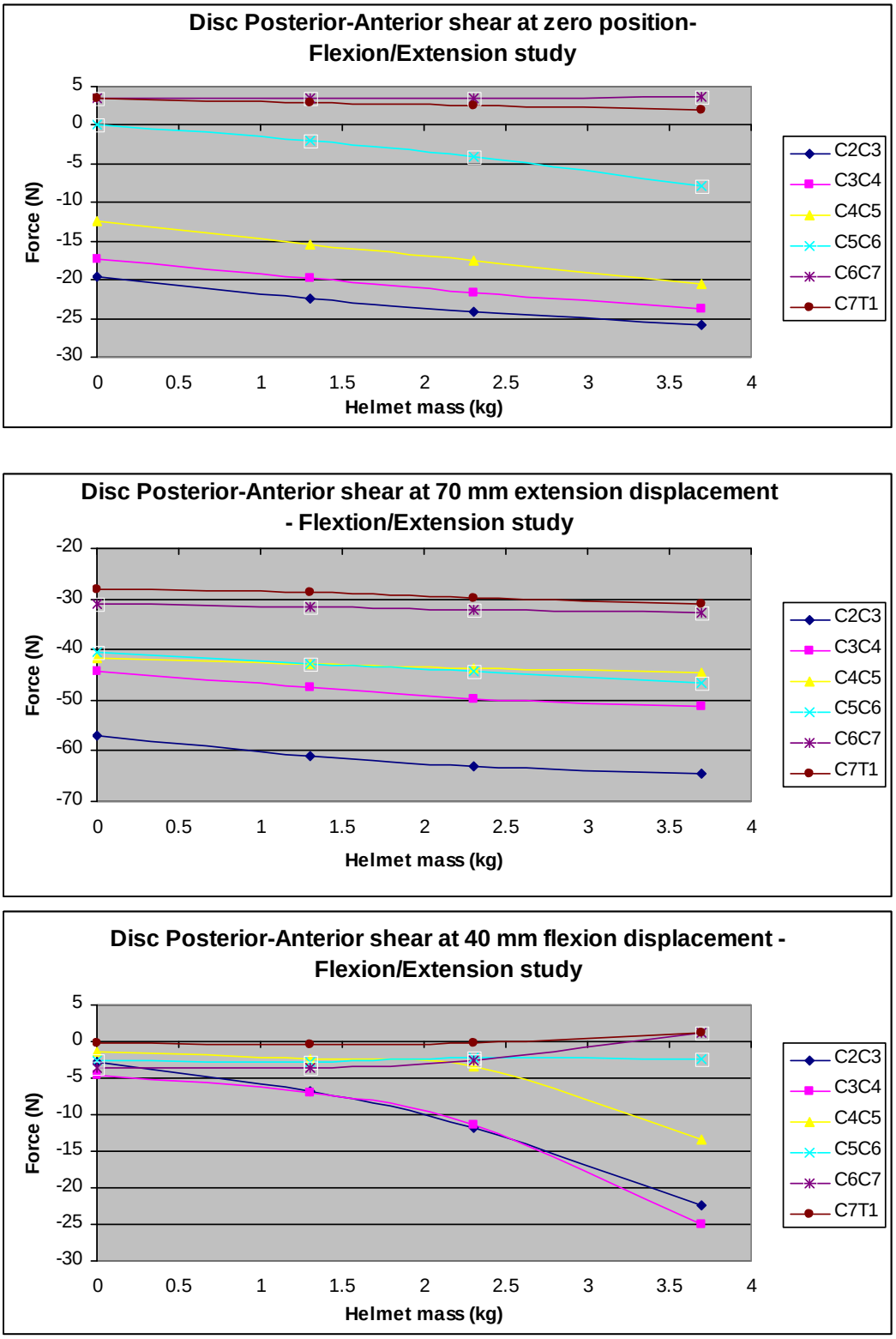

Figure D.1: Sensitivity analysis for flexion/extension case study

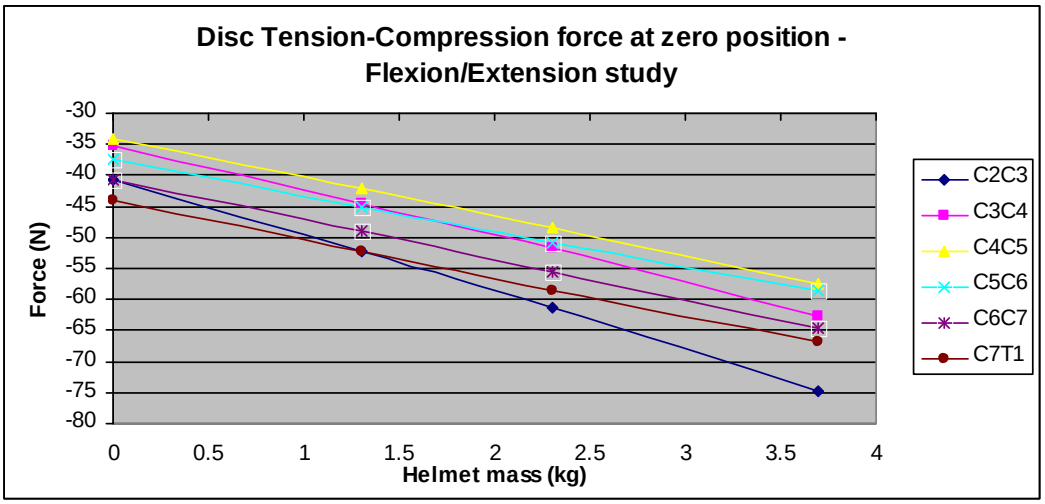

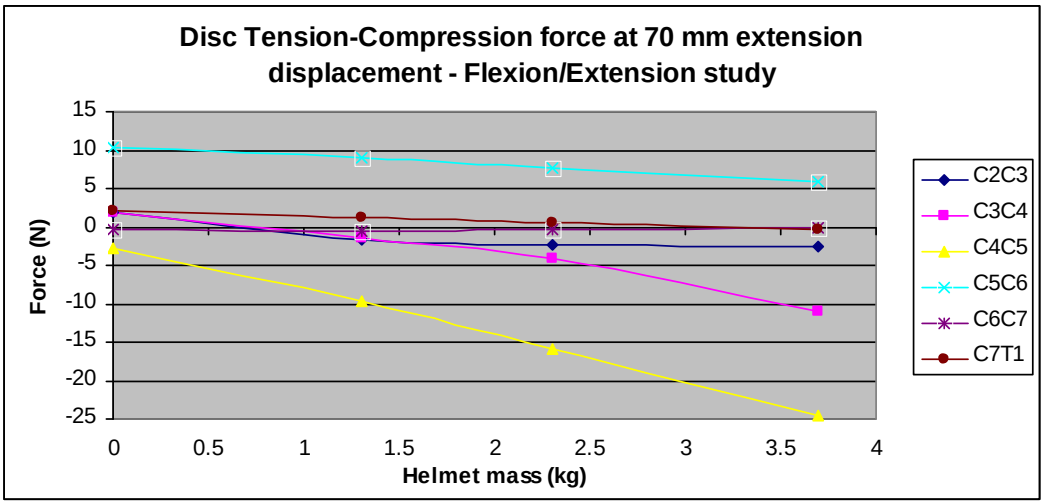

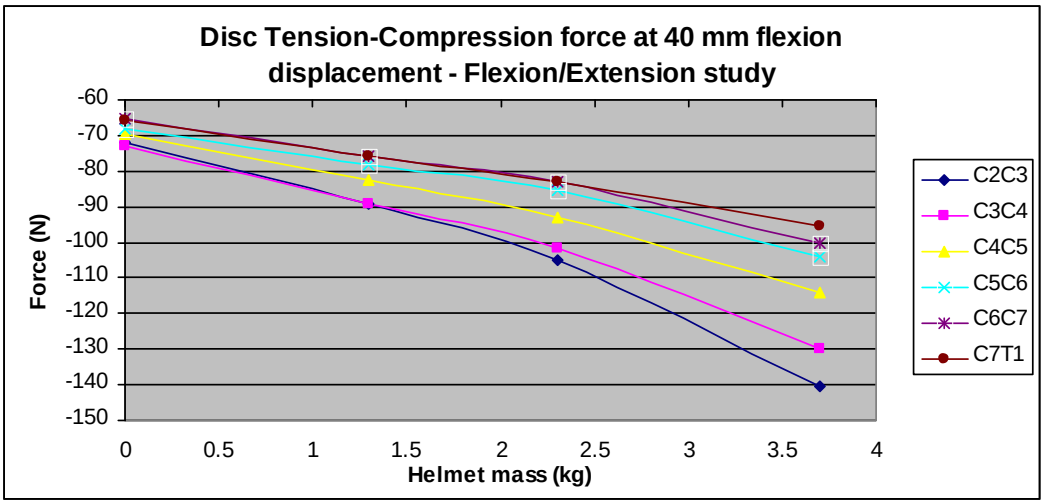

Figure D.1: Sensitivity analysis for flexion/extension case study (continued)

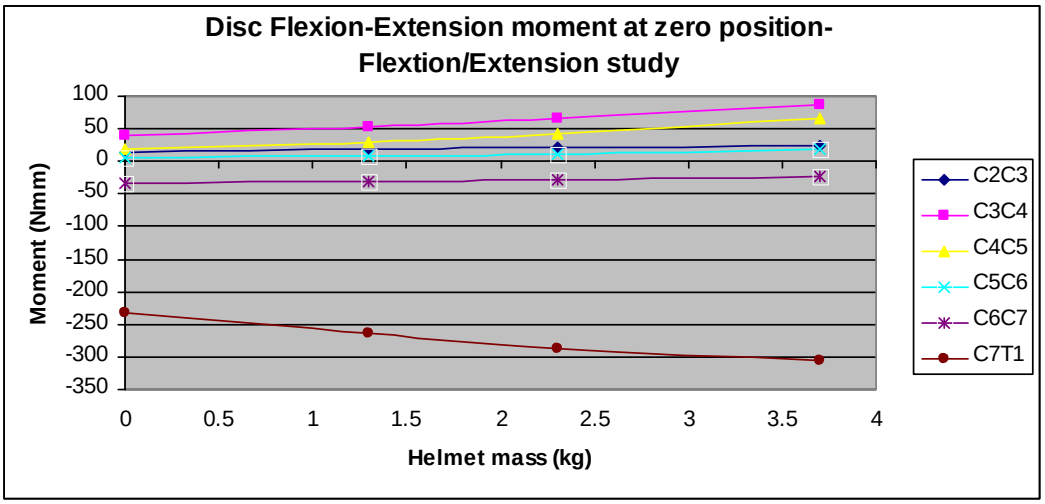

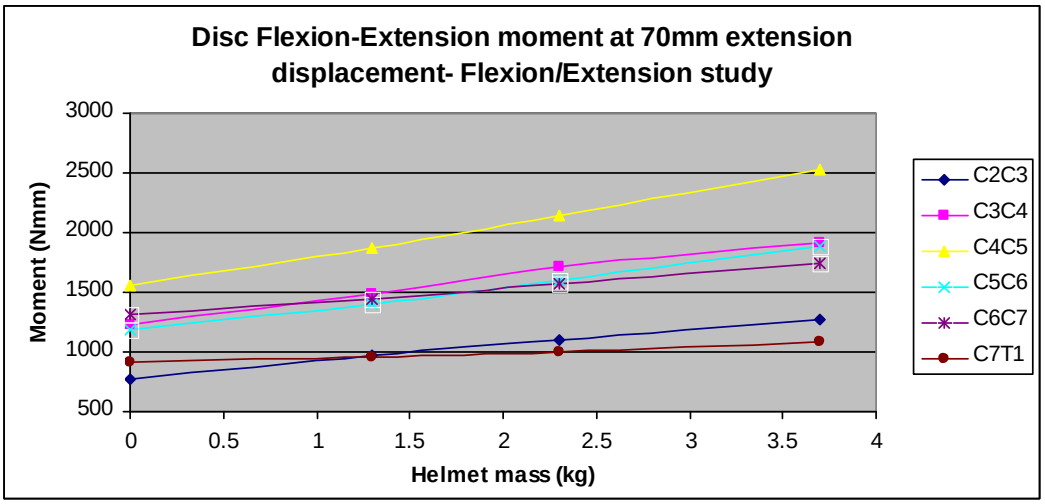

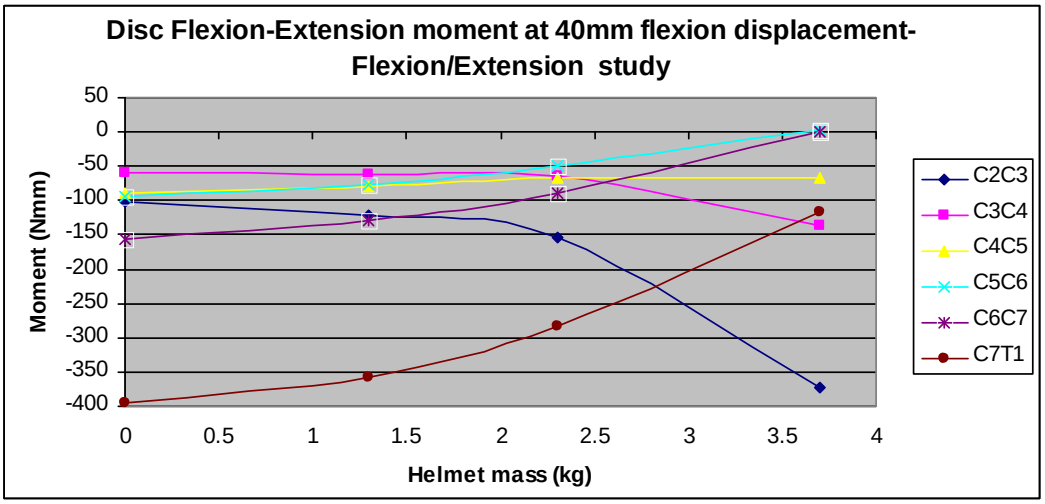

Figure D.1: Sensitivity analysis for flexion/extension case study (continued)

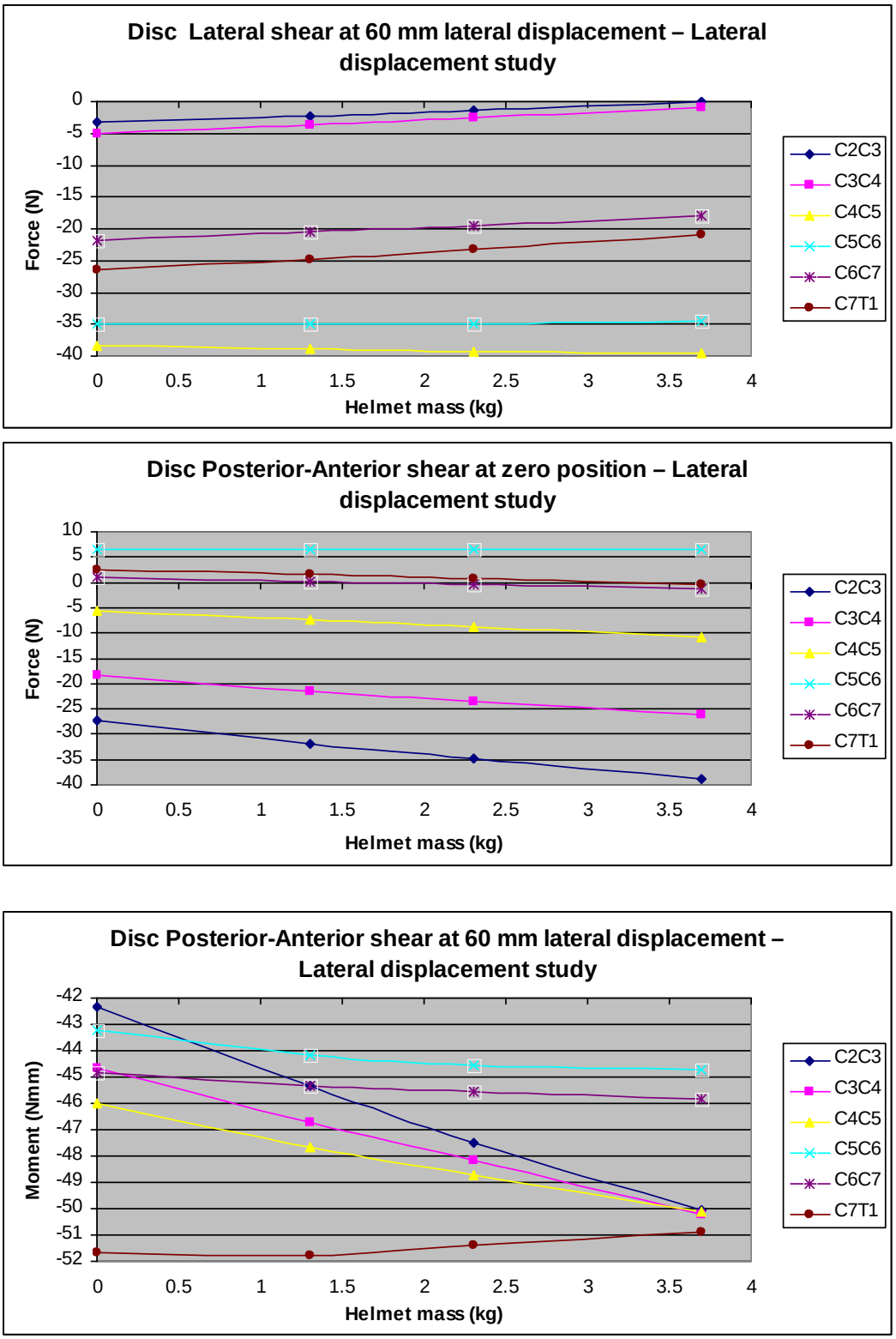

Figure D.2: Sensitivity analysis for lateral displacement case study

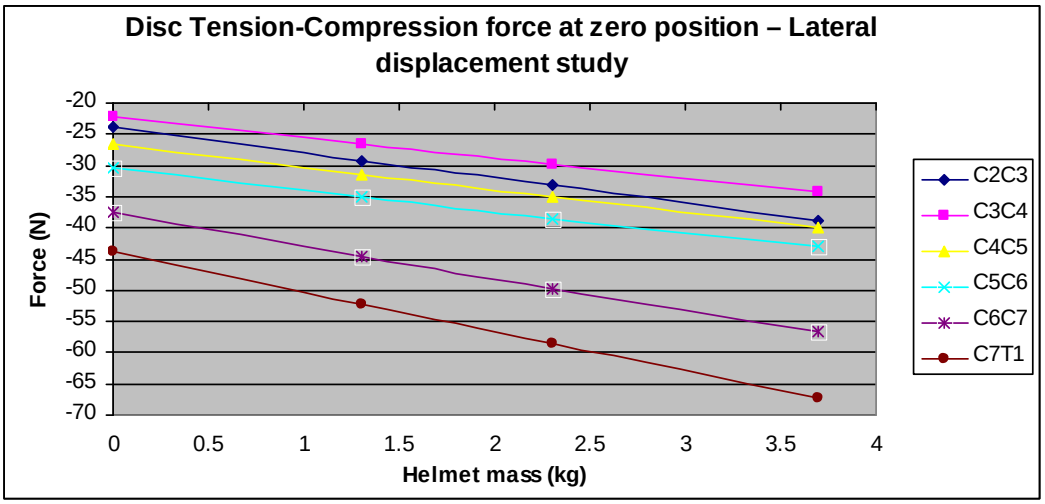

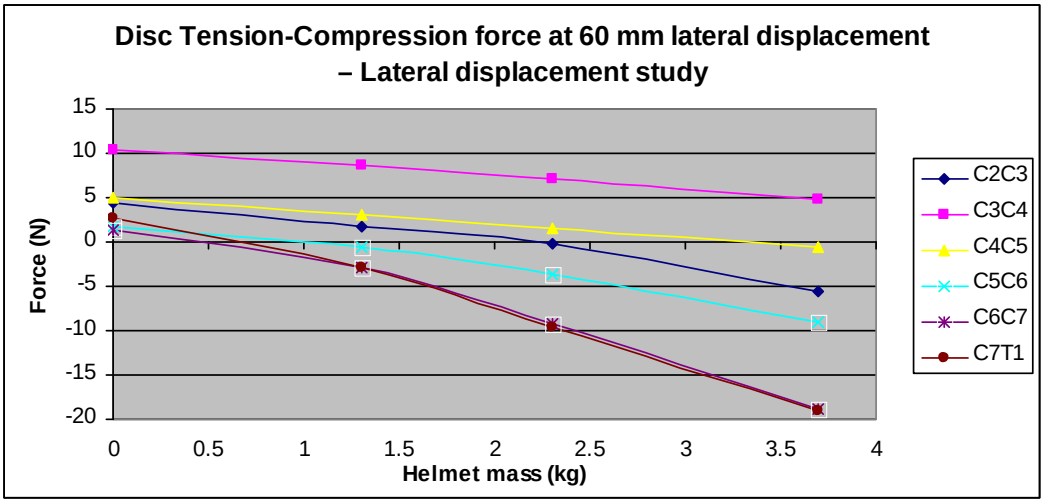

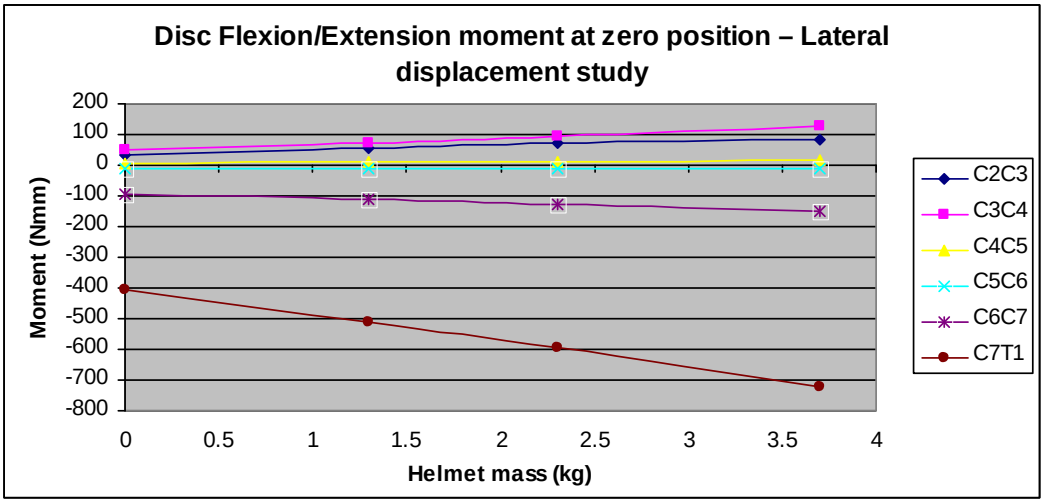

Figure D.2: Sensitivity analysis for lateral displacement case study (continued)

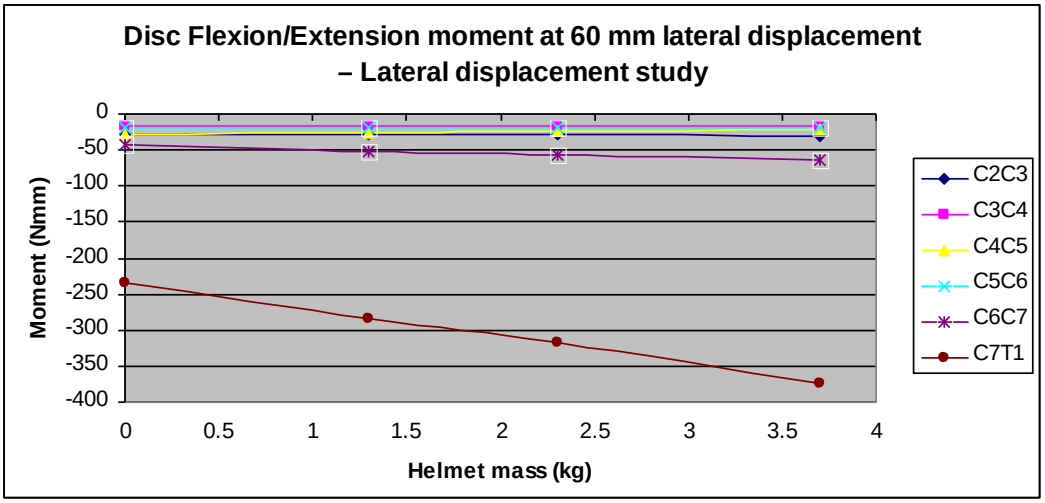

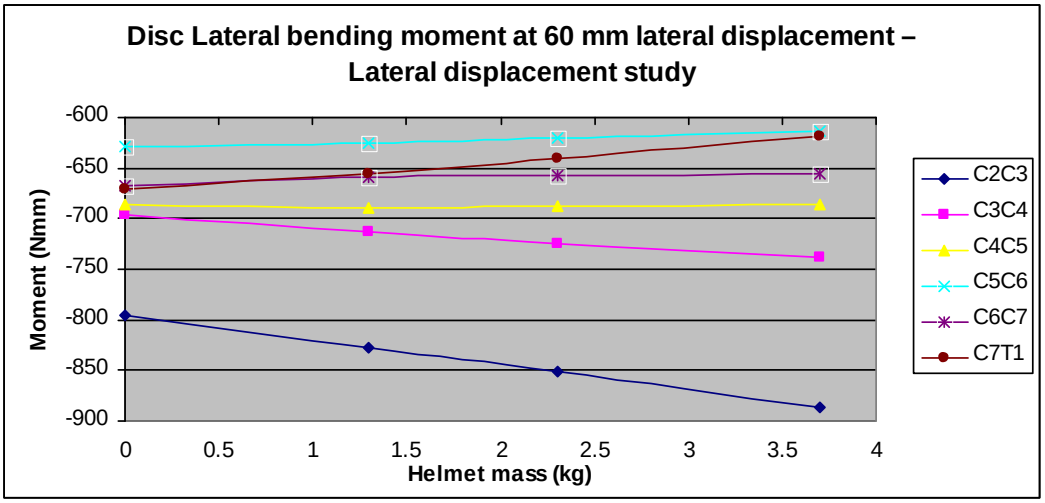

Figure D.2: Sensitivity analysis for lateral displacement case study (continued)

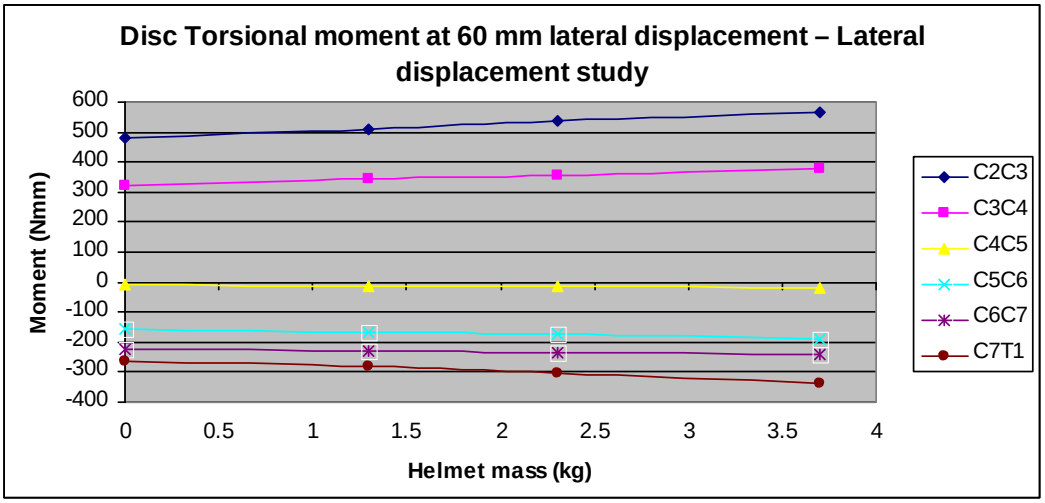

Figure D.3: Sensitivity analysis for torsional moment case study

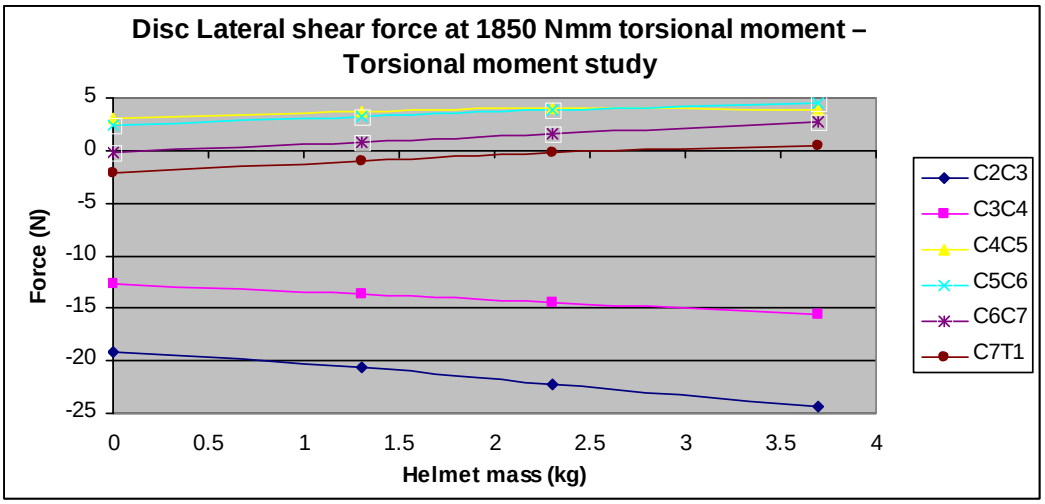

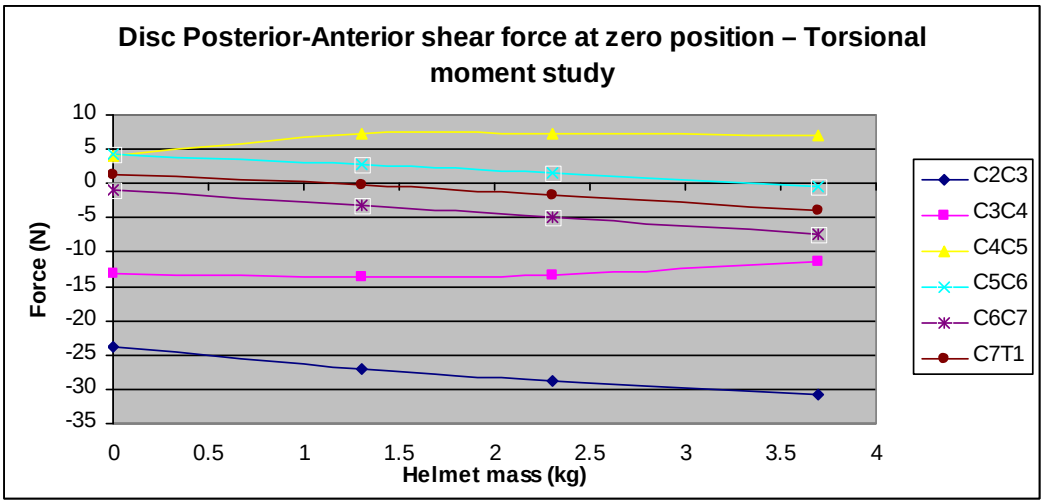

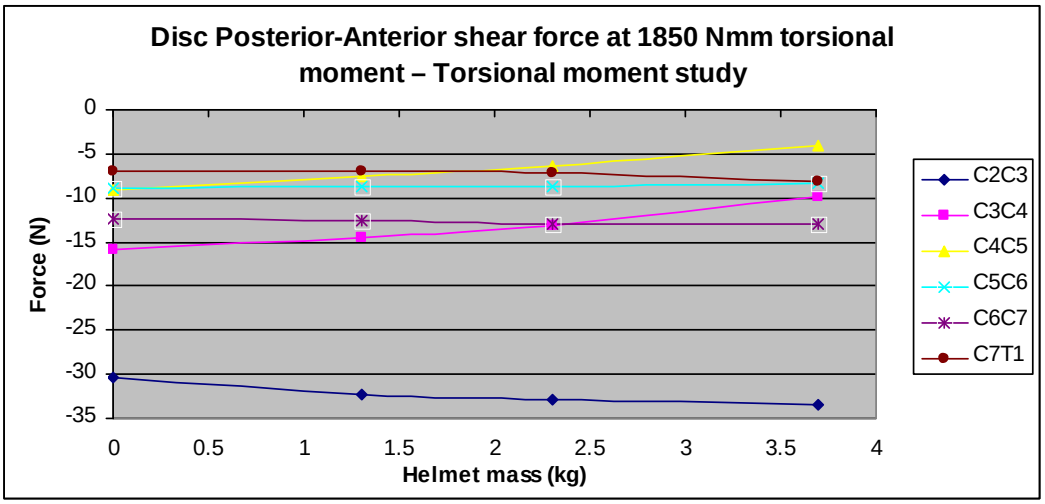

Figure D.3: Sensitivity analysis for torsional moment case study (continued)

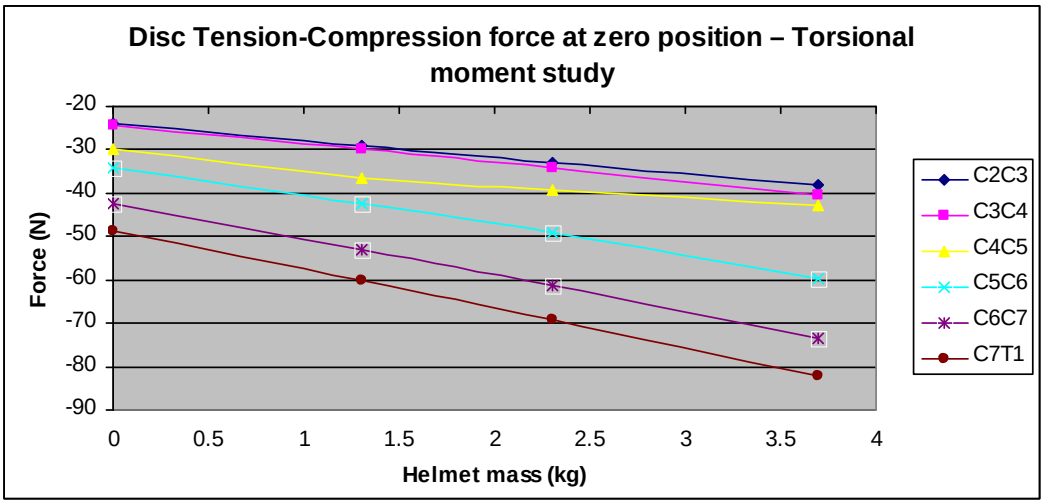

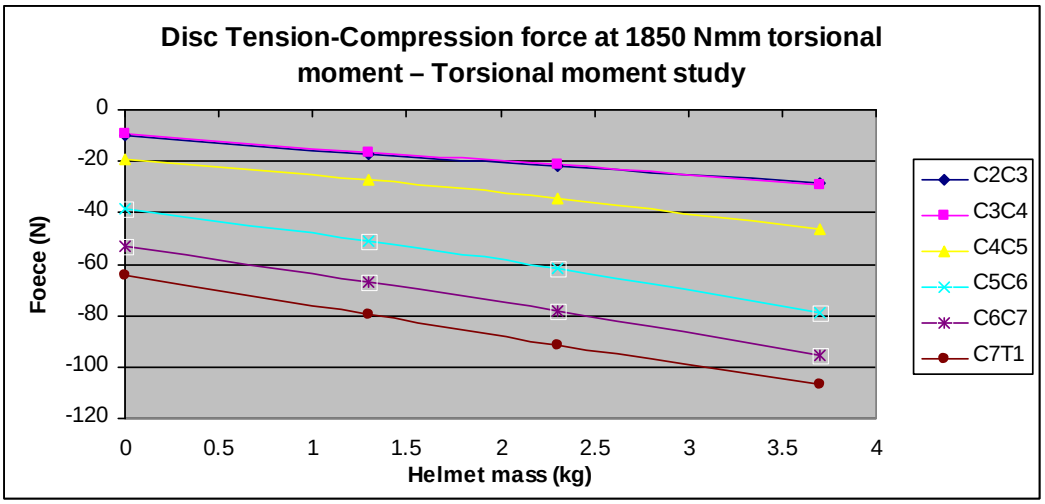

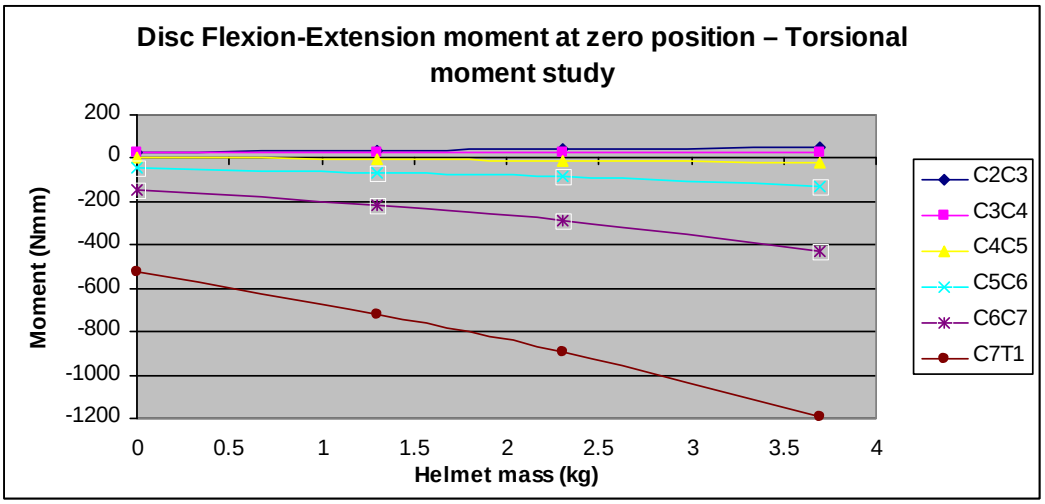

Figure D.3: Sensitivity analysis for torsional moment case study (continued)

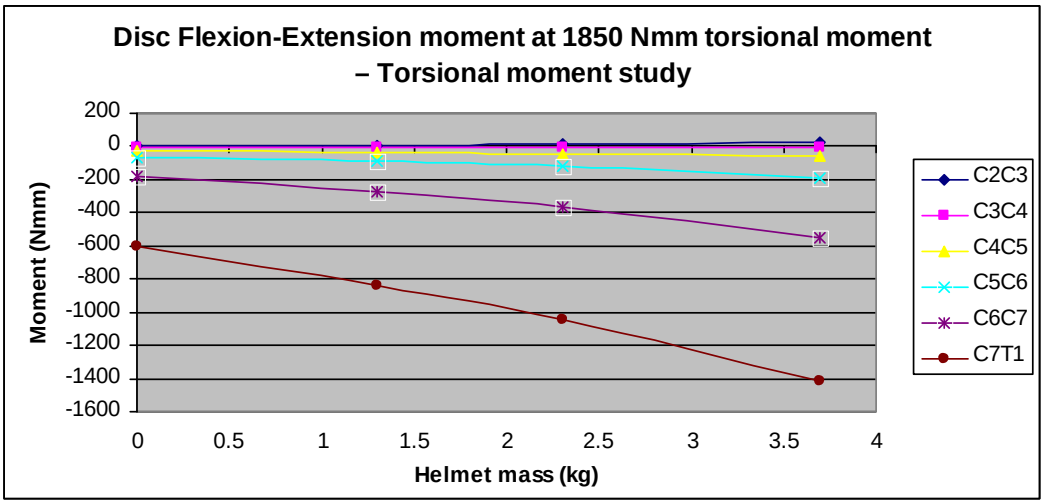

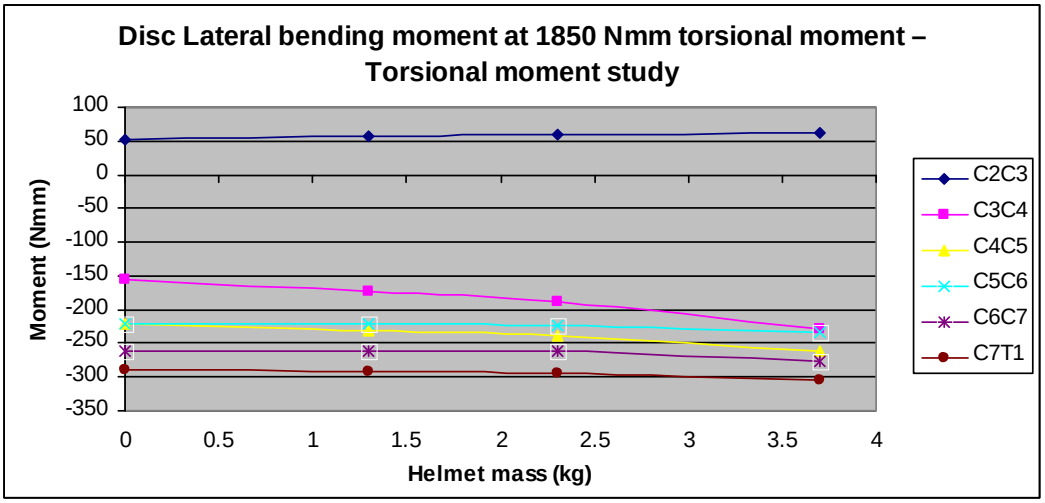

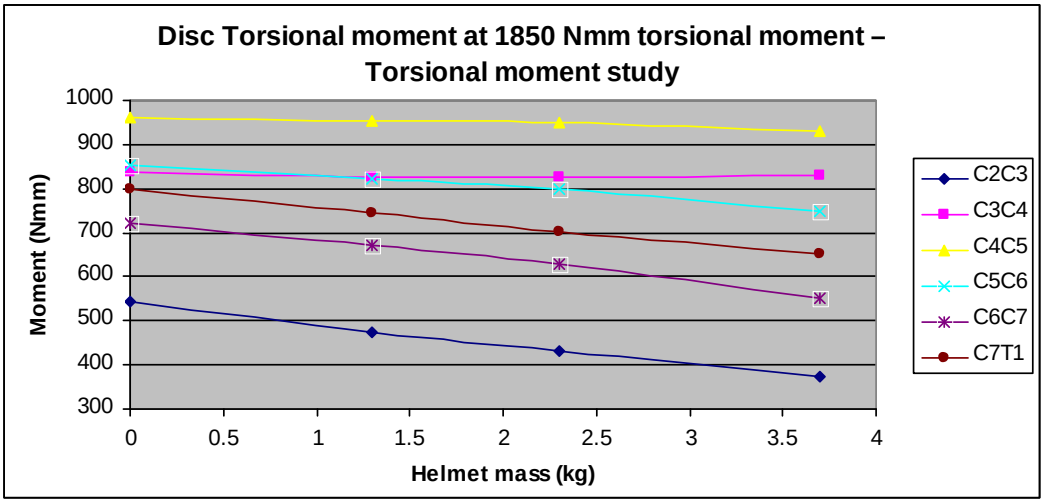

Figure D.3: Sensitivity analysis for torsional moment case study (continued)

References

Acar M., Loptic D W. V., 2007, Development of a multi-body computational model of human head and neck

Adams, M.A. and P.J. Roughley, What is intervertebral disc degeneration, and what causes it? Spine (Phila Pa 1976), 2006. 31(18): p. 2151-61.

Alem N, Nusholtz G, Melvin J., Superior–inferior head impact tolerance levels. Ann Arbor, MI: University of Michigan; 1982, 271pp.

Alem NM, Nusholtz GS, Melvin JW., Head and neck response to axial impacts. In: Proceedings of the 28th Stapp Car Crash Conference,; Warrendale, PA. 1984, p. 275–88.

Allard P., Thirty P. S., Bourgault A., Drouin G., Pressure Dependence of the Area Micrometer Method in Evaluation of Cruciate Ligament Cross-Section, J. Orthop. Res., 1979, l,pp.265-267.

Amiel D., Frank C., Harwood F., Fronek J., Akeson W., Tendons and ligaments: A Morphological and Biochemical Comparison, J. Orthop. Res., 1984, 1, pp.257-265.

Anderson L, D'Alonzo R., Fractures of odontoid process of the axis. J Bone Joint SurgAm A; 1974, 56:1663–74.

Atkinson T. S., Haut R. C., Altiero N.J., A Poroelastic Model that Predicts Some Phenomological Responses of Ligaments and Tendons, ASME J. Biomech. Eng., 1997,119,pp.400-405.

Augustus A. White, M.M.P., Clinical Biomechanics of the Spine. 2nd ed. 1990: Lippincott, Williams, and Wilkins.

Ault H. K., Hoffman A. H., A Composite Micromechanical Model for Connective Tissues: Part I, Theory, ASME J. Biomech. Eng., 1992, 114(1), pp.137-141.

Bach J. M., Hull M. L., Patterson H. A., Direct Measurement of Strain in the Posterolateral Bundle of the Anterior Cruciate Ligament, J. Biomechanics, 1997, 30(3), pp. 281-283.

Barbenel J. C., Evans J. H., Finlay J. B., Stress-Strain Time Relations for Soft Connective Tissues, In: Kenedi, Editor, Perspectives in Biomedical Engineering, New York, McMillan, 1973, pp. 165-172.

Bensoussan A., Lions J. L., Papanicolaou G., Asymptotic Analysis for Periodic Structures, Amsterdam, North-Holland, 1978.

Beskos D. E., Jenkins J. T., A Mechanical Model for Mammalian Tendon, J. Appl. Math., 1975, 42, pp. 755-758.

Betsch D. F., Baer E., Structure and mechanical properties of rat tail tendon. Biorheology, 1980, 17:83–94.

Beynnon B., Howe J. G., Pope M. H., Johnson R. J., Fleming B. C., The Measurement of Anterior Cruciate Ligament Strain in vivo, Int. Orthop., 1992, 16(1), pp. 1-12.

Bogduk, N. and S. Mercer, Biomechanics of the cervical spine. I: Normal kinematics. Clin Biomech (Bristol, Avon), 2000. 15(9): p. 633-48.

Brand R. A., What Do Tissues and Cells Know of Mechanics? Ann Med., 1997, 29(4), pp. 267-269.

Brolin K., 2002, Cervical Spine Injuries - Numerical Analyses and Statistical Survey

Butler D. L., Grood E. S., Noyes F. R., Zemicke R. F., Brackett K., Effects of Structure and Strain Measurement Technique on the Material Properties of Young Human Tendons and Fascia, J. Biomechanics, 1984, 17(8), pp. 579-596.

Camacho,D. L.,Nightingale, R.W.,Robinette, J. J.,Vanguri, S. K., Coates, D. J., and Myers, B. S. ,1997, Experimental flexibility measurements for the development of a computational head–neck model validated for near-vertex Head impact. In Proceedings of the 41st Stapp Car Crash Conference, Society ofAutomotiveEngineers,SAEpaper 973345, pp. 473–486.

Chimich D., ShriveN., Frank C., Marchuk L., and Bray R., Water Content Alters Viscoelastic Behavior of the Normal Adolescent Rabbit Medial Collateral Ligament, J. Biomechanics, 1992, 25, pp. 831-837.

Ching R, Tenser A, Anderson P, Daly C., Comparison of residual stability in thoracolumbar spine fractures using neutral zone measurements. J Orthop Res; 1995, 13:533–41.

Comninou M., Yannas LV., Dependence of Stress-Strain Nonlinearity of Connective Tissues on the Geometry of Collagen Fibers, J. Biomechanics, 1976, 9, pp. 427-433.

Daniel D.M.;Akeson W.H., O'Connor J.J., Knee Ligaments: Structure, Function, Injury and Repair, New York, Raven Press, 1990.

Danto M. I., Woo S. L. Y., The Mechanical Properties of Skeletally Mature Rabbit Anterior Cruciate Ligament and Patellar Tendon over a Range of Strain Rates, J. Orthop. Res., 1993, 11(1), pp. 58-67.

Decraemer W. F., Maes M.A., Vanhuyse V. J., An Elastic Stress-Strain Relation for

Soft Biological Tissues Based on a Structural Model, J. Biomechanics, 1980, 13, pp. 463-468.

Decraemer W. F., Maes M. A., Vanhuyse V. J., Vanpeperstraete P., A Nonlinear Viscoelastic Constitutive Equation for Soft Biological Tissues Based upon a Structural Model, J. Biomechanics, , 1980-b, 13, pp. 559-564

Diamant J., Keller A., Baer E., Litt M., Arridge R. G. C., Collagen: Ultrastructure and Its Relation to Mechanical Properties as a Function of Ageing., Proc. R. Soc. Lond., 1972, 180, pp. 293-315.

Doherty B., Heggeness M., The Quantitative Anatomy of the Atlas, Spine, 1994, 19(22), 2497-2500.

Doherty B., Heggeness M., The Quantitative Anatomy of the Second Cervical Vertebra, Spine, 1995, 20(5), 513-517.

Dong Y., Hong M., Jianyi L., Lin M., Quantitative Anatomy of the Lateral Mass of the Atlas, Spine, 2003, 28, pp. 860-863

Dvorak J., Panjabi M., Novotny J. E., Antinnes J. A., In vivo Flexion/Extension of the Normal Cervical Spine. J. Orthop Res., 1991, 9, pp. 828- 834.

Ethier C. Ross and Simmons Craig A., Introductory biomechanics from cells to organisms, 2007

Farsa M., whole cervical spine finite element model, 2006

Francis C. Dimensions of the cervical vertebrae, Anatomical Record, 1995, 122, pp. 603-609.

Ford K. A., Albert W. J., Harrison M. F., Neary J. P., Croll J., Callaghan J. P., 2011, Neck loads and posture exposure of helicopter pilots during simulated day and night flights

Foust DR, Chaffin DB, Snyder RG, Baum JK., Cervical range of motion and dynamic response and strength of cervical muscles. In: Proceedings of the 17th Stapp Car Crash Conference,; Oklahoma City, OK. 1973, p. 285–308.

France E. P., Daniels A. U., Goble E. M., Dunn H. K., Simultaneous Quantization of Knee Ligament Forces, J. Biomechanics, 1983, 16(8), pp. 553-564.

Frisen M., Magi M., Sonnerup L., Viidik A., Rheological Analysis of Soft Collagenous Tissue, Part I: Theoretical Considerations, J. Biomechanics, 1969, 2, pp.13-20.

Fujie H., Mabuchi K., Woo S. L. Y., Live ay G. A., Arai S., Tsukamoto Y., The Use of Robotics Technology to Study Human Joint Kinematics: A New Methodology, ASME J. Biomech. Eng., 1993, 115, pp. 211-217.

Fung. Y. C., Biomechanics. Mechanical Properties of Living Tissues. Springer-Verlag, New York, 2nd edition, 1993.

Fung Y. C., Perrone N., Aliker M., Stress-Strain History Relations of Soft Tissues in Simple Elongation, Englewood Cliffs, N.J. Prentice-Hall, 1972.

Gardiner J. C., Cordaro N., Weiss J. A., Elastic and Viscoelastic Shear Properties of the Medial Collateral Ligament, Trans. 46th Meeting Orthop. Res. Soc., 2000, 25, pp. 63.

Gardiner J. C., Weiss J. A., Simple Shear Testing of Parallel-Fibered Planar Soft Tissues, ASME J. Biomech. Eng., 2001.

Gardiner J. C., Weiss J. A., Strain in the Human Medial Collateral Ligament During Valgus Loading, Trans. 46th Meeting Orthop. Res. Soc., 2000, 25, pp. 774.

Glos D. L., Butler D. L., Grood E. S., Levy M. S., In vitro Evaluation of an Implantable Force Transducer (IFT) in a Patellar Tendon Model, ASME J. Biomech. Eng., 1993, 115, pp. 335-343.

Goel V. K., Biomechanics of the Spine: Clinical and Surgical Perspective, CRC Press, 1990.

Gray, H., W.H. Lewis, and Bartleby.com Inc., Anatomy of the human body, Bartleby.com: New York, 2000.

Guedes J. M., Nonlinear Computational Models for Composite Materials Using Homogenization, Ph.D. Dissertation, University of Michigan, 1990.

Hashin Z., Rosen B. W., The Elastic Moduli of Fiber-Reinforced Materials, ASME J. Appl. Mech., 1964, 31, pp. 223-232.

Hildebrandt J., Fukaya H., Martin C. J., Simple Uniaxial and Uniform Biaxial Deformation ofNearly Isotropic Incompressible Tissues, Biophysical J., 1969, 9, pp. 781-791.

Hirokawa S., Yamamota K., Kawada T., A Photoelastic Study of Ligament Strain, IEEE Trans. Rehabil. Eng., 1998, 6(3), pp. 300-308.

Holdsworth H., 1963, Fractures, dislocations and fractures-dislocations of the spine. J Bone Joint SurgBr B; 2001, 45:6–20.

Hollis J. M., Takai S., Adams D. J., HoribeS., WooS. L. Y., The Effects of Knee Motion and External Loading on the Length of the Anterior Cruciate Ligament (ACL): A Kinematic Study, ASME J. Biomech. Eng., 1991, 113(2), pp. 208-214.

Holzapfel G. A., Biomechanics of Soft Tissue, 2000-a

Holzapfel G. A., Nonlinear Solid Mechanics. A Continuum Approach for Engineering. John Wiley & Sons, Chichester, 2000-b

Hughes D. W., Kirby M. C., Sikoryn T. A., Apsden R. M., Cox A. J., Comparison of Structure, Mechanical Properties, and Functions of Lumbar Spinal Ligaments, Spine, 1990, 15(8), pp. 787-795.

Hurschler C., Loit-Ramage B., Vanderby R., A Structurally Based Stress-Stretch Relationship for Tendon and Ligament, ASME J. Biomech. Eng., 1997, 119, pp. 392-399.

Jager, Johannes M. K. , 1998, Mathematical Head-Neck Models for Acceleration Impacts

Johannes L., Verlag G. T., Clinical anatomy ofthe cervical spine, 1993.

Karin Blorin, Cervical Spine Injuries - Numerical Analyses and Statistical Survey, 2002

Kastelic J., Palley I., and Baer E., The Multicomposite Ultrastructure of Tendon, Conn. Tiss. Res., 1978, 6, pp. 11-23.

Kastelic J., Palley I., Baer E., A Structural Mechanical Model for Tendon Crimping, J. Biomechanics, 1980, 13, pp. 887-893.

Kevin L. Troyer, Comprehensive Viscoelastic Characterization of Human Lower Cervical Spine Ligaments (PHD Thesis), 2010

Komi P., Relevance of in vivo Force Measurements to Human Biomechanics, J. Biomechanics, 1990, 23, pp. 23-34.

Kwan M. K., Lin T. H., Woo S. L.Y., On the Viscoelastic Properties of the Anteromedial Bundle of the Anterior Cruciate Ligament, J. Biomechanics, 1993, 26, pp. 447-452.

Lam T., Frank C., Shrive N., Calibration Characteristics of a Video Dimension Analyzer System, J. Biomechanics, 1992, 25(10), pp. 1227-31.

Lanir Y., A Structural Theory for the Homogeneous Biaxial Stress-Strain Relationships in Flat Collagenous Tissues, J. Biomechanics, 1979, 12, pp. 423- 436.

Lanir Y., A Microstructure Model for the Rheology of Mammalian Tendon, ASME J. Biomech. Eng., 1980, 102, pp. 332-339.

Lanir Y., Constitutive Equations for Fibrous Connective Tissues, J. Biomechanics, 1983, 16(1), 1-12.

Larson SJ., Vertebral injury and instability. In: Holtzman RNN, editor. Spinal instability. New York: Springer; 1993, p. 101–37.

Larson SJ, Maiman DJ., In: Surgery of the lumbar spine. New York, NY: Thieme; 1999, p. 334.

Lee T. Q., Woo S. L. Y., A New Method for Determining Cross-Sectional Shape and Area of Soft Tissues, ASME J. Biomech. Eng., 1988, 110, pp. 110-114.

Levine A, Edwards C., Treatment of injuries in C1–C2 complex. Orthop Clin North Am; 1986, 17:31–44.

Liao H., Belkoff S. M., A Failure Model for Ligaments, J. Biomechanics, 1999, 32(2), pp. 183-188.

Liggins A. B., Shemerluk R., Hardie R., Finlay J. B., Technique for the Application of Physiological Loading to Soft Tissue in vitro, J. Biomed. Eng., 1992, 14(5), pp. 440-441

Liu Y. K., Krieger K. W., Njus G., Quantitative Geometry of Young Human Male Cervical Vertebrae, NTIS Report No. AFAMRL-TR, 1982, pp. 80-138.

Lowery D., Wald M., Browne B., Tigges S., Hoffman J., Mower W., Epidemiology of Cervical Spine Injury in Victims, Ann. Emergency Medicine, 2001, 38 (1), pp. 12-16.

Madsen Jens Bay, Adams Solver Training notes, 2007

Mercer S., Bogduk N., The Ligaments and Annulus Fibrosus of Human Adult Cervical Intervertebral Discs, Spine, 1999, 24, pp. 619-628.

Minns, R. J., Soden P. D., Jackson D. S., The role of the fibrous components and ground substance in the mechanical properties of biological tissues: A preliminary investigation. J. Biomech., 6:153–165, 1973.

Moore, R.J., The vertebral end-plate: what do we know? Eur Spine J, 2000. 9(2): p. 92-6.

Moroney, S. P., Schultz, A. B., Miller, J. A. A., and Andersson, G. B. J., 1988, Load-displacement properties of lower cervical spine motion segments. J.Biomech., 21(9), 769–779.

Mow V. C., Kuei S. C., Lai W. M., Armstrong C. G., Biphasic Creep and Stress Relaxation of Articular Cartilage: Theory .and Experiments, ASME J. Biomech. Eng., 1980, 102, pp. 73-84.

Murray G, Persellin R., Cervical fracture complicating ankylosing spondylitis. Am J Med; 1981, 4:1033–41.

Myklebust JB, Pintar F, Yoganandan N, Cusick JF, Maiman D, Myers TJ, Sances A., Tensile Strength of Spinal Ligaments, Spine, 1988, 13, pp. 526-531.

Naderi S., Guvencer M., Korman E., An Anatomical Study of the C-2 Pedicle, Journal of Neurosurgery, 2004, 3, pp. 306-310

Nissan M., Gilad I., A Study of Vertebra and Disc Geometric Relations of the Human Cervical and Lumbar Spine, Spine, 1986, 11(2), pp. 154-157

Nimni M. E., Harkness R. D., Molecular structure and functions of collagen. In M. E. Nimni, editor, Collagen, pages 3–35. CRC Press, Boca Raton, FL., 1988.

Panjabi M., Duranceau J., Goel V., Cervical Human Vertebrae Quantitative Three-dimensional Anatomy of the Middle and Lower Regions, Spine, 1992, 17, pp. 299-306.

Panjabi M., Oda T., Crisco J. J., Bueff H. H., Grob D, Vorak J. D., 1992, Role of tectorial membrane in the stability of the upper cervical spine

Panjabi M., Oxland T., Parks E., Quantitative Anatomy of Cervical Spine Ligaments, Part I: Upper Cervical Spine, J. Spinal Disord., 1991, 4(3), pp. 270-27.

Panjabi M., Oxland T., Takata K., Goel V., Duranceau J., Krag M., Articular Facets of the Human Spine, Quantitative Three-Dimensional Anatomy, Spine, 1993, 18(10), pp.1298-1310.

Panjabi M., Takata K., Goel V., Federico D., Oxland T., Duranceau J., Krag M., Thoracic Human Vertebrae, Quantitative Three-Dimensional Anatomy, Spine, 1991-b, 16(8), pp. 888-901.

Pech P., Bergstrom K., Rauschning W., Haughton W., Attenuation Values, Volume Changes and Artifacts in Tissue due to Freezing, Acta. Radiol., 1987, 28, pp.779-782

Penning, L. and J.T. Wilmink, Rotation of the cervical spine. A CT study in normal subjects. Spine, 1987. 12(8): p. 732-8.

Pintar FA, Yoganandan N, Gennarelli TA., Head–neck tension biomechanical models for pediatric and small female populations. In: Proceedings of the 43rd AAAM Conference; Barcelona, Spain, 1999, p. 357–66.

Pintar F. A., Yoganandan N., Kumaresan S., 2001, Biomechanics of the cervical spine Part 2. Cervical spine soft tissue responses and biomechanical modeling

Pintar F, Yoganandan N, Voo L, Cusick J, Maiman D, Sances Jr., A. Dynamic characteristics of human cervical spine. SAE Trans; 1995, 104:3087–94

Pintar FA, Yoganandan N, Voo L., Effect of age and loading rate on human cervical spine injury threshold. Spine; 1998, 23:1957–62.

Przybylski G., Patel P., Carlin G., Woo S., Quantitative anthropometry of the subatlantal cervical longitudinal ligaments, Spine, 1998, 23, pp. 893-898.

Quapp K. M., Weiss J. A., Material Characterization of Human Medial Collateral Ligament, ASME J. Biomech. Eng., 1998, 120, pp. 757-763.

Ramachandran G. N., Chemistry of collagen. In G. N. Ramachandran, editor, Treatise on Collagen, pages 103–183. Academic Press, New York, 1967.

Rauschning W., Surface cryoplaning, a Technique for Clinical Anatomical Correlations, Ups J. Med. Sci., 1986, 91, pp. 251-255.

Rothman RH, Simeone FA., 3rd ed. The spine, vol. 1. Philadelphia, PA: Saunders; 1992, p. 969.

Saldinger P., Dvorak J., Rahn B., Perren S.., Histology of the Alar and Transverse Ligaments, Spine, 1990, 15, pp. 257-261.

Schaffler M., Alson M., Heller J., Garfin S., Morphology of the Dens, A Quantitative Study, Spine, 1992, 17(7), 738-743.

Shabana,A.A., Computational Dynamics. John Wiley & Sons, 1994

Shabana Ahmed A., Dynamics of Multibody Systems, 2005

Sharma M., Langrana N.A., Rodriguez J., Role of Ligaments and Facets in Lumbar Spinal Stability, Spine, 1995, 20, pp. 887-900.

Simon B. R., Wu J. S., Carlton M. W., Evans J. H., Kazarian L. E., Structural Models for Human Spinal Motion Segments Based on a Poroelastic View of the Intervertebral Disc, ASME J. Biomech. Eng., 1985, 107(4), pp. 327-335.

Tan S. H., Teo E. C., Chua H. C., Quantitative three-dimensional anatomy of cervical ,thoracic and lumbar vertebrae of Chinese Singaporeans, European Spine Journal, 2004, 13, pp.137-146.

Tani T, Yamamoto H, Kimura J., Cervical spondylotic myelopathy in elderly people: high incidence of conduction block at C3-4 or C4-5. J Neurol NeurosurgPsychiatry 1999, 1;66:456–64.

Thorngren K, Liedberg E, Aspelin P., Fractures of thoracic and lumbar spine in ankylosing spondylitis, Arch Orthop Trauma Surg; 1981, 98:101– 7.

Troyer Kevin L, Comprehensive viscoelastic characterization of human lower cervical spine ligaments, 2010

Truesdell C., Toupin R., The Classical Field Theories, In Handbuck der Physik, Berlin, Springer- Verlag, 1960, pp. 226-793.

Urban, J.P.G., S. Roberts, and J.R. Ralphs, The nucleus of the intervertebral disc from development to degeneration. American Zoologist, 2000. 40(1): p. 53-61.

Viidik A., A Rheological Model for Uncalcified Parallel-Fibred Collagenous Tissue, J. Biomechanics, 1968, 1, pp. 3-11.

Walsh, W.R., Repair and regeneration of ligaments, tendons, and joint capsule. Orthopedic biology and medicine. 2006, Totowa, N.J.: Humana Press. x, 324 p.

Weiss J. A., A Constitutive Model and Finite Element Representation for Transversely Isotropic Soft Tissues, PhD Thesis, Department of Bioengineering, University of Utah, 1994

Weiss J., Gardiner J., Computational Modeling of Ligament Mechanics, Critical Reviews in Biomedical Engineering, 2001, 29, pp. 1-70

Weiss J., Lai A., Loui S., and Nisbet J., Behavior of Human Medial Collateral Ligament in Unconfined Compression, Trans. 46th Meeting Orthop. Res. Soc., 2000, 25, pp. 781.

White III A, Johnson R, Panjabi M, et al., Biomedical analysis of clinical stability in cervical spine. Clin Orthop; 1975, 109(III):85–95.

White III A, Panjabi M., Clinical biomechanics of spine. 2nd ed., Philadelphia, PA: JB Lippincott; 1990, 722pp

Woo S. L. Y., Gomez M. A., Akeson W. H., Mechanical behaviors of soft tissues: Measurements, modifications, injuries and treatment. In The Biomechanics of Trauma, A. M. Nahum and J. Melvin (Eds), Norwalk. Appleton Crofts. 1985, 107-133.

Woo S. L-Y., Kwan M.K., A Structural Model to Describe the Non-Linear Stress- Strain Behavior for Parallel-Fibered Collagenous Tissues, Journal of Biomechanical Engineering, 1989

Woo S. L. Y., Mechanical Properties of Tendons and Ligaments: I. Quasi-static and Nonlinear Viscoelastic Properties, Biorheology, 1982, 19, pp. 385-396.

Wu, H.C. and R.F. Yao, Mechanical-Behavior of Human Annulus Fibrosis. Journal of Biomechanics, 1976. 9(1): p. 1-&.

Xu R., Burgar A., Ebraheim N., Yeasting R., The Quantitative Anatomy of the Laminas of the Spine, Spine, 1999, 24(2), pp.l 07-113.

Yahia L. H., Drouin G., Study of the Hysteresis Phenomenon in Canine Anterior Cruciate Ligaments, J. Biomedical Eng., 1990, 12, pp. 57-62.

Yin F. C., Tompkins W. R., Peterson K. L., Intaglietta M., A Video-Dimension Analyzer, IEEE Tans. Biomed. Eng., 1972, 19, pp. 376-381.

Yoganandan N, Sances Jr. A, Maiman DJ, Myklebust JB, Pech P, Larson SJ., Experimental spinal injuries with vertical impact. Spine; 1986, 11:855–60.

Yoganandan N, Pintar FA, Sances Jr. A, Maiman DJ., Strength and motion analysis of the human head–neck complex. J Spinal Disord; 1991, 4:73–85.

Yoganandan N, Pintar FA, Gennarelli T, Eppinger RH, Voo LM., Geometrical effects on the mechanism of cervical spine injury due to head impact. In: Proceedings of the IRCOBI; Barcelona, Spain. 1999, p. 261–70.

Yoganandan N, Pintar FA, Kleinberger M., Cervical spine vertebral and facet joint kinematics under whiplash. J Biomech; 1998, 120:305–7.

Yoganandan N, Pintar FA, editors. Frontiers in whiplash trauma: clinical and biomechanical. The Netherlands: IOS Press, 2000

Yoganandan N, Pintar FA, Maiman DJ, Cusick JF, Sances Jr. A, Walsh PR., Human head–neck biomechanics under axial tension. Med EngPhys; 1996, 18:289–94.

Yoganandan N, Haffner M, Maiman DJ, Nichols H, Pintar FA, Jentzen J, et al. , Epidemiology and injury biomechanics of motor vehicle related trauma to the human spine. SAE Trans; 1990, 98:1790–807.

Yoganandan N, Myklebust JB, Ray G, Sances Jr. A., Mathematical and finite element analysis of spinal injuries. CRC Rev Biomed Eng; 1987, 15:2 9–93.

Yoganandan N, Pintar FA, Butler J, Reinartz J, Sances Jr. A, Larson SJ., Dynamic response of human cervical spine ligaments. Spine; 1989, 14:1102–10.

Yoganandan N, Kumaresan S, Pintar F, Gennarelli T. Pediatric biomechanics. In: Nahum A, Melvin J, editors. Accidental injury: biomechanics and prevention. New York: Springer. In press. 1993

Zwiers U., The Fundamentals of Multibody Dynamics, 2001